UNIVERSIDADE FEDERAL DA BAHIA
FACULDADE DE MEDICINA
FUNDAÇÃO OSWALDO CRUZ
INSTITUTO GONÇALO MONIZ

Programa de Pós-Graduação em Patologia Humana e Experimental

TESE DE DOUTORADO

IDENTIFICAÇÃO DE BIOMARCADORES DIAGNÓSTICOS E PROGNÓSTICOS DA SÍNDROME INFLAMATÓRIA DA RECONSTITUIÇÃO IMUNE ASSOCIADA À TUBERCULOSE EM PACIENTES COINFECTADOS COM HIV-1

RAFAEL TEIXEIRA TIBÚRCIO DOS SANTOS

Salvador - Bahia

2022

UNIVERSIDADE FEDERAL DA BAHIA

FACULDADE DE MEDICINA

FUNDAÇÃO OSWALDO CRUZ

INSTITUTO GONÇALO MONIZ

Programa de Pós-Graduação em Patologia Humana e Experimental

IDENTIFICAÇÃO DE BIOMARCADORES DIAGNÓSTICOS E PROGNÓSTICOS DA SÍNDROME INFLAMATÓRIA DA RECONSTITUIÇÃO IMUNE ASSOCIADA À TUBERCULOSE EM PACIENTES COINFECTADOS COM HIV-1

RAFAEL TEIXEIRA TIBÚRCIO DOS SANTOS

Tese de Doutorado apresentada ao Programa de Pós-graduação em Patologia Humana e Experimental como requisito para obtenção do grau de Doutor.

Orientação: Prof. Dr. Bruno de Bezerril Andrade

Salvador - Bahia

2022

Ficha Catalográfica elaborada pela Biblioteca do
Instituto Gonçalo Moniz/ FIOCRUZ – Bahia - Salvador

S2371i Santos, Rafael Teixeira Tibúrcio dos

Identificação de biomarcadores diagnósticos e prognósticos da síndrome inflamatória da reconstituição imune associada à tuberculose em pacientes coinfectados com HIV-1. / Rafael Teixeira Tibúrcio dos Santos. _ Salvador, 2022.

107 f.: il.: 30 cm

Orientação: Prof. Dr. Bruno de Bezerril Andrade

Tese (Doutorado em Patologia Humana) – Universidade Federal da Bahia, Faculdade de Medicina, Instituto Gonçalo Moniz, Fundação Oswaldo Cruz, Salvador, 2023.

1. SIRI. 2. Linfócitos T. 3. Inflamação sistêmica. 4. Ativação celular. 5. Metabolismo celular. I. Título.

CDU 616-002.5:616.98

"IDENTIFICAÇÃO DE BIOMARCADORES DIAGNÓSTICOS E PROGNÓSTICOS DA SÍNDROME INFLAMATÓRIA DA RECONSTITUIÇÃO IMUNE ASSOCIADA À TUBERCULOSE EM PACIENTES COINFECTADOS COM HIV-1".

Rafael Teixeira Tibúrcio dos Santos

FOLHA DE APROVAÇÃO

Salvador, 20 de dezembro de 2022

COMISSÃO EXAMINADORA

Dra. Simone Gonçalves da Fonseca
Professora
UFGO

Dra. Theolis Costa Barbosa Bessa
Pesquisadora
IGM/FIOCRUZ

Dra. Natália Machado Tavares
Pesquisadora
IGM/FIOCRUZ

Dr. Antonio Ricardo Khouri Cunha
Pesquisador
IGM/FIOCRUZ

Dr. Bruno de Bezerril Andrade
Pesquisador
IGM/FIOCRUZ

FONTES DE FINANCIAMENTO

"O presente trabalho foi realizado com apoio da Coordenação de Aperfeiçoamento de Pessoal de Nível Superior - Brasil (CAPES) – Código de Financiamento 001”

AGRADECIMENTOS

À minha mãe, por sua doçura, atenção, pelos sacrifícios, por celebrar cada vitória minha como se fosse sua, e pelo amor incomensurável que foi minha força motriz durantes estes 4 anos de doutorado.

Ao meu pai, pelo companheirismo, incentivo e ensinamentos, pelas palavras amigáveis e de conforto ao longo desses anos.

Aos meus familiares, especialmente, a meu TUGA (*the Uncle and godfather*), Denilton e à minha avó e madrinha Dirce, por todo apoio e confiança.

Ao meu orientador Dr. Bruno Bezerril e colegas do MONSTER, pelo aprendizado, incentivo e apoio.

Aos queridos professores do PgPat, pelas oportunidades, pelas portas abertas e pelas preciosas contribuições.

Aos meus amigos e companheiros da Plataforma de Vigilância Molecular e colegas do PgPAT, por fazer meus dias mais alegres e por proporcionarem um excelente e harmonioso ambiente de trabalho.

Aos meus amigos de biologia e da vida: Cleiton Lima, Lana Adriele, Gisele Conceição, Leon Dimitri, Fernanda Lessa, Marina Borges, Thiago Antunes e muitos outros, o apoio de vocês foi fundamental durante minha trajetória.

À Universidade Federal da Bahia e ao Departamento de Patologia e Medicina Legal/ Faculdade de Medicina - UFBA, pelo vínculo do programa de pós-graduação em Patologia Humana.

À Coordenação de Aperfeiçoamento de Pessoal de Nível Superior (CAPES) pelo fomento, apoio financeiro e consolidação do programa de pós-graduação em Patologia Humana.

Ao IGM, por todo apoio

“Poderia viver encerrado numa casca de noz e julgar-me o rei do espaço infinito, não tivesse eu sonhos atormentados.”

(**Shakespeare)**

SANTOS, Rafael Teixeira Tibúrcio dos. **Identificação de biomarcadores preditores e diagnósticos da síndrome inflamatória da reconstituição imune associada à tuberculose em pacientes coinfectados com HIV-1**. 2022. 107 f. Tese (Doutorado em Patologia Humana e Experimental) – Universidade Federal da Bahia. Faculdade de Medicina. Instituto Gonçalo Moniz, Fundação Oswaldo Cruz, Salvador, 2022

RESUMO

INTRODUÇÃO: A síndrome inflamatória de reconstituição imune associada à tuberculose (TB-SIRI) é um agravamento clínico dos sintomas de tuberculose observados em uma fração de pacientes coinfectados com HIV após o início da terapia antirretroviral (TARV). É bem conhecido que a TB-IRIS ocorre em função de inflamação exacerbada e dano tecidual em resposta à produção elevada de IFN-γ derivado de células T $CD4^+$. Concomitante a reconstituição linfócitaria, diversas alterações imunopatológicas dão suporte ao fenômenos patológicos associados a SIRI. Sabe-se que perturbações metabólicas subjacentes às alterações qualitativas das funções de diversas células imunológicas culminam na exacerbação da inflamação sistêmica e hiperativação celular. Além disso, vários estudos destacam o papel das células imunes adaptativas na patogênese da IRIS, mas até que ponto a ativação dos linfócitos T contribui para o desenvolvimento da SIRI ainda precisa ser esclarecido. **OBJETIVO**: Identificação de biomarcadores associados a TB-SIRI através da bioprospecção de metabolitos plasmáticos e marcadores de ativação e perfil de memória de linfócitos T $CD4^+$ e $CD8^+$ em indivíduos TB coinfectados com HIV mediante ao início do tratamento antirretroviral (TARV). **MÉTODOS**: Este foi um estudo retrospectivo de pacientes TB-HIV do sul da Índia antes e semanas após o início do TARV, em que houve a caracterização fenotípica dos linfócitos e determinação do grau de inflamação sistêmicas nestes pacientes. **RESULTADOS**: Observamos que a SIRI está relacionada com alterações no metabolismo de aminoácidos e lipídios. Tais vias metabólicas foram correlacionadas com mediadores pro-inflamatórios elevados durante a SIRI. O segundo manuscrito desta tese revelou que pacientes que desenvolveram SIRI possuíam uma linfopenia de células T $CD4^+$ acentuada antes do início da TARV e possuíam elevadas frequências de células T $CD8^+$. Além disso, os episódios de IRIS foram associados às disfunções da dinâmica de ativação linfocitária, com elevação de linfócitos T $CD4^+$ HLA-DR^+ e células T $CD4^+$ e $CD8^+$ expressando granzima B. Desenvolvemos modelos baseados em algoritmos de aprendizado de máquinas que foram capazes de predizer e diagnosticar IRIS levando em consideração as frequências de linfócitos expressando moléculas associadas a ativação celular. No terceiro manuscrito, observamos que a reconstituição do compartimento de células T $CD8^+$ de memória é predominada por células de memória efetora em pacientes que desenvolvem SIRI. Por sua vez, a magnitude da variação das frequências dessas células esta correlacionada positivamente com as abundancias de citocinas pro-inflamatórias. Em pacientes que manifestaram SIRI associada a TB, ocorre retenção de células T $CD8^+$ expressando CXCR3 em sítios persistentemente inflamados e a frequência destas células foi capaz de distinguir os pacientes com grande acurácia. **CONCLUSÃO**: Os dados apresentados nesta tese ratificam o papel da ativação linfocitária na imunopatogênese da SIRI, sendo que as subpopulações destas células e o perfil de alteração metabólicas são capazes de diagnosticar ou predizer a manifestação desta síndrome.

Palavras-chave: SIRI. Linfócitos T. Inflamação sistêmica. Ativação celular. Metabolismo celular.

SANTOS, Rafael Teixeira Tibúrcio dos. **Identification of predictive and diagnostic biomarkers of tuberculosis-associated immune reconstitution inflammatory syndrome in HIV-coinfected patients**. 2022. 107 f. Tese (Doutorado em Patologia Humana e Experimental) – Universidade Federal da Bahia. Faculdade de Medicina. Instituto Gonçalo Moniz, Fundação Oswaldo Cruz, Salvador, 2022

ABSTRACT

INTRODUCTION: Tuberculosis-associated immune reconstitution inflammatory syndrome (SIRI) is a clinical picture of tuberculosis symptoms observed in a disease of patients co-infected with HIV shortly after initiation of antiretroviral therapy (ART). It is well known that TB-IRIS occurs as a function of exacerbated inflammation and tissue damage in response to the overproduction of IFN-γ derived from CD4+ T cells. Concomitant to several lymphocyte reconstitution, changes and different layers of biological organization as alterations and support to the pathological phenomena associated with SIRI. Several immunological studies stand out, but that contribute to the great evolution of the role of genetics in the development of T lymphocytes, but that contribute to the great evolution of the development of T lymphocytes, remains highlighted. **OBJECTIVE**: To evaluate the lymphocyte profile of patients starting antiretroviral treatment. This thesis was joined by another manuscript that investigated the application of multi-omics techniques to bioprospecting for indicators associated with TB-SIRI. **METHODS**: This was a retrospective study of TB-HIV patients from South India before and weeks after initiation of ART, in which there was a phenotypic characterization of lymphocytes and determination of the degree of systemic inflammation in these patients. **RESULTS**: We observed that SIRI is related to alterations in amino acid and lipid metabolism. Such metabolic pathways have been correlated with elevated pro-inflammatory mediators during SIRI. The second manuscript of this thesis revealed that patients who developed IRIS had marked CD4+ T-cell lymphopenia before starting ART and had high frequencies of CD8+ T-cells. In addition, IRIS episodes were associated with dysfunctions of lymphocyte activation dynamics, with elevation of CD4+ HLA-DR+ T lymphocytes and $CD4^+$ and CD8+ T cells expressing granzyme B. We developed models based on machine learning algorithms that were able to predict and diagnose IRIS taking into account the frequencies of lymphocytes expressing molecules associated with cell activation. In the third manuscript, we observed that the reconstitution of the memory CD8+ T cell compartment is predominated by effector memory cells in patients who develop IRIS. In turn, the magnitude of the frequency variation of these cells is positively correlated with the abundance of pro-inflammatory cytokines. In patients who manifested TB-associated SIRI, there is retention of CD8+ T cells expressing CXCR3 in persistently inflamed sites and the frequency of these cells was able to distinguish patients with great accuracy. **CONCLUSION**: The data presented in this thesis confirm the role of lymphocyte activation in the immunopathogenesis of IRIS, and the subsets of these cells and the profile of metabolic alterations are capable of diagnosing or predicting the manifestation of this syndrome.

Keywords: TB-IRIS. T lymphocytes. Systemic inflammation. Cell activation. Cellular metabolism.

LISTA DE FIGURAS

LISTA DE ABREVIATURAS

CPI	Complexo de pré-integração
CXCR3	C-X-C motif chemokine receptor 3
Glut 1	Transportador de glicose 1
HLA-DR	Human leukocyte antigen – DR isotype
IFN-γ	Interferon γ
IL-12p70	Interleucina 12 subunidade proteica 70
IL-6	Interleucina 6
IL-8	Interleucina 8
Ki-67	Marker of proliferation ki-67
MCH	Complexo principal de histocompatibilidade
MTBC	Complexo *Mycobacterium tuberculosis*
Mtb	*Mycobacterium tuberculosis*
PD-1	Programmed cell death protein 1
P-TEFβ	*Positive transcription elongation factor* β
TLR	Toll like receptors
TNF- α	Fator de necrose tumoral α
TR	Transcriptase reversa

LISTA DE ARTIGOS

Esta tese é baseada nos seguintes manuscritos, os quais serão referidos pelos seus numerais romanos

Manuscrito I Plasma Metabolomics Reveals Dysregulated Metabolic Signatures in HIV-Associated Immune Reconstitution Inflammatory Syndrome. *Front Immunol*. 2021; 12:693074.

Manuscrito II Dynamics of T-Lymphocyte Activation Related to Paradoxical Tuberculosis-Associated Immune Reconstitution Inflammatory Syndrome in Persons with Advanced HIV. *Front Immunol*. 2021; 12: 757843.

Manuscrito III Frequency of CXCR3+ CD8+ T-Lymphocyte Subsets in Peripheral Blood Is Associated with the Risk of Paradoxical Tuberculosis-Associated Immune Reconstitution Inflammatory Syndrome Development in Advanced HIV Disease. *Frontiers in immunology*, *13*, 873985.

SUMÁRIO

1 **INTRODUÇÃO**

1.1 ASPECTOS GERAIS DA INFECÇÃO PELA *MYCOBACTERIUM TUBERCULOSIS*

1.1.1 **O agente etiológico**

O complexo *Mycobacterium tuberculosis* (MTBC) é composto por um grupo de espécies de micobactérias aeróbias, em forma de bastonete, ácido-resistente que compartilham um alto grau de similaridade genética (> 99% de similaridade das sequências de nucleotídeos) (ACHTMAN, 2008). Sabe-se que os membros do MTBC são os principais agentes causadores da tuberculose (TB) em seres humanos. As principais espécies que compreendem tal complexo são *M. bovis*, *M. tuberculosis, M. africanum e M. microti* (GAGNEUX, 2018). Como bacilos ácidos resistentes, sua parede celular é rica em ácidos graxos de cadeia longa contendo ácido micólico, responsável pela resistência destas bactérias à detergentes, assim como pelo seu lento crescimento em cultura e persistência no interior de células hospedeiras. Outros constituintes de sua parede celular incluem peptidioglicanos conjugados a micolatos de arabionogalactana (arabionse e galactose) (Figura 1).

Além disso os membros do MTBC são patógenos profissionais com nenhum reservatório animal ou ambiental descrito (GAGNEUX, 2018). Acredita-se que o MTBC emergiu como patógenos a partir de ancestrais bacterianos ambientais que foram fagocitados por protozoários de vida livre (amebócitos). Esta capacidade de infectar amebócitos propiciou a seleção do ancestrais do MTBC que adquiriram uma série de adaptação para a vida no meio intracelular (JANG et al, 2008). Diferentemente de uma miríade de outros patógenos, a transmissão das espécies que compõe o MTBC é diretamente relacionada sua virulência, tendo a obrigatoriedade de causar a forma pulmonar da doença para que possam ser transmitidas (BRITES; GAGNEUX, 2012).

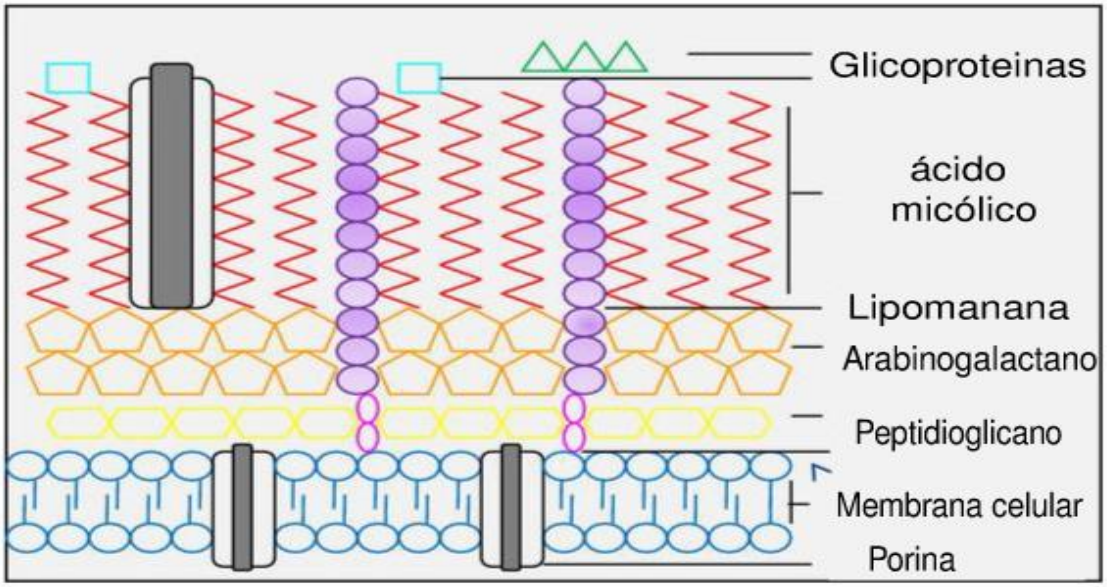

Figura 1 - Principais componentes estruturais da parede celular de *Mycobacterium tuberculosis*. Nota-se que a membrana interna é constituída principalmente por peptidoglicanos ligados de maneira covalente à camada de arabinogalactanos. A camada mais externa é basicamente composta por ácido micólico e glicolipídios.
Fonte: (Kleinnijenhuis et al, 2011)

1.1.2 **Aspectos epidemiológicos da infecção por *Mycobacterium tuberculosis***

A TB figura como uma das doenças infectocontagiosas mais antigas já registradas nas diferentes populações humanas. Estima-se que a *Mtb* tenha emergido como organismo patogênico há cerca de 20 mil anos em populações no leste do continente africano (BROWN, 1941). Evidências paleopatológicas sugerem a existência de TB acometendo tecidos ósseos em espécimes do período neolítico (entre 8000 e 5000 anos antes de Cristo) (BARBERIS et al, 2017). Além disso o material genético deste bacilo foi encontrado em lesões de múmias encontradas no Egito e também restos mortais m na América do sul (ZIMMERMAN; BULL, 1979; CAVE, 2013).

A complexa interação entre fatores biológicos do agente patológico e do hospedeiro humano somados às questões ambientais (como padrões de migração e condições de vida) contribuem significativamente para a permanência do bacilo nas populações humanas (BRITES; GAGNEUX, 2011). O aumento densidade populacional e intensificação do processo de urbanização que ocorreu na Europa logo após o advento da revolução industrial no século XVIII contribuiu significativamente para o aumento da incidência de TB naquele período (FRITH, 2014). Acredita-se que ao longo dos últimos 200 anos, infecções atribuídas a *Mtb* tenham sido responsáveis pela morte de aproximadamente 1 bilhão de pessoas ao redor de todo

o mundo (PAULSON, 2013). Atualmente, a TB ainda permanece como umas das principais causas de morte que pode ser atribuída a um único agente etiológico.

O relatório Global da Tuberculose estimou que, em 2020, aproximadamente 10 milhões de pessoas desenvolveram TB, das quais 1,2 milhões pereceram em virtude de tal doença (WORLD HEALTH ORGANIZATION, 2021). Nota-se que a carga da TB não é homogeneamente distribuída, sendo que a maior fração dos casos registrados em 2020 estavam concentrados no Sudeste Asiático (43%) e no continente Africano (25%) **(Figura 2a)**. O grupo de países que concentram os maiores números de casos inclui Índia (26%), China (8.5%), Indonésia (8,4%), Filipinas (6 %), Paquistão (5,8%), Nigéria (4,6%), Bangladesh (3,6%) e África do Sul (com 3,3%) **(Figura 2b)**.

Notou-se que nas últimas décadas, a incidência da TB globalmente entrou em declínio, porém ainda não o satisfatório para atingir a meta do STOP TB que visa a eliminação da TB até 2035 (WORLD HEALTH ORGANIZATION, 2015). Salienta-se que o impacto da TB global está substancialmente associado à sua elevada taxa de mortalidade (estimada em 16% dos casos). Ademais, o número de fatalidades também é influenciado pela existência de coinfecção pelo vírus da imunodeficiência humana (HIV) e pela emergência de bacilos multirresistente às ferramentas quimioterápicas atualmente disponíveis (WORLD HEALTH ORGANIZATION, 2021).

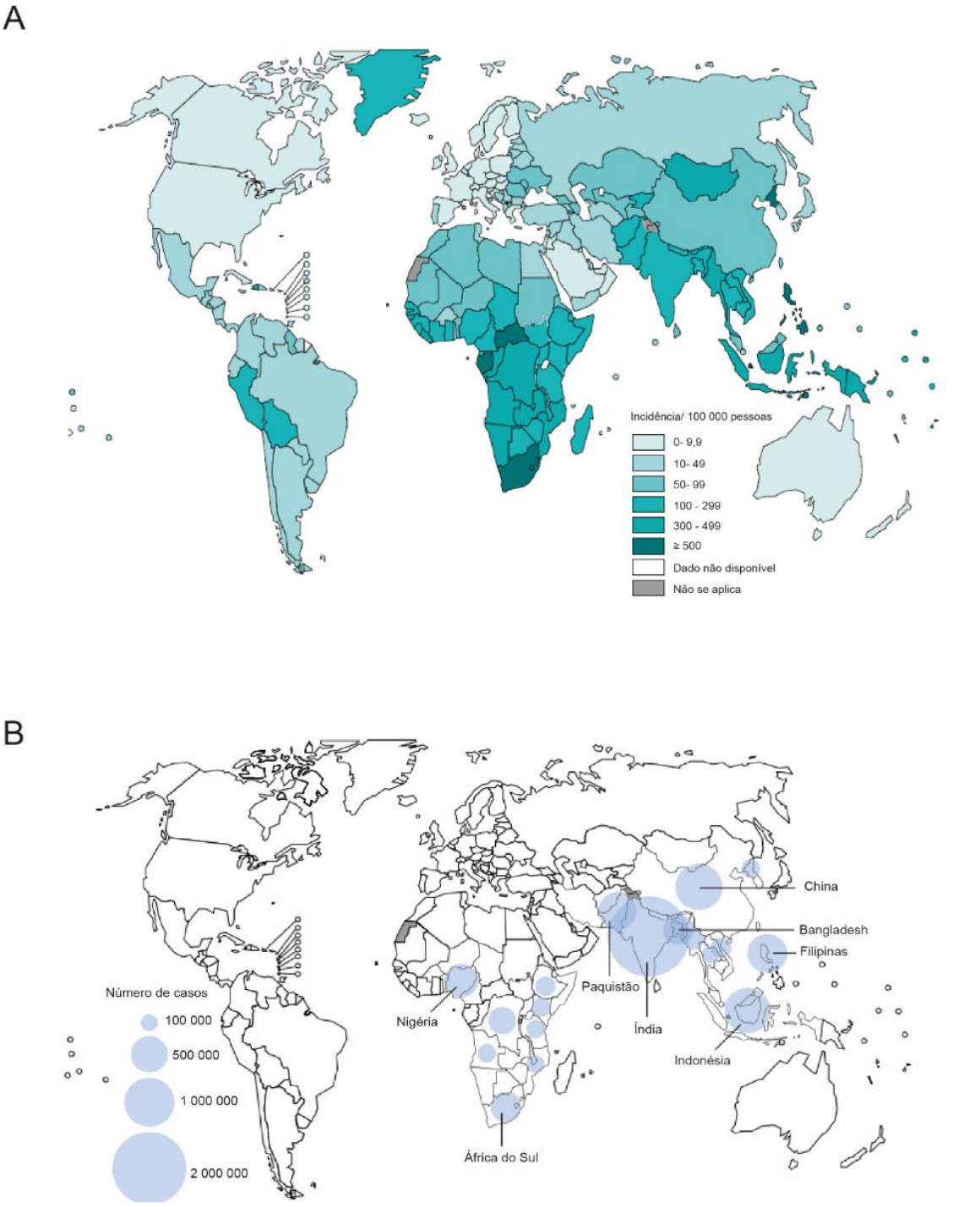

Figura 2 – Taxas estimadas de incidência de Tuberculose em 2020 – Incidência da Tuberculose pulmonar no mundo em 2020 (a) e países com maior concentração dos casos de TB registrados em 2020 (b).
Fonte: (WORLD HEALTH ORGANIZATION, 2021)

1.1.3 **Modo de transmissão**

1.1.3.1 A cascata de transmissão da tuberculose

A compreensão da sequência de eventos subjacentes à transmissão da TB faz-se imprescindível para a mitigação da carga desta patologia e para a geração de estratégias de controle mais eficazes. Apesar de a TB poder acometer qualquer órgão, os pulmões são a principal interface entre o bacilo e o hospedeiro. Churchyard et al (2017) sugerem que um esquema que ilustra a cascata de eventos da transmissão da TB que inclui: (1) a presença de individuo infectado (caso fonte), (2) a geração e eliminação de partículas infecciosas por vias aéreas, (3) estabilidade das gotículas aerossolizadas no ar e retenção do potencial infeccioso, (4) inalação destas partículas por indivíduos suscetíveis, (5) infecção destes indivíduos, e por fim (6) potencial desenvolvimento da TB (CHURCHYARD et al, 2017) **(Figura 3)**.

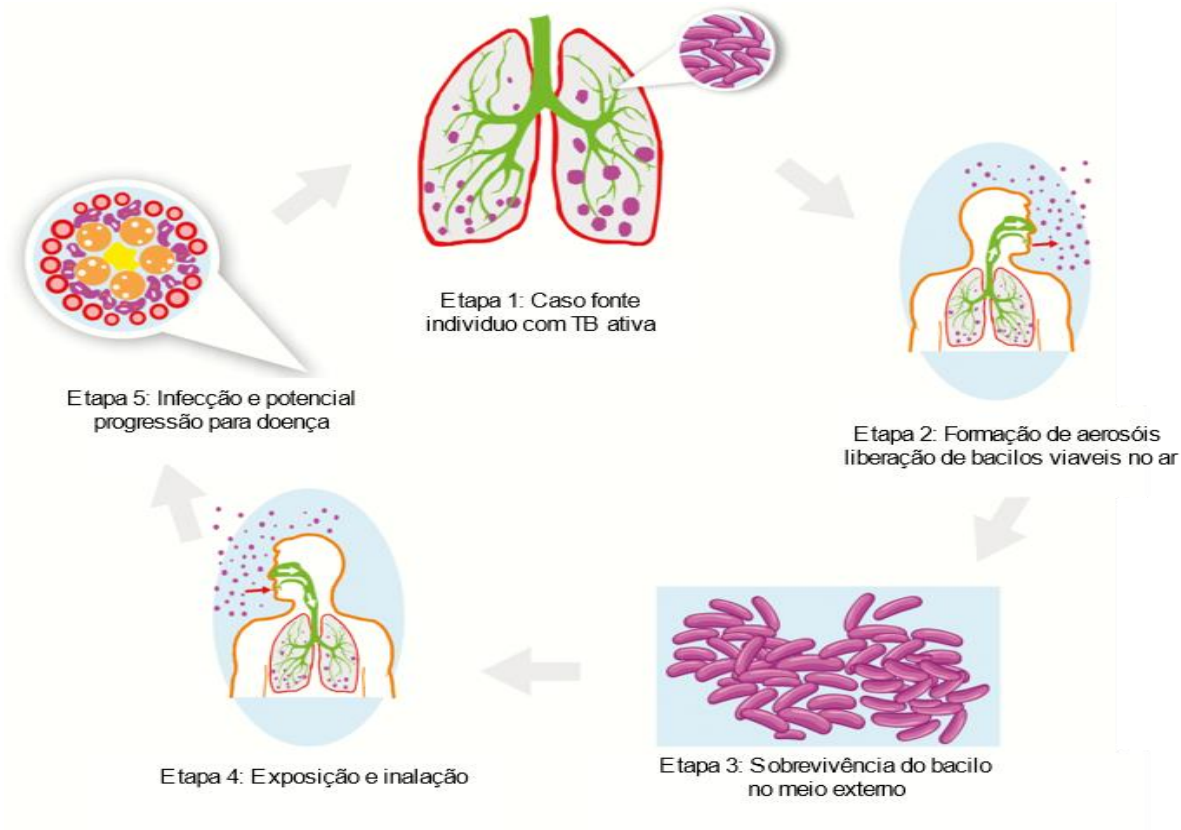

Figura 3 - Cascata da transmissão da TB. A transmissão do bacilo *Mycobacterium tuberculosis* tem início com a formação de partículas aerossolizadas oriundas de um paciente fonte com TB pulmonar ativa. Subsequentemente, os bacilos devem ser capazes de sobreviver às agressões do ambiente externo até que sejam inalados por indivíduos expostos. A deposição das gotículas contendo bacilos viáveis no trato respiratório do indivíduo exposto é o evento inicial do processo de infecção.
Fonte: (CHURCHYARD et al., 2017)

1.1.3.2 Eventos determinantes para a transmissão

Indivíduos com TB pulmonar ativa constituem a principal fonte de geração de partículas infecciosas aerossolizadas que são eliminadas através da tosse, fala e espirro. Tipicamente estas partículas possuem diâmetro inferior a 5µm e o seu potencial de transmissão é influenciado por uma combinação de eventos aerodinâmicos (como velocidade de sedimentação e tempo de suspensão no ar), físico-químicos (pH, tamanho da partícula, carga elétrica), anatômicos e ambientais (como temperatura, umidade, ventilação e radiação ultravioleta) (WANG et al, 2021). Ademais, aspectos biológicos do bacilo, como espessura da parede celular e sua hidrofobicidade conferem proteção contra agressões externas relacionadas à desidratação (quando em temperatura ambiente) e reidratação (quando tem acesso ao aparelho respiratório do hospedeiro recém infectado) (BRENNAN, 2003).

Diversos estudos apontam que a transmissão do *Mtb* é multifatorial e pode ser apenas determinado probabilisticamente (RUSSEL et al, 2010; RILEY et al, 1995). Fatores determinantes da transmissão incluem elementos patológicos clássicos da TB como a formação de cavitações pulmonares (sobretudo em indivíduos imunocompetentes) associada com maior secreção de bacilos e disponibilidade de tratamento eficaz aos indivíduos infectados com intuito de cessar a cadeia de transmissão. Estudos sugerem que a infectividade de um indivíduo com TB pulmonar ativa está diretamente associada com a quantidade de bacilos presentes no escarro (que pode ser mensurada através da técnica de esfregaço de escarro) (LOHMANN et al, 2012). Ademais, o status imunológico e nutricional dos indivíduos expostos, coinfecção por HIV, tabagismo ou diabete influenciam substancialmente as taxas de transmissão.

1.1.4 **Eventos entre o estabelecimento da infecção e manifestações clínicas**

1.1.4.1 O papel da imunidade inata na resposta contra *Mtb*

Ao ganhar acesso ao trato respiratório dos indivíduos expostos, a maior parte dos bacilos são aprisionados nas porções superiores sendo subsequentemente expelidos pela ação das células ciliadas (TEITELBAUM et al, 1999). O sistema de mucosas do trato respiratório confere a primeira linha de defesa contra uma miríade de patógenos, sendo a função de barreira estabelecida pelas células epiteliais de vital importância para limitar o acesso do *Mtb* no organismo (DENG et al, 2012). Entretanto, uma porção destes bacilos pode ser depositado nos alvéolos pulmonares. Neste ponto, os macrófagos alveolares residentes interagem ativamente

com o bacilo. Estas células constituem importantes membros do sistema imune inato que contribui para a homeostase pulmonar através fagocitose de restos celulares, reciclagem de surfactantes, reconhecimento de organismos invasores e disparo de resposta inflamatória local (HUSSELL et al, 2014). Salienta-se que a funcionalidade dos macrófagos alveolares é substancialmente influenciada por padrões moleculares e sinais imunológicos presentes no microambiente dos pulmões, dentre eles: a disponibilidade de oxigênio, exposição à surfactantes, assim como interação com células epiteliais do tipo I e tipo II (JOSHI et al, 2018). Os eventos bem-sucedidos de fagocitose são seguidos pelo remodelamento metabólico e epigenético dos macrófagos alveolares, culminando na produção de diversos fatores intracelulares associados à destruição da *Mtb* (MARIMANI; AHMAD; DUSE, 2018). Dentre estes mecanismos, destaca- se o cercamento das invaginações da membrana plasmática ao redor do bacilo formando uma estrutura intracelular conhecida como fagossomos. Então, há mobilização de elementos que favorecem a coalescência dos fagossomos albergando Mtb com lisossomos (organelas repletas de enzimas hidroliticas e espécies reativas de oxigênio). Desta maneira, a fusão destas duas organelas dá origem ao fagolisossomo, cujo conteúdo ácido é responsável pela destruição do *Mtb* (TABARAN et al, 2020). Entretanto, durante o curso do processo evolutivo, *Mtb* desenvolveu diversas estratégias que tornam o mecanismo de fagocitose ineficiente. Dentre eles, destacam-se a liberação de lipídios bioativos que compõe a parede celular (por exemplo, Lipoarabinomanana [LAM]) e ação do sistema de secreção ESX que interferem na formação do fagolisossomo (TABARAN et al, 2020). Ademais estes mecanismos também modulam outras respostas microbicidas dos macrófagos alveolares permitindo a replicação do Mtb (PODINOVSKAIA et al, 2013) Uma vez que a resposta elicitada pelos macrófagos alveolares seja ineficiente para conter a progressão do processo infeccioso, Mtb é capaz de invadir o tecido intersticial do pulmão através da infecção direta do epitélio alveola ou via macrófagos alveolares que migram para a região do parênquima pulmonar (PAI et al, 2016) (Figura 4).

Concomitantemente aos primeiros eventos de interação bacilo-hospedeiro, macrófagos infectados produzem moléculas inflamatórias (como citocinas, quimiocinas e mediadores lipídicos) que são capazes de recrutar e ativar outros leucócitos. Tem-se então a amplificação da resposta imunológica local contra o bacilo e início do processo inflamatório. Após um breve período de estagnação (aproximadamente 3 dias), ocorre a replicação em escala exponencial dos bacilos no sítio infeccioso (UPADHYAY; MITTAI; PHILLIPS, 2018). Neste momento da infecção, o infiltrado celular é composto principalmente por neutrófilos (tipo de leucócito mais abundante na circulação sanguínea) que tem papel dual na TB. Durante o processo de diapedese

(passagem da circulação para o foco da infecção), os neutrófilos interagem com diversas proteínas da matriz extracelular que promovem a ativação das suas atividades microbicidas, incluindo aumentada taxa de fagocitose, produção de citocinas pró-inflamatórias (como TNF-α, IL-6, IL-1β), secreção de grânulos enzimáticos, além da liberação de material genético associado a enzimas capazes de aprisionar e patógenos extracelulares – as NETs (do inglês, *neutrophil extracelular traps*) (AMULIC et al, 2012). Diversos estudos apontam a importância dos neutrófilos nos processos imunopatogênicos da TB. Teixeira e colaboradores demonstraram em um modelo experimental murino que interferência na sinalização mediada por GM-CSF (fator estimulador de colônias de granulócitos e macrófagos) implica na hiperativação de neutrófilos e na formação de NETs, por sua vez, associada ao crescimento bacteriano e maior gravidade da TB (MOREIRA-TEIXEIRA et al, 2020). Um estudo conduzido por Walker e colaboradores apontou que os neutrófilos são a principal fonte de produção exacerbada de metaloproteinase 8 (MMP-8) que contribui para destruição da matriz extracelular (WALKER et al, 2017). Assim, estes estudos e outros sugerem que a elevação do infiltrado e ativação de neutrófilos contribuem para o aumento do processo inflamatório que favorece o estabelecimento da *Mtb*.

Os eventos iniciais da imunopatogênese da TB também incluem o recrutamento de outras células mieloides importante no controle da infecção. Dentre estes tipos celulares, destacam-se os monócitos que possuem considerável plasticidade fenotípica capazes de dar origem a certos tipos de macrófagos e células dendríticas (DCs). Coletivamente, as DCs e macrófagos compõem o grupo de células apresentadoras de antígeno profissionais (do inglês, APCs) que responsáveis pelo reconhecimento de padrões moleculares associadas à *Mtb*, captura e processamento antígenos. Subsequentemente, as APCs elevam a expressão de moléculas coestimuladoras (como CD80 e CD86) e migraram para órgão linfoides secundário a fim de apresentar antígenos à linfócitos T naïve (SONG et al, 2018). Durante o período que antecede o estabelecimento de uma resposta adaptativa robusta o suficiente para conter o crescimento bacilar, *Mtb* pode realizar disseminação linfo-hematogênica para outros sítios do pulmão ou outros órgãos (PAI et al, 2016).

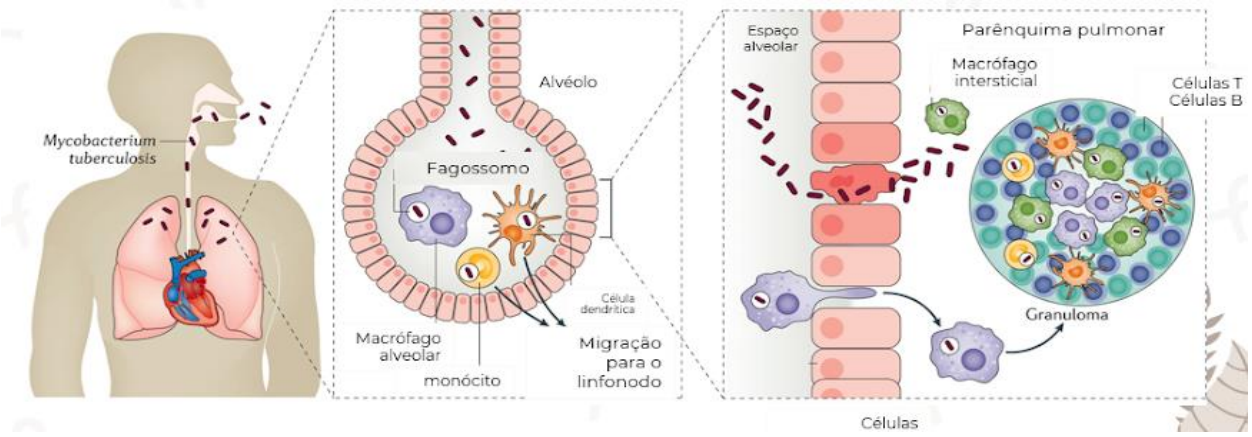

Figura 4 – Eventos iniciais da imunopatogênese da Tuberculose. Após a inalação de partículas aerossolizadas contendo bacilos viáveis, os macrófagos alveolares residentes interagem com *Mtb.* Em casos bem-sucedidos, a infecção termina neste ponto com atuação apenas destes tipos celulares. Entretanto, *Mtb* é capaz de subverter os mecanismos microbicidas dos macrófagos e prolifera no interior destes. Há intensa produção de mediadores inflamatórios e morte celular. DCs e monócitos são recrutados para o sítio da infecção e auxiliam no estabelecimento de respostas imune contra o bacilo. Após a captura e processamento de antígenos micobacterianos, DCs migram para o linfonodo onde irão ativar células T. A incapacidade das células imune inata em conter a infecção resulta na migração de *Mtb* para o parênquima pulmonar por via direta (infecção de células do epitélio alveolar) ou pela transmigração de macrófagos infectados. Posteriormente, células do ramo adaptativo participam da formação de estruturas patológicas associadas à contenção do processo infeccioso.
Fonte: Pai et al, 2016.

1.1.4.2 O desenvolvimento de resposta imune adaptativa

Cerca de 2 a 4 semanas após a infecção, as células T $CD4^+$ infiltrantes são capazes de produzir fatores que promovem a ativação completa dos macrófagos infectados e facilitam a destruição do Mtb. Alternativamente, uma resposta de hipersensibilidade tardia elicitada pelos antígenos bacilares promove a morte de macrófagos não ativados albergando Mtb e amplifica a destruição tecidual (JASENOSKY et al, 2015). A progressão Tb é ditada pela dinâmica dos dois fenômenos descritos acima.

Salienta-se que a resposta adaptativa mediada pelos linfócitos T é um elemento central na imunopatogênese da TB. Os linfócitos T $CD4^+$ reconhecem epítopos associados ao Mtb apresentados através MHC (complexo de histocompatibilidade maior) II presente nas superfícies das APCs. Subsequentemente, os linfócitos passam por um processo de ativação (caracterizado por uma extensa modificação da sua arquitetura genética), que culmina em sua diferenciação em células efetoras e expansão clonal de populações especificas para o antígeno apresentado. Classicamente, destacam-se dois tipos de células T auxiliadoras: as células Th1 (caracterizadas pela produção de INF-γ e IL-2) e células Th2 (que produzem citocinas anti-inflamatórias como IL-4, IL-10 e IL-13) (SARAVIA; CHAPMAN; CHI, 2019). A resposta do tipo Th1 é imprescindível para o recrutamento de monócitos e neutrófilos, além de contribuir para ativação dos macrófagos infectados (SARAVIA; CHAPMAN; CHI, 2019). As células Th1

são caracterizadas pela expressão de *T-box transcriptor factor* (T-bet), fator de transcrição estimulado por IFN-γ, que atua na manutenção e amplificação da resposta Th1 (SZABO et al, 2000). Contudo, em certos contextos, esse tipo de resposta não é suficiente para impedir a progressão da infecção. Células Th17 também são reconhecidas por exercerem um papel duplo na imunopatogênese da TB. Por um lado, a atuação das células Th17 favorece a migração de células Th1 para o ambiente pulmonar e o estabelecimento das respostas contra o bacilo. Entretanto, a hiperativação das células Th17 promove elevação do processo inflamatório, aumento do influxo de neutrófilos patogênicos e dano tecidual excessivo (PATEL; KUCHROO; VIJAY, 2015).

Ademais, um outro fenótipo de células T $CD4^+$ - as células T regulatórias (Treg) que são capazes de suprimir as funções de outros linfócitos ativados- desempenham um papel relevante na patogênese da TB. Durante as etapas iniciais da infecção, as células Treg estão associadas a um atraso no estabelecimento da resposta imune adaptativa mediada por células Th1. Por outro lado, durante a fase crônica da TB, tais células estão relacionadas com a proteção contra o dano tecidual excessivo (CARDONA; CARDONA, 2019). Desta maneira, a resposta célula mediada por células T $CD4^+$ está intimamente associada a um balanço entre as respostas pro-inflamatórias, que promovem a eliminação do bacilo, e a resposta anti-inflamatório que limita o dano colateral da resposta imune.

1.1.4.3 Formação do granuloma

A extensa proliferação da Mtb em macrófagos com limitada capacidade de microbicida é acompanhada da liberação de quimiocinas e citocinas aumentam o influxo de linfócitos para o sítio infecioso (FLYN; CHAN; LIN, 2011). Produtos bacterianos e padrões moleculares associados ao dano celular durante os ciclos de infecção amplificam o recrutamento de outros leucócitos, como macrófagos não ativados e DCs. Tem-se então o estabelecimento de uma estrutura patológica associada à contenção da infecção – o granuloma (Figura 5). As lesões granulomatosas são formadas mediada ao acúmulo de macrófagos ativados na lesão primária. A arquitetura patológica dos granulomas pode ser sucintamente descrita como um cinturão composto por linfócitos T e B circundando um agregado compacto de células epitelióides (CADENA; FORTUNE; FLYNN, 2018). Estas últimas por sua vez, representam macrófagos que passaram por um remodelamento morfológico, onde suas membranas plasmáticas estão fortemente unidas, lembrando a forma de células epiteliais. A fusão dos macrófagos também dá origem às células gigantes multinucleadas ou células espumosas, caracterizadas pelo

acúmulo de corpúsculos lipídicos em seu citoplasma (RAMAKRISHNAN, 2012). No centro do granuloma, há grande concentração de bactérias e células mortas compondo uma área de extensa necrose (centro caseoso). O ambiente necrótico associado a baixas de tensões de oxigênio e pH ácido podem auxiliar na contenção do crescimento bacilar. Subsequentemente, algumas lesões granulomatosas podem ser cicatrizadas através do processo de fibrose seguido de calcificação (CADENA; FORTUNE; FLYNN, 2017).

Os granulomas formados nesta fase da imunopatogênese da TB podem apresentar uma grande heterogeneidade quanto ao seu tamanho e composição celular, bem como na sua capacidade de limitar a infecção. Salienta-se que os granulomas são encontrados tanto em pacientes com TB latente quanto com doença ativa e que o simples estabelecimento do granuloma não pode ser interpretado como uma medida de controle da infecção (FLYN; CHAN; LIN, 2011). Alternativamente, o estado de latência pode ser interpretado como o resultado da dinâmica entre os aspectos biológicos do patógeno e a capacidade protetora da resposta imunológica.

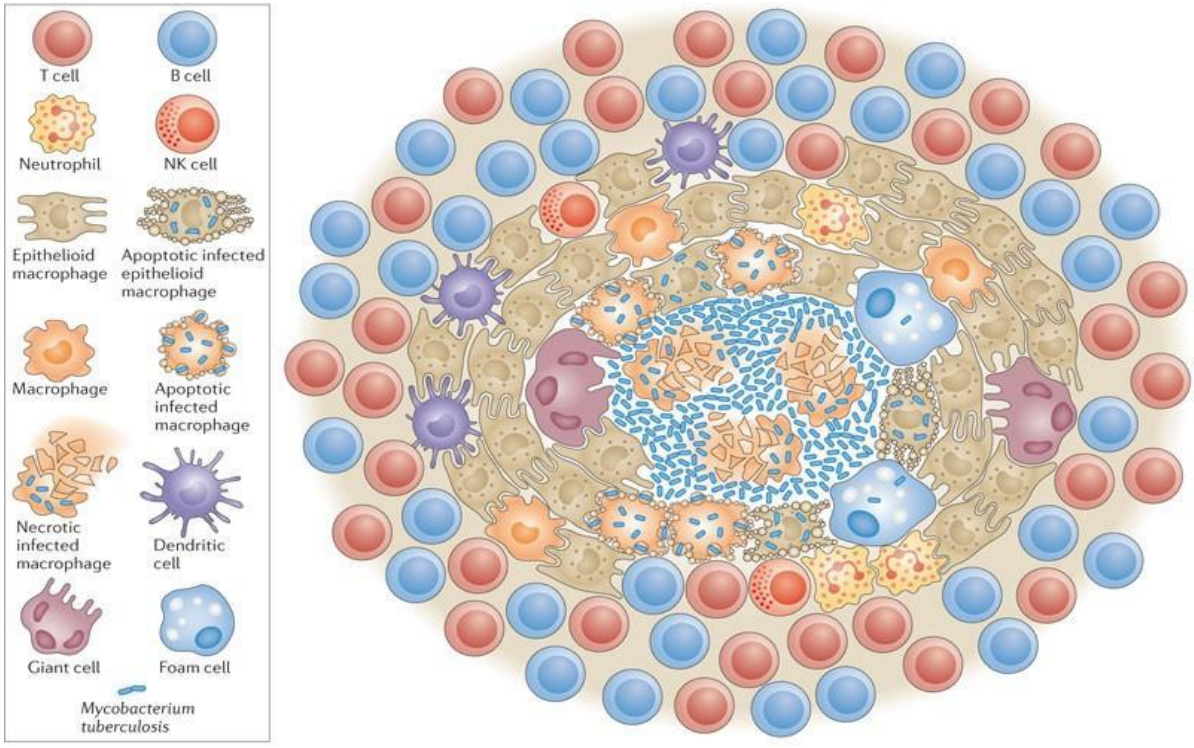

Figura 5 - Estrutura do Granuloma. O granuloma compreende uma estrutura patológica associada à contenção da infecção de *Mtb*. Macrófagos em contato com o bacilo realizam uma gama de especializações funcionais incluindo a formação de células gigantes, células espumosas e células epitelióides. O centro do granuloma é uma área com predominância de processos necróticos onde há intensas taxas de morte celular e densidade de *Mtb*. DCs e Natural Killer auxiliam na manutenção do granuloma. A região mais externa do granuloma é composta por um cinturão de linfócitos T e B.
Fonte: (CADENA; FORTUNE; FLYNN, 2017).

1.1.5 **O espectro de manifestações clínicas da Tuberculose**

Diversos fatores imunológicos determinam o desfecho da interação primária entre Mtb e o hospedeiro. Os eventos que sucedem a exposição ao bacilo podem culminar na eliminação dos mesmo por intermédio da resposta imune inata concatenada à resposta imune adaptativa (PHILLIPS; ERNST, 2011). Alguns indivíduos estabelecem respostas granulomatosas apropriadas para a contenção da infecção, caracterizando assim o estágio latente da TB. Estima-se que cerca de 2 bilhões de pessoas estejam infectadas de maneira latente por *Mtb*, o que compõe 1/3 da população mundial (WORLD HEALTH ORGANIZATION, 2013). Alternativamente, defeitos na funcionalidade dos granulomas podem culminar na Tb ativa e pacientes com esta forma da doença podem apresentar a forma pulmonar, extrapulmonar ou ambas (RAVIMOHAN et al, 2018). Desta maneira, a TB pode ser melhor compreendida como um espectro dinâmico entre a infecção e manifestação da doença ativa, onde os pacientes podem avançar ou retroceder neste continuum de acordo com a robustez de sua resposta imunológica ou presença de outras patologias (PAI et al, 2016). A Figura 6 ilustra o espectro de manifestações clínicas associadas a TB.

A TB pulmonar pode ser dicotomicamente classificada como primária ou pós-primaria (reativação). Os principais sintomas da Tb pulmonar incluem tosse com produção de escarro, falta de apetite, febre sobretudo no fim da tarde, sudorese noturna, hemoptise e perda de peso (LODDENKEMPER; LIPMAN; ZUMIA, 2016). A TB primária ocorre quando o indivíduo não possui imunidade prévia ao *Mtb* e tipicamente esta é a forma mais observada em crianças e indivíduos imunocomprometidos, sobretudo em regiões geográficas de alta carga de TB (LAWN; ZUMLA, 2011). Na TB primária, as zonas inferiores do pulmão são os sítios majoritariamente afetados. A lesão inicial (foco de Ghon) é tipicamente periférico e acompanhado por linfodenopatia hilar ou paratraqueal transiente. Os sintomas mais comumente associados à esta forma de TB são febres e dor torácida (LAWN; ZUMLA, 2011). Em uma porção dos indivíduos com TB primária, as lesões expandem rapidamente acompanhada de necrose central e cavitação – tem-se então o desenvolvimento da TB primária progressiva (HUNTER, 2011; HUNTER; JAGANNATH,2007). Neste caso, pode ocorrer disseminação bacilar do parênquima pulmonar para os vasos linfáticos, compressão dos brônquios promovidas por linfonodos aumentados, além da ruptura destes nas vias áreas. Por outro lado, a Tb pós-primaria (também conhecida como secundária) está associada a reativação de infecções previamente contidas pela ação do sistema imunológico e acontece na presença de respostas imunológicas com especificidade antigênica para o bacilo (HUNTER, 2011). Esta

forma da TB é a principal forma encontrada em indivíduos adultos. A lesão esta tipicamente localizada na porção apical dos lobos superiores, onde as relativamente altas tensões de oxigênio propiciam o crescimento bacilar (HUNTER, 2011). Neste cenário, o nível de comprometimento do parênquima pulmonar é bastante variável, desde pequenos infiltrados à cavitações. Em certos indivíduos, o conteúdo liquefeito da necrose é transportado pelas vias áreas e ocorre disseminação broncogênica. Assim, pode haver o surgimento de lesões satélites com posterior progressão para cavitações no parênquima pulmonar (HUNTER; JAGANNATH,2007).

Por definição, a TB é classificada como extrapulmonar quando a doença se manifesta em outro órgão fora do parênquima pulmonar em virtude da disseminação do bacilo durante os estágios iniciais da infecção. A TB extrapulmonar é mais frequentemente observada em pacientes coinfectados com HIV e o risco de desenvolvimento desta forma da TB esta inversamente correlacionada com as contagens de células T $CD4^+$ (NAING et al, 2013; JONES et al, 1993). Outra população substancialmente vulnerável a Tb extrapulmonar são crianças devido ao seu sistema imunológico incapaz de estabelecer respostas protetoras robustas (LEWINSOHN et al, 2004). Os sítios mais frequentes de TB extrapulmonar são linfonodos, pleura, trato gastrointestinal, ossos, meninges e pericárdio (LAWN; ZUMLA, 2011).

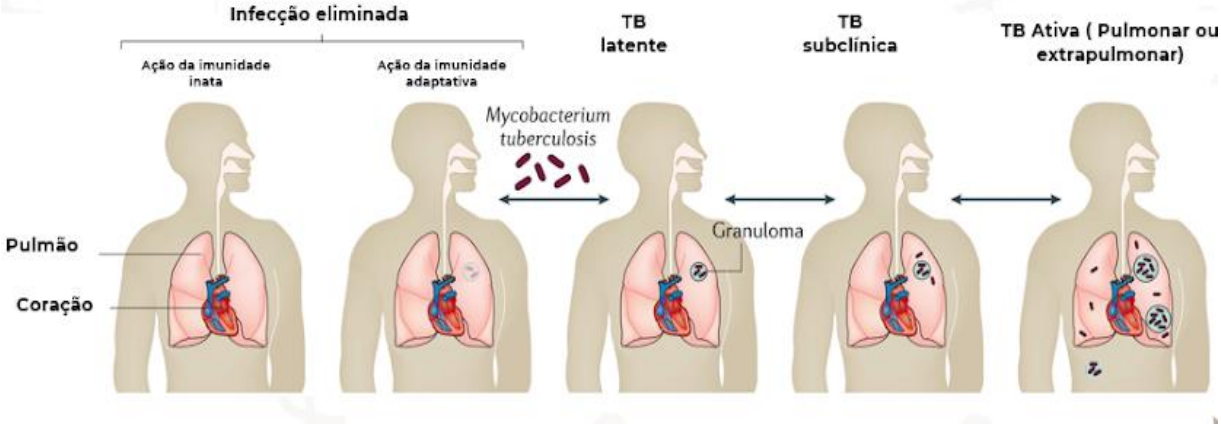

Figura 6 - Espectro de manifestações clínicas da TB. Diversos fatores inerentes à biologia da *Mtb* e do status imunológico do indivíduo exposto determinam a progressão da infecção. Em muitos casos, a ação da imunidade inata é suficiente para eliminar os bacilos invasores. As respostas mediadas pelas células da imunidade adaptativa, sobretudo as células T $CD4^+$ auxiliam no processo de eliminação do patógenos. Quando essas respostas são insuficientes, tem-se a formação do granuloma e estabelecimento da forma latente da TB. A repressão da progressão da TB primária ou reativação de doença está intimamente relacionada à capacidade do hospedeiro de manter respostas imunológicas apropriadas contra o bacilo. Devido a heterogeneidade de tais respostas, muitas vezes as infecções são desassistidas de sintomas clínicos conspícuos (TB subclínica). No outro polo deste continuum, tem-se a TB ativa (podendo se manifestar nos pulmões ou em outros sítios – TB extrapulmonar). Esta última forma geralmente compreende à TB disseminada e é frequentemente observada em pacientes com avançado grau de imunossupressão e em crianças.
Fonte: (PAI et al, 2016).

1.1.6 **Diagnóstico e tratamento da tuberculose**

O diagnóstico da TB faz-se imprescindível para o controle desta doença e para o melhor manejo do paciente. Entretanto, diversos fatores contribuem para o atraso no diagnóstico oportuno e satisfatório, incluindo sistemas de saúdes com infraestrutura insuficiente, escassez de ferramentas diagnósticas apropriadas e sintomatologia branda em alguns pacientes (STORLA; YIMER; BJUNE, 2008). A ferramenta de escolha para a realização de testes diagnósticos de TB deve levar em consideração o propósito da investigação, seja a detecção da TB latente (ILTB) ou ativa (revisado em PAI; BEHR; DOWDY et al, 2016).

1.1.6.1 Diagnóstico e tratamento da tuberculose latente

O diagnóstico da ILTB é frequentemente realizado através do teste tuberculínico (TST) ou IGRA (do inglês, IFN-γ release assays). O TST (também conhecido como reação de Mantoux) consiste na aplicação intradérmica de proteínas derivadas do bacilo e mensuração da resposta de hipersensibilidade tardia aos antígenos de Mtb. O mecanismo celular que fundamenta o TST é o recrutamento de células T $CD4^+$ previamente sensibilizadas à antígenos de Mtb ao local da inoculação dos antígenos purificados. Embora o TST seja relativamente barato e facilmente aplicável, requisitando mínima infraestrutura laboratorial para sua execução, tal teste é limitado pelo seu baixo poder de discriminar a resposta induzida pela vacinação prévia com BCG e resposta inespecíficas à outras micobactérias (FARHAT et al, 2006). Por sua vez, o IGRA consiste em um teste *in vitro* que mensura a capacidade de linfócitos T de sangue periférico em produzir INF-γ quando estimulados com ESAT-6 e CFP-10. A vantagem do IGRA frente ao TST, é que os antígenos incorporados no ensaio são mais específicos para a Mtb, excluindo assim o efeito confundidor de infecção por outras micobactérias (PAI; ZWERLING; MENZIES, 2008). De maneira geral, ambos testes possuem baixo valor preditivo, possuem reduzida sensibilidade em pacientes imunossuprimidos, além de serem incapazes de distinguir a ILTB de Tb ativa (CASTRO et al, 2010). Em 2018, a organização mundial da saúde considerou fundamental o tratamento da ILTB como uma estratégia de mitigação da TB (WORLD HEALTH ORGANIZATION, 2018). Sobretudo, o tratamento é indicado para grupos que exibem grande risco de progressão para a Tb pulmonar ativa, incluindo pessoas vivendo com HIV, crianças menores de 5 anos em contato com indivíduos com TB ativa. O tratamento recomendado consiste na utilização de isoniazida por 6

ou 9 meses acrescido de rifampicina pelo período de 4 meses (BRASIL; MINISTÉRIO DA SAÚDE; SECRETARIA DE VIGILÂNCIA EM SAÚDE, 2013).

1.1.6.2 Diagnóstico e tratamento da tuberculose ativa

O diagnóstico da TB ativa baseia-se primariamente em 4 tipos de tecnologia: (1) técnicas de imagem (como raio X e tomografia computadorizada), (2) métodos de cultura bacteriana, (3) técnicas de microscopia, e (4) testes moleculares. A radiografia do tórax figura como uma das principais de técnicas de triagem para a TB pulmonar. Dependendo da disponibilidade de recursos, ela pode ser empregada como uma técnica rotineira para a detecção de Tb pulmonar, ou em países com maior vulnerabilidade econômica, o raio X do tórax pode ser utilizado como acompanhamento em indivíduos incapazes de produzir escarro e aqueles que apesar da forte suspeita clínica de TB. A cultura micobacteriana pode ser realizada em meio sólido ou líquido e é considerado o padrão-ouro para o diagnóstico de TB. O crescimento lento em laboratório associado à necessidade de profissionais treinados, infraestrutura laboratorial avançada (incluindo laboratórios de biossegurança nível 3) constituem as principais desvantagens deste método (SHAW; WYNN-WILLIAMS, 1954). A pesquisa de bacilos álcool ácido resistentes (BAAR) por baciloscopia dieta é realizada através da coloração pelo método de Ziehl-Neelsen, constituindo o pum método valioso para o diagnóstico de TB. Além disso, essa metodologia é vantajosa devido ao seu baixo custo e sua grande sensibilidade (em torno de 60%) (DAVIS et al., 2013). Fatores que limitam esta técnica incluem a variabilidade da sensibilidade do teste de acordo com a gravidade da TB e o tempo de coleta das amostras. Além disso, a detecção de Mtb através desta metodologia é dificultada em paciente que vivem com HIV. O advento das técnicas baseadas na amplificação do ácido nucleico nos anos 90 propiciou avanços significativos no controle da TB. O emprego do teste molecular rápido (Gene XPERT) baseado na reação em cadeia da polimerase (ou PCR) é capaz de detectar o DNA do bacilo além de identificar possíveis mutações associadas a resistência a drogas (como a rifampicina). Esta técnica é vantajosa pelo menor tempo associado ao resultado do diagnostico (que acontecem em cerca de 2 horas) (LAWN; NICOL, 2011; DAVIS et al, 2013). O tratamento da TB ativa tem como objetivos principais: a prevenção da morbidade e mortalidade, da emergência de bacilos multirresistentes, assim como a interrupção da cadeia de transmissão. As quatro drogas que são consideradas como agentes de primeira linha para o tratamento da Tb ativa associada a Mtb não resistente a drogas incluem: a rifampicina, pirazinamida, etambutol e isoniazida (BRASIL; MINISTÉRIO DA SAÚDE; SECRETARIA DE VIGILÂNCIA EM SAÚDE, 2013).

1.2 ASPECTOS GERAIS DA CO-INFECÇÃO TB E VÍRUS DA IMUNODEFICIÊNCIA HUMANA

A infecção pelo HIV constitui o principal fator de risco independente para o desenvolvimento da TB ativa (KWAN; ERNST, 2011). Nota-se que indivíduos vivendo com HIV estão aproximadamente 26 vezes mais propensos a desenvolver TB durante o curso de suas vidas (WORLD HEALTH ORGANIZATION, 2017). No ano de 2020, a OMS estimou cerca de 214 mil mortes associadas a coinfecção TB-HIV, representando aproximadamente 25% das mortes atribuídas a infecção pelo HIV (UNAIDS, 2021). Ademais, as taxas de mortalidade atribuídas a tal infecção estão assimetricamente distribuídas ao redor do globo, sendo o continente africano responsável pela concentração de 2/3 da mortalidade atribuída a TB-HIV (WORLD HEALTH ORGANIZATION, 2021). Nota-se que a infecção pelo HIV é capaz de causar mudanças significativas no status imunológico dos pacientes com TB, que se distanciam de um perfil caracterizado pela presença de cavitações para um perfil paucibacilar e com acometimento da TB extrapulmonar (BADRI et al, 2001; MANAS ET AL, 2004).

1.2.1 **O vírus da imunodeficiência humana**

O HIV, agente etiológico da síndrome da imunodeficiência adquirida (AIDS), é um lentivírus membro da família Retroviridae. Os retrovírus estão associados com uma miríade de patologias em vertebrados, sendo a sua quintessência molecular a enzima Transcriptase reversa (TR), responsável pela conversão do RNA viral em DNA durante as etapas subsequentes à entrada do vírus nas células hospedeiras (SIERRA et al, 2005). Sabe-se que o HIV constitui uma população heterógena de vírus zoonóticos que foram transmitidos para seres humanos em múltiplas ocasiões a partir de espécies de primatas não-humanos (HAHN et al, 2000). O HIV é dicotomicamente subdividido nos grupos 1 e 2, que exibem diferentes padrões de distribuição epidemiológica e apresentam distintos graus de patogenicidade em humanos (Sharp et al 2000). O grupo HIV-1 constitui a linhagem de vírus com maior contribuição para a epidemia de AIDS em escala global, ao passo que o HIV-2 é endêmico de regiões da África ocidental. Além disso, o HIV-1 é dividido nos subgrupos M, N, O e P (SHARP et al, 2011; GIOVANETTI et al, 2020). No que diz respeito a morfologia do HIV, sabe-se que este vírus possui aproximadamente 70 a 130 nm em diâmetro, capsídeo com estrutura icosahedral recoberto por um envelope de natureza lipídica e proteínas estruturais espalhadas ao longo de sua superfície (a proteína extracelular gp120 e a transmembrana gp41) (ZHU et al, 2006; ZANETTI et al, 2006; LIU et

al, 2008). Estas últimas proteínas estruturais associam-se na forma de um heterodímero trimêrico que medeia a interação entre o vírus e a célula hospedeira.

O ciclo de replicação do HIV tem início através do estabelecimento de ligação de alta afinidade entre a proteína viral gp120 e o receptor CD4 da célula hospedeira (KWONG et al, 1998; RIZZUTO et al, 1998). O CD4 é uma molécula de aproximadamente 55-KDa encontrada predominantemente na superfície de linfócitos T auxiliares e, em menor grau, em células do compartimento mieloide, tais como monócitos, macrófagos e células dendríticas/ células de Langherans (MORRISON; OFFNER; VANDERNBARK, 1994). Subsequentemente ao engajamento entre gp120 e a molécula de CD4, tem-se uma mudança conformacional no heterodímero com eventual exposição de sítios de ligações adicionais para correceptores presentes nas células (CCR5 e CXCR4). Assim, ocorre a inserção do peptídeo de fusão localizado na gp41 e posterior coalescência das membranas celulares e do envelope viral (WEISSENHORN et al, 1997; BUZON et al, 2010). As próximas etapas incluem o desmantelamento do capsídeo, início da polimerização promovida pela atividade da TR e formação do complexo de pré-integração (CPI) (composto pelo RNA viral, enzimas e proteínas acessórias em intima associação com proteínas do capsídeo e matriz viral). CPI, então, facilita a formação de provírus que será destinado ao núcleo celular, onde será integrado. Uma vez integrado ao genoma do hospedeiro, o provírus será transcrito através da atividade de polimerases de RNA do hospedeiro com auxílio de fatores de alongamento da transcrição, como o P-TEFβ (TAHIROV et al, 2010). Há então produção de moléculas de RNA mensageiro que servirão como molde para a síntese de proteínas virais, após a etapa de exportação nuclear. No citoplasma, ocorre a tradução do RNA mensageiro e as proteínas recém-sintetizadas são incorporadas nas partículas virais nascentes. Após a montagem do vírus, ocorre a etapa de brotamento e extrusão das partículas virais no meio extracelular (VON SCHWEDLER et al, 2003; FISHER et al, 2007).

1.2.2 **Aspectos epidemiológicos e clínicos da Síndrome da imunodeficiência adquirida (AIDS)**

Apesar do advento de ferramentas preventivas e terapêuticas eficazes, a AIDS ainda figura como uma importante questão de saúde pública em escala global. Estima-se que atualmente 38 milhões de pessoas estejam infectadas pelo HIV e que aproximadamente 680 mil pereçam anualmente como consequência desta infecção (UNAIDS, 2021). Atualmente, a África subsaariana, América latina e sudeste asiático concentram a maior parte dos registros de

infecção pelo HIV-1. O HIV é transmitido a partir do contato íntimo com fluidos (sangue, sêmen, fluidos vaginais) de um indivíduo infectado através de práticas sexuais desprotegidas, e em menor proporção via transmissão vertical (de mães para filhos) ou, no passado, via transfusão sanguínea (BAETEN et al, 2003; BOILY et al, 2009).

Faz-se importante ressaltar que é infecção pelo HIV é multifatorial e multifásica, sendo as etapas clínicas da infecção subdivididas em: manifestações agudas (síndrome retroviral aguda), fase de latência clínica e desenvolvimento de AIDS (estágio mais avançado da infecção). A síndrome retroviral aguda é uma manifestação clínica que sucede os eventos iniciais da entrada do vírus no organismo (GURUNATHAN et al, 2009). Ela ocorre em média após certa de 2 a 6 semanas após a exposição e é caracterizada pela ocorrência de sinais clínicos relativamente inespecíficos e autolimitantes, incluindo febre baixa, linfadenopatia, cefaleia, manifestações gastrointestinais, anorexia, faringite não-exsudativa (GURUNATHAN et al, 2009). Em aproximadamente 70 % dos casos, a apresentação clínica ocorre como uma síndrome que se assemelha a mononucleose. Subsequentemente, ocorre o estabelecimento de respostas imunológicas adaptativas que controlam a replicação viral e persistência do HIV em sítios privilegiados, caracterizando assim a fase de latência clínica (GROSSMAN et al, 2006). Com a progressiva destruição de células T $CD4^+$ e gradual elevação dos níveis de inflamação sistêmica e ativação imunológica, o indivíduo infectado entra em um estado de imunossupressão avançada, tornando-se susceptível a ocorrência de doenças oportunistas, caracterizando a fase de AIDS. Os critérios utilizados para o diagnóstico de AIDS incluem contagens de linfócitos T $CD4^+$ inferiores a 200 células/µl ou ocorrência de infecções oportunistas independentemente da contagem de células T $CD4^+$. As doenças oportunistas definidoras da AIDS incluem neurotoxoplasmose, sarcoma de Kaposi, pneumocitose, TB pulmonar e extrapulmonar, candidíase esofágica.

1.2.3 **Efeito da infecção pelo HIV na imunidade contra *Mycobacterium tuberculosis***

A infecção pelo HIV é caracterizada pela depleção de linfócitos T $CD4^+$ e mitigação funcional de componentes importantes das respostas imunológicas frente à patógenos e células neoplásicas (MOIR et al, 2011). Indivíduos com níveis de linfócitos T $CD4^+$ inferiores a certos limiares possuem maior propensão a desenvolver doenças e neoplasias oportunísticas definidoras de AIDS. Sabe-se que o HIV promove a destruição linfocitária através de diversos mecanismos, incluindo efeitos citopatológicos diretos da replicação viral na célula hospedeira,

assim como a morte celular em decorrência da ativação e exaustão celular exacerbada (MOIR et al, 2011).

Diversos estudos apontam a influência da infecção pelo HIV em reduzir as respostas mediadas por células do sistema imune inato contra *Mtb*. Foi demonstrado que macrófagos infectados pelo HIV apresentam menor capacidade de realizar apoptose, além menor capacidade de acidificar os fagolisossomos contendo os bacilos (O'GARRA,2013). Além disso, um estudo conduzido em pacientes HIV^+ com TB disseminada admitidos em um hospital sul-africano revelou altos níveis de ativação de células imune inatas, sobretudo aumento na frequência de monócitos intermediários e produção de citocinas pró-inflamatórias como IL-6 e TNF-α (JANSSEN, 2017). Outras evidências sugerem a capacidade de tal vírus em mitigar as respostas de DCs e consequentemente limitar o estabelecimento de respostas adaptativas contra a *Mtb* (ABRAHEM, 2020).

A redução das respostas imunológicas no contexto de coinfecção TB-HIV associado a hiperativação das células imune facilitam a progressão do HIV e depleção de linfócitos T $CD4^+$ específicos para *Mtb* (BRUCHFIELD; CORREIA-NEVES; KALLENIUS et al, 2015). Geldmacher et al demonstram que macrófagos de pacientes HIV-TB possuem limitada capacidade de secreção de MIP-1β (que se liga ao CCR5), desta maneira reduzindo a capacidade do sistema imune de antagonizar a entrada do vírus (GELDMACHER; NGWENYAMA; SCHUETZ et al, 2010). Um estudo conduzido em modelo experimental de primatas não-humanos demonstrou que o vírus da imunodeficiência Símia (SIV), geneticamente relacionado ao HIV, é capaz de promover a depleção de células T CD4+ especificas para *Mtb* durante os estágios iniciais da infecção do bacilo (aproximadamente 2 semanas pós-infecção). Ademais, este estudo também revelou que as células T CD4 são preferencialmente depletadas nos granulomas, assim sugerindo que retrovírus são capazes de mitigar a das respostas contenção contra TB bem precocemente (FOREMAN et al, 2022). Além disso, outros estudos demonstram que a infecção crônica pelo HIV está associada ao aumento da expressão de marcadores de ativação em células T. Destacam-se as moléculas HLA-DR, sobretudo em células T de memória efetora (KESTENS et al ,1992).

A estimulação antigênica crônica também promove a exaustão dos linfócitos T (um estado de hipfuncionalidade marcado pela perda da capacidade de secretar citocinas e baixo potencial de proliferação), demonstrado pelo aumento na expressão de PD-1 (SHARPE; PAYKEN, 2017). Sabe-se também que a infecção pelo HIV impacta de maneira substancial a respostas de células T $CD8^+$ especificas contra antígenos de Mtb. Por sua vez, estes linfócitos são capazes de secretar grânulos contendo perforina e granzima B que coletivamente estimulam

a apoptose de células-alvo infectadas (TANIUCHI et al, 2018). Sabe-se que o HIV promove alterações substanciais nos perfis de memória imunológica e de polifuncionalidade de células T (DEEKS et al, 2015). Outras células da imunidade adaptativa que tem sua resposta contra Mtb influenciada pela infecção do HIV incluem as células B, células iNKT e células T regulatórias (Figura 7). Por conta da redução na magnitude das respostas imunológicas, a progressão da Tb em indivíduos co-infectados com HIV é substancialmente diferente de suas contrapartes imunocompetentes (ESMAIL et al, 2018).

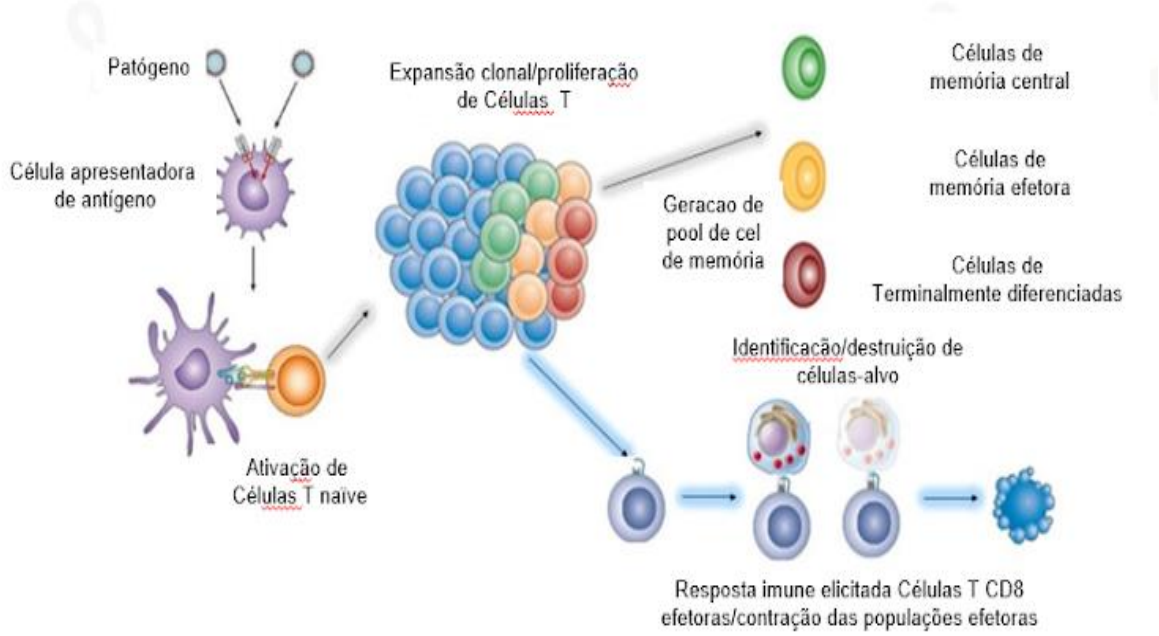

Figura 7 – Processo de ativação de células T. Células T são fundamentais para o estabelecimento de respostas protetoras contra diversos patógenos. Células apresentadoras de antígenos são responsáveis pelo reconhecimento e concatenação da informação acerca de organismos invasores. Células T naïve reconhecem epítopos patogênicos presentes nos MHC-II de APCs. Os eventos que sucedem este reconhecimento são caracterizados pelo profundo remodelamento sinalizatório e da arquitetura epigenética das células T. Elas então adquirem grande capacidade proliferativa (evidenciado pela expressão de marcadores como Ki-67), diferenciam-se em células efetoras e migram para o sítio infeccioso a fim de eliminar a ameaça. Células T CD4 são capazes de se diferenciar em subtipos de células auxiliares responsáveis pela produção de conjuntos de citocinas relacionadas a perfis de resposta imunológica específicos (ex: Th1 e Th2). Já as Células T $CD8^+$ são capazes de liberar grânulos contendo Granzima B e perforina que estimula a apoptose de células infectadas. Posteriormente, os linfócitos T passam por um processo de contração populacional. Entretanto, uma fração destas células permanece como células de memória, dotadas da capacidade de responder mais robustamente frente a um reencontro com seu antígeno cognato.
Fonte: adaptado de (BEVAN, 2004).

1.3 ASPECTOS GERAIS DA SÍNDROME INFLAMATÓRIA DA RECONSTITUIÇÃO IMUNE ASSOCIADA A TB

1.3.1 **Caracterização da Síndrome Inflamatória da reconstituição Imune**

O advento da terapia antirretroviral (TARV) reduziu significativamente as taxas de morbimortalidade associadas à infecção pelo HIV, uma vez que tal terapia promove a

restauração da imunidade concomitante à supressão viral. Desta forma, estes pacientes que exibem alto grau de linfopenia crônica e elevada susceptibilidade a infecções oportunistas são beneficiados pela restauração parcial da imunidade. Entretanto, em uma parcela destes indivíduos, o início do TARV e reconstituição numérica e funcional das células T CD4+ estão associados ao desenvolvimento da síndrome inflamatória da reconstituição imune (SIRI).

A SIRI é caracterizada como a deterioração clínica associada a respostas inflamatórias exacerbadas direcionadas contra patógenos oportunistas, apesar do eficiente controle da viremia e aumento significativo dos linfócitos T $CD4^{+.}$ A *Mtb* figura como umas das principais patógenos oportunistas associadas a SIRI. Outros agentes etiológicos frequentemente associados a manifestação de SIRI incluem *Cryptococcus neoformans*, membros do complexo *M. avium*, citomegalovírus, *Toxoplasma gondii, Pneumocystis jirovecci.*

A SIRI associada à TB pode ser dicotomicamente classificada em paradoxal e "desmascarada". A SIRI paradoxal é caracterizada pela deterioração clínica de um paciente infectado HIV-1 previamente diagnosticado com TB. Estes pacientes recebem tratamento anti-tubercular, obtendo boas respostas do quadro clínico. Aproximadamente 2 a 4 semanas após o início do TARV, estes indivíduos apresentam agravamento dos sintomas associados a TB. A SIRI "desmascarada" ocorre quando os pacientes não previamente diagnosticados com TB e consequentemente não estão sob o tratamento antitubercular no início do TARV.

1.3.2 **Aspectos epidemiológicos e fatores de risco**

A incidência da TB-SIRI está intimamente associada ao cenário epidemiológico da TB, e estima-se que 8 a 54% dos pacientes desenvolvam SIRI nos primeiras semanas após a introdução do TARV (Narita et al,1998; Narendran et al 2013; Muller et al 2010).Sabe-se que o desenvolvimento da SIRI é multifatorial, entretanto a maior parte dos estudos na literatura consideram os seguintes fatores como os mais relevantes para a manifestação da SIRI: (1) intensa depleção de células T CD4+ previamente ao início do tratamento (inferior a 100 células/μL), (2) curto intervalo de tempo entre o início do tratamento ATT e TARV e (3) carga viral elevada (Naidoo et al, 2012; Valin et al, 2010). Estes fatores são de certo modo intrinsicamente vinculado com apresentação tardia de pacientes diagnosticados com HIV em estágios avançados da infecção. Outros fatores de risco para SIRI incluem o grau de disseminação do patógeno e predisposição genética (presença dos alelos *TNFA-308*1* e *IL6-174*G*). A SIRI associada à TB exibe um amplo espectro de manifestações clinicas que dependem substancialmente do sitio de infecção da *Mtb*. Os principais sintomas incluem febre,

suores noturnos, linfadenopatia, piora do quadro respiratório (tosse e dispneia) e agravamento de infiltrado nos pulmões (Meintjes et al, 2012). O tempo médio dos episódios de SIRI é de 14 dias (Meintjes et al, 2012), com registros de manifestações precoces (7 dias após o início da TARV).

1.3.3 **Imunopatogênese da SIRI associada à TB**

Diversos estudos destacam o papel da expansão de células T $CD4^+$ mediante a remoção de estímulos deletérios como um dos principais fatores que influenciam a SIRI. Entanto, as células da imunidade inata estão entre as principais células que contribuem para a exacerbação do processo inflamatório neste cenário. Sabe-se que as células do compartimento mieloide (como monócitos e macrófagos) requisitam múltiplos sinais para sua completa ativação e consequente aquisição de funções efetoras (GREENE et al, 2021). Comumente, um destes sinais é fornecido pelo reconhecimento de produtos do *Mtb* por receptores de padrão molecular presentes na superfície das células mieloides. Entre estes receptores, destacam-se o *toll-like receptors* (TLRs), uma família importante de receptores lectina do tipo C, induz a atividade biológicas de fatores de transcrição relacionados com a indução respostas pro-inflamatórias. Desta maneira, a célula que albergando bacilos previamente reconhecidos submetem-se a um remodelamento parcial de seu perfil transcricional e epigenético. Diz-se que a célula em questão foi "primada".

De maneira concomitante a este processo, o bacilo presente no interior de fagossomos, consequência do processo de fagocitose, coalesce com os lisossomos, organelas ricas em conteúdo ácido, capaz de degradar patógenos ocorrendo então a formação do fagolisossmo. Sabe-se que porções do patógeno degradado são processados e translocados para o complexo principal de histocompatibilidade (MCH), plataformas moleculares relacionadas com a apresentação de antígenos para as células da imunidade adaptativa. Mediante ao evento de apresentação de antígeno para linfócitos T com receptores TCR cognatos para o antígeno, tem-se a liberação do segundo sinal responsável pela complementação da ativação destas células. Tipicamente, os linfócitos T CD4+ são responsáveis pela liberação de interferon-γ para as células infectadas com MTB. Por sua vez, o IFNY age permitindo a síntese e liberação de citocinas pró-inflamatórias como TNF-α e IL6 que elicitam programas de destruição dos bacilos.

Em contexto de depleção acentuada dos linfócitos T CD4+, os bacilos são capazes de replicar eficientemente na ausência de sinais que complementam a ativação de suas células

hospedeiras. Há então um acúmulo de células parcialmente ativadas nestes hospedeiros. A supressão viral mediada pelo TARV promove então a reconstituição das populações de células T CD4+ especificas para os antígenos bacilares. Desta forma, estas células são capazes de fornecer os sinais adicionais para a ativação completa das células fagocitarias, caracterizando um cenário de hiperresponsividade aos antígenos de *Mtb* e consequente produção exacerbada de mediadores inflamatórios e dano tecidual considerável.

1.3.4 **Diagnóstico e tratamento da SIRI**

O diagnóstico de SIRI é limitado devido a escassez de ferramentas ou biomarcadores eficientes com grau de validação, sobretudo em países de recursos tecnológicos limitados. Uma vez que o grau de imunossupressão também impacta significativamente a manifestação de SIRI, a apresentação tardia também está associada com uma maior dificuldade de diagnóstico de SIRI. No ensejo de diagnóstico de SIRI, as manifestações clínicas observadas devem ser distinguidas dos efeitos adversos provocados pela TARV ou tratamento antituberculár, além de possíveis interações medicamentosas. Desta maneira, a SIRI é diagnosticada principalmente através de critério clínicos e de exclusão. Trabalho seminal conduzido por French e colaboradores (2004) definiu o principal critério diagnostico de SIRI qualquer manifestação atípica associada a uma infecção oportunista acompanhada pelo decréscimo de, no mínimo, 1 $\log_{10}$ cópias de RNA viral no plasma após o início do tratamento. Critérios secundários propostos pelos autores incluíam aumento quantitativo dos linfócitos T CD4 e resposta imunológica contra o patógeno em questão. Posteriormente, esta definição foi estendida levando em consideração achados de deterioração radiológicas. O tratamento da SIRI é realizado através da administração de corticoides e anti-inflamatórios não esteróides (MEINTJES et al, 2018). Um trabalho conduzido por Meintjes e colaboradores demonstrou que a administração de predsiona em uma dose de 1,5kg/kg/dia estava associada a redução da mortalidade em pacientes com SIRI moderada (MEINTJES et al, 2018). Comumente, casos leves não são acompanhados de intervenções medicamentosas, uma vez que seus sintomas são auto-limitantes.

2 **JUSTIFICATIVA**

Nas últimas décadas, avanços no entendimento da imunopatogênese da infecção pelo HIV-1 possibilitaram o advento de opções terapêuticas mais eficazes associadas com a diminuição das taxas de mortalidade e morbidade, permitindo assim um melhor manejo de pessoas vivendo com HIV (PVH). Além disso, a introdução da TARV reduziu de forma drástica a ocorrência de infecções oportunistas, como a infecção pelo *Mtb*. Entretanto, devido a fatores vinculados à baixa cobertura da TARV em certas regiões do planeta e por dificuldade inerentes à escassez de ferramentas eficazes no diagnóstico de TB em PVH, tal patologia ainda figura como a principal causa de morte neste grupo de indivíduos. Ademais, em uma fração de pacientes virgens de tratamento, o início da TARV está associado com surgimento paradoxal da síndrome inflamatória da reconstituição imune através de mecanismos imunopatológicos ainda pouco esclarecidos. Apesar do amplo conhecimento acerca dos fatores de risco, tais como alta carga viral pré-TARV, estado avançado de imunossupressão relacionado com acentuada linfocitopenia de células T $CD4^+$, assim como curto intervalo de tempo entre o início da terapia antituberculár e a TARV, métodos prognósticos e/ou diagnósticos de SIRI ainda são consideravelmente incipientes.

Sabe-se que a imunopatogênese da SIRI é intrinsecamente vinculada à uma resposta imunológica exacerbada disparada por células do compartimento mieloide contra antígenos de *Mtb* frente à reconstituição da população de linfócitos T $CD4^+$ e concomitante supressão do HIV (Quinn et al, 2020). Mahnke e colaboradores (2012) evidenciaram a expansão de subpopulações polifuncionais de células T $CD4^+$ especificas para antígenos de *Mtb* durante a desenvolvimento da SIRI. Além disso, Barber e colaboradores (2010) demonstraram, em um modelo experimental murino de SIRI associada a infecção por *Mycobacterium avium*, que a propagação de células T $CD4^+$ Th1 produtoras INF-γ está intimamente correlacionada com alterações funcionais de células mieloides localizadas na circulação e em tecidos. Considera-se que a completa ativação de células inatas mediada pelo IFN-γ proveniente da reconstituição linfocitária acarreta a produção excessiva de mediadores solúveis, culminando em um processo inflamatório sistêmico e decorrente dano tecidual. Deste modo, evidencia-se a importância das respostas imunológicas mediadas por linfócitos contra antígenos micobacterianos no cerne da imunopatogênese da SIRI.

Considerando o alto grau de heterogeneidade fenotípica e funcional das populações de linfócitos e que a coinfecção HIV/*Mtb* altera diversos processos da homeostase imunológica e metabólicas, investigamos neste trabalho a relevância da dinâmica de ativação imune assim

como o estabelecimento de memória imunológica no desenvolvimento da SIRI associada à TB e o potencial destas populações celulares como biomarcadores de SIRI. Consideramos conveniente, então, subdividir tal trabalho em duas partes que contemplam as principais abordagens do estudo: (1) a prospecção de biomarcadores para o prognóstico/diagnóstico de SIRI através da aplicação de técnicas multi-ômicas e (2) investigação do processo de ativação e perfil de memória de linfócitos T $CD4^+$ e $CD8^+$ no desenvolvimento da SIRI.

3 **PARTE 1**

3.1 HIPÓTESE

Pacientes HIV-1^{+} que desenvolvem SIRI associada à TB apresentam persistente perturbações metabólicas a nível sistêmico correlacionadas com o perfil inflamatório e alterações transcricionais em diferentes estágios pré- e pós- início do tratamento.

3.2 OBJETIVOS

3.2.1 **Objetivo geral**

Caracterizar longitudinal dos perfis metabolômico, inflamatório e transcricional de indivíduos HIV/TB durante o início do tratamento e correlacionar com o risco de SIRI.

3.2.2 **Objetivos específicos**

- Determinar a abundância de metabólitos plasmáticos da população de estudo através de cromatografia líquida de ultra-alta performance acoplada à espectrometria de massa;
- Quantificar as concentrações de moléculas inflamatórias presente na circulação da população de estudo através de ensaios multiplex de eletroquimioluminescência;
- Caracterizar o perfil de transacional do sangue total dos pacientes arrolados no estudo;
- Correlacionar os níveis plasmáticos de metabolitos em indivíduos que desenvolveram SIRI com os níveis de moléculas inflamatórias e expressão gênica;
- Avaliar o potencial dos metabólitos diferencialmente expressos (MDEs) em predizer e/ou diagnosticar SIRI associada à infecção por micobactérias ou por outros patógenos na população de estudo.

3.3 MANUSCRITO I

PLASMA METABOLOMICS REVEALS DYSREGULATED METABOLIC SIGNATURES IN HIV-ASSOCIATED IMMUNE RECONSTITUTION INFLAMMATORY SYNDROME

Este estudo examinou os perfis metabolômico, inflamatório e transcricional do plasma de indivíduos HIV-1 antes e depois da introdução da TARV, a sua correlação com o desenvolvimento de SIRI, assim como avaliou o potencial destas moléculas como biomarcadores de predição e diagnóstico da SIRI.

Resumo:
A síndrome inflamatória da reconstituição imune (SIRI) associada a tuberculose está associada com um elevado grau de perturbação no status metabólico do hospedeiro. No presente estudo, observamos que indivíduos que desenvolveram a SIRI apresentaram diferenças na abundância de lipídeos e amino ácidos nos estágios pré e pós TARV. Desta maneira, evidenciou-se uma associação biológica entre o estresse oxidativo, via de metabolismo do triptofano e vias de sinalização mediadas por lipídios no contexto de imunopatogênese da SIRI. Ademais, detectamos correlações estatisticamente significantes entre as vias de metabolismo de lipídios e aminoácidos com os níveis de citocinas pró-inflamatórias IL-12p70 e IL-8 no momento de deflagração da SIRI, evidenciando assim uma relação recíproca entre a ativação imune e metabolismo celular. A aplicação de ferramenta de aprendizado de máquinas, tais como arvore de decisão e analise de componente principal, permitiu a identificação e avaliação do potencial prognóstico/diagnóstico dos metabolitos plasmáticos na população estudada. Nossos achados notabilizam os impactos das alterações imunometabólicas em pacientes HIV^+ na imunopatogênese da SIRI e na exacerbação de manifestações inflamatórias e da ativação imune.

Este artigo foi publicado no periódico internacional *Frontiers in immunology* (Fator de impacto = 7.5)

Publicado em 21 de junho de 2021, doi: 10.3389/fimmu.2021.693074

frontiers in Immunology

ORIGINAL RESEARCH
published: 15 June 2021
doi: 10.3389/fimmu.2021.693074

Plasma Metabolomics Reveals Dysregulated Metabolic Signatures in HIV-Associated Immune Reconstitution Inflammatory Syndrome

Luxin Pei[1,2†], Kiyoshi F. Fukutani[3,4,5†], Rafael Tibúrcio[3,4,6], Adam Rupert[7], Eric W. Dahlstrom[8], Frances Galindo[1], Elizabeth Laidlaw[1], Andrea Lisco[1], Maura Manion[1], Bruno B. Andrade[3,4,5,6,9,10‡] and Irini Sereti[1*‡]*

[1] Laboratory of Immunoregulation, National Institute of Allergy and Infectious Diseases (NIAID), National Institutes of Health (NIH), Bethesda, MD, United States, [2] Department of Biology, Johns Hopkins University, Baltimore, MD, United States, [3] Multinational Organization Network Sponsoring Translational and Epidemiological Research (MONSTER) Initiative, Salvador, Brazil, [4] Laboratory of Inflammation and Biomarkers, Gonçalo Moniz Institute, Oswaldo Cruz Foundation, Salvador, Brazil, [5] Curso de Medicina, Centro Universitário Faculdade de Tecnologia e Ciências (UniFTC), Salvador, Brazil, [6] Faculdade de Medicina, Universidade Federal da Bahia, Salvador, Brazil, [7] Leidos Biomedical Research Inc., Frederick National Laboratory for Cancer Research, Frederick, MD, United States, [8] Rocky Mountain Laboratories, National Institute of Allergy and Infectious Diseases (NIAID), National Institutes of Health (NIH), Hamilton, MT, United States, [9] Wellcome Centre for Infectious Disease Research in Africa, Institute of Infectious Disease and Molecular Medicine, University of Cape Town, Cape Town, South Africa, [10] Division of Infectious Diseases, Department of Medicine, Vanderbilt University School of Medicine, Nashville, TN, United States

Immune reconstitution inflammatory syndrome (IRIS) is an inflammatory complication associated with an underlying opportunistic infection that can be observed in HIV-infected individuals shortly after the initiation of antiretroviral therapy, despite successful suppression of HIV viral load and $CD4^+$ T cell recovery. Better understanding of IRIS pathogenesis would allow for targeted prevention and therapeutic approaches. In this study, we sought to evaluate the metabolic perturbations in IRIS across longitudinal time points using an unbiased plasma metabolomics approach as well as integrated analyses to include plasma inflammatory biomarker profile and whole blood transcriptome. We found that many lipid and amino acid metabolites differentiated IRIS from non-IRIS conditions prior to antiretroviral therapy and during the IRIS event, implicating the association between oxidative stress, tryptophan pathway, and lipid mediated signaling and the development of IRIS. Lipid and amino acid metabolic pathways also significantly correlated with inflammatory biomarkers such as IL-12p70 and IL-8 at the IRIS event, indicating the role of cellular metabolism on cell type specific immune activation during the IRIS episode and in turn the impact of immune activation on cellular metabolism. In conclusion, we defined the metabolic profile of IRIS and revealed that perturbations in metabolism may predispose HIV-infected individuals to IRIS development and contribute

OPEN ACCESS

Edited by:
Jean-Pierre Routy, McGill University, Canada

Reviewed by:
Julien Van Grevenynghe, Université du Québec, Canada
Rachel Lai, Imperial College London, United Kingdom
Pierre Corbeau, Université de Montpellier, France

***Correspondence:**
Bruno B. Andrade
bruno.andrade@fiocruz.br
Irini Sereti
isereti@niaid.nih.gov

†These authors have contributed equally to this work

‡These authors have contributed equally to this work

Specialty section:
This article was submitted to Inflammation, a section of the journal Frontiers in Immunology

Received: *09 April 2021*
Accepted: *27 May 2021*
Published: *15 June 2021*

Citation:
Pei L, Fukutani KF, Tibúrcio R, Rupert A, Dahlstrom EW, Galindo F, Laidlaw E, Lisco A, Manion M, Andrade BB and Sereti I (2021) Plasma Metabolomics Reveals Dysregulated Metabolic Signatures in HIV-Associated Immune Reconstitution Inflammatory Syndrome. Front. Immunol. 12:693074. doi: 10.3389/fimmu.2021.693074

to the inflammatory manifestations during the IRIS event. Furthermore, our findings expanded our current understanding IRIS pathogenesis and highlighted the significance of lipid and amino acid metabolism in inflammatory complications.

Keywords: immune reconstitution inflammatory syndrome (IRIS), cell metabolism, metabolomics, immune activation, HIV

INTRODUCTION

Antiretroviral therapy (ART) effectively controls HIV viral replication and leads to the restoration of immune function, which has greatly improved the life expectancy of people living with HIV (PWH). Growing evidence suggests that a fraction of HIV-infected patients, however, can still develop severe inflammatory complications and experience clinical deterioration within the first few weeks following the initiation of ART despite successful suppression of HIV viral load and recovery of $CD4^+$ T cells (1). This condition, termed immune reconstitution inflammatory syndrome (IRIS), presents with clinical manifestations such as worsening lymphadenopathy, fever, malaise, and worsening pulmonary infiltrates even with microbiologic control of the underlying co-infection. Notably, mycobacterial co-infections, such as *Mycobacterium tuberculosis* (TB) and *Mycobacterium avium* complex (MAC), are frequently associated with IRIS that can lead to higher morbidity and mortality rates (2–5). The incidence of IRIS can vary from <5% to as high as 50% and is dependent on several risk factors including severe lymphopenia prior to starting ART as well as disseminated infection with high antigen load (6). Current management for IRIS involves clinical observation, drainage of inflammatory collections, use of non-steroid anti-inflammatory drugs (NSAIDs), or use of corticosteroids for either prevention or treatment in high-risk TB patients (5, 7, 8).

A comprehensive understanding of IRIS is evolving, and it is now well appreciated that IRIS pathogenesis is characterized by dysregulated host innate and adaptive immune responses to the underlying co-infection. More specifically, IRIS is associated with hyperactivation of polyfunctional antigen-specific $CD4^+$ T cells resulting in exaggerated production of pro-inflammatory cytokines such as TNF and IFN-γ (3, 9–14). Additionally, patients who develop IRIS display monocyte activation with increased production of pro-inflammatory cytokines along with altered gene expression profile both prior to ART initiation and during the IRIS event (6, 15). Elevated levels of soluble plasma biomarkers, cytokines, and chemokines associated with both adaptive and innate immune activation have also been described in IRIS including IL-6, IL-8, granulocyte-macrophage colony-stimulating factor (GM-CSF), sCD14 and the afore mentioned TNF and IFN-γ (3, 6, 16–18). IL-6, IL-8, GM-CSF, and sCD14 are of innate immune origins reflecting pathogen activation of monocytes and macrophages (6, 16, 18). Chemokine IL-8 is also responsible for neutrophil recruitment to sites of inflammation (16). The increased levels of IFN-γ and TNF indicate a T-helper 1 bias in IRIS T cell responses. Furthermore, the role of pro-inflammatory cytokines in mediating IRIS pathogenesis is elucidated through blockade or ablation of IFN-γ, TNF, and IL-6 in a MAC-IRIS murine model as well as in IRIS patients who are refractory to steroid treatment (10, 11, 19). Such robust systemic inflammation observed in IRIS may be reflected in substantial immunometabolic shifts (5). Indeed, IRIS was recently linked with higher metabolic activity monitored by nuclear imaging technique ^{18}F-fluorodeoxyglucose positron emission tomography (FDG-PET). FDG-PET results showed higher total glycolytic activity and standardized uptake values in IRIS patients, which was also supported by increased expression of glucose transporter 1 (GLUT-1) on both $CD4^+$ T cells and $CD14^+$ monocytes (20).

A large number of studies underscores the importance of intracellular metabolism for the maintenance of both T cell and monocyte functions, since immune cells must cope with different catabolic and anabolic demands in response to antigen activation and other inflammatory stimuli. In particular, metabolic reprogramming characterized by glycolytic shift and increased mitochondria function greatly contributes to T cell effector function and macrophage activation (21–28). Therefore, the identification of immunometabolic requirements as well as dysfunctional metabolic pathways may further unravel the nuances surrounding IRIS pathogenesis.

The application of metabolomics offers an untargeted global approach for the identification of distinct metabolic signatures. Metabolomics studies have demonstrated that immune activation associated with mycobacterial infections or autoimmune conditions substantially change the metabolic state of the immune system, which, in turn, could also affect the host response to the pathogen (29–34). To comprehend how metabolic disturbances contribute to IRIS development and progression, we devised an unbiased plasma metabolomics approach to identify altered metabolite composition at longitudinal time points in PWH who developed IRIS compared to those who did not upon ART commencement. Our findings suggested alterations of the metabolic profile in IRIS patients mainly occurred before the initiation of ART and during the IRIS event with perturbed lipid and amino acid metabolism that further correlated with plasma inflammatory biomarkers.

MATERIALS AND METHODS

Study Design and Patient Cohort

HIV infected ART-naïve patients with $CD4^+$ T cell count <100 cells/μL were enrolled in a prospective observational study at the National Institutes of Health [PET Imaging and lymph node assessment of IRIS in persons with AIDS (PANDORA)

NCT02147405]. The study was approved by the ethics committee and all participants signed informed consent prior to any study procedures. ART was started within 2 weeks of study enrollment following standard treatment guidelines. IRIS was diagnosed based on the AIDS Clinical Trials Group IRIS definition criteria including $CD4^+$ T-cell count increased by ≥50 cells/μl or >two-fold from pre-ART levels and/or HIV plasma RNA reduced by >0.5 $\log_{10}$ copies/mL, and patient experienced signs and symptoms of inflammatory conditions attributed to a specific pathogen or condition that were not consistent with the development of a new infection, predicted clinical course of a pre-existing infection, or side effects of ART (4).

Metabolomics

Cryopreserved plasma samples from 13 IRIS and 17 non-IRIS HIV-infected patients at the pre-ART, 1-2 months, and 12 months after ART initiation time points were collected. Non-targeted metabolomics analysis was performed at Metabolon, Inc using previously published method (35). Briefly, plasma samples underwent methanol extraction, and the resulting extract was used for metabolite analysis by ultra-high-performance liquid chromatography/tandem mass spectrometry in both positive and negative ion modes along with gas chromatography/mass spectrometry to maximize compound detection and accuracy. Metabolites were then identified by comparing the spectral signature of sample metabolites to a reference library at Metabolon, Inc. Spectral peaks were used for metabolite identification by a proprietary visualization and interpretation software. Area under the curve for the spectral peaks was used for metabolite quantification. Raw data generated from peak quantification were then normalized to correct for variation in multi-day experiments, where each compound was normalized to a median equal to one. The raw values after normalization are included in **Supplementary Table 1**.

Plasma Biomarker Measurements

Concentrations of inflammatory biomarkers, including soluble PD-1, soluble CD14, IL-6r, MCP1, GMCSF, TNF, IL-8, IL-6, IL-2, IL-1β, IL-12p70, IL-10, IFN-γ, and MPO, were measured in cryopreserved plasma samples at the pre-ART and month 1 time points using a custom Meso Scale Discovery electrochemiluminescence multiarray kit following manufacturer recommendations. D-dimer was measured by an enzyme-linked fluorescent assay on a VIDAS instrument (bioMérieux, Durham, North Carolina).

Statistical Methods

Comparisons of patients' baseline characteristics between the IRIS, non-IRIS, and mycobacterial-IRIS groups were performed using the nonparametric Mann-Whitney *U* test. Frequencies of female sex and race were assessed using Chi-square test. BMI at the pre-ART, month 1, and month 12 time points were compared using the Wilcoxon signed rank test.

Differentially expressed metabolites (DEMs) were determined by multiple t-tests in a $\log_2$ transformed matrix comparing individual metabolite levels of IRIS and non-IRIS patients. FDR correction was not made for the identification of DEMs given the exploratory nature of the study. Venn diagram was used to visualize unique and shared differentially expressed metabolites. Hierarchical cluster analysis was performed using the Ward's method (with 100X bootstrap), and principal component analysis (PCA) was performed using JMP Statistical Discovery PRO (Version 13). Decision trees were employed to identify a minimal set of markers allowing separation between IRIS from non-IRIS, and mycobacterial IRIS and other types of IRIS using J48 algorithm implemented in the WEKA program (Waikato Environment for Knowledge Analysis, version 3.6.11, University of Waikato, New Zealand) (36). In order to estimate the classification accuracy of decision tree models, we performed the sensitivity and specificity measurement using the receiver–operating characteristic curve (ROC) in JMP Statistical Discovery PRO (Version 13).

Co-expression module analysis for metabolic pathways was executed using the CEMiTool package (37). This package computes and identifies modules based on co-expressed/regulated pathways that were altered in a specific sample group. Module pathways were annotated based on reference library provided by Metabolon Inc. The file was in a *.gmt set and the enrichment values of each patient was used in correlation plots. The correlation profiles between metabolic pathways and plasma biomarkers at different time points were examined using Spearman correlation matrices. Only statistically significant correlations (p-values < 0.05 with r values above 0.7 and below -0.7) were included in the network visualization. Circos plots were used to illustrate the networks as previously reported (38).

RNA Extraction and Library Preparation

Whole blood samples from the pre-ART, month 1, and month 12 post-ART longitudinal time points were collected and sequenced in 2 batches indicated in **Supplementary Table 1**. All whole blood samples were extracted using the PAXgene 96 Blood RNA Kit (Qiagen, Valencia, CA) following manufacturer's instructions. RNA quality was assessed using 2100 Bioanalyzer RNA Pico 6000 kit (Agilent Technologies, Santa Clara, CA). Following total RNA extraction, each sample was subjected to purification steps using Agencourt RNAClean XP beads and Globin Removal Mix and instructions provided in the TruSeq Stranded Total RNA Sample Preparation Guide (Illumina, Guide, Part# 15021048, Rev E).

For the first set of samples, the TruSeq Stranded Total RNA Sample Preparation Kit was used to prepare sequencing libraries exactly as specified in the manufacturer's recommended procedure followed by the usage of the RNA Adapter Plate for dual indexing (Illumina, Guide, Part# 15021048, Rev. E). The final libraries were assessed on the 2100 Bioanalyzer using the DNA 1000 chip (Agilent Technologies) and quantified using the Kapa Quantification Kit for Illumina Sequencing (Kapa Biosystems, Boston, MA) on the CFX384 Real-Time PCR Detection System (Bio-Rad Laboratories, Inc, Hercules, CA). Libraries were then prepared for clustering to the flow cell. On-board cluster generation and paired-end 76 base pair sequencing were completed on the NextSeq550 (Ilumina, Inc, San Diego, CA) using a High Output 150 cycle reagent kit. Three more NextSeq runs were completed to increase the mapping

density. For the second set of samples, the TruSeq Stranded mRNA Sample Preparation Kit was used to prepare sequencing libraries exactly as specified in the manufacturer's recommended procedure followed by the usage of the RNA Adapter Plate for dual indexing (Illumina, Guide, Part# 15031047, Rev. E). The final libraries were assessed on the 2100 Bioanalyzer using the DNA 1000 chip (Agilent Technologies). The fragment size distribution of the libraries was within the manufacturer's specifications. TruSeq libraries were quantified on the CFX96 Touch real-time PCR instrument (BioRad, Hercules, CA) using the Kapa Library Quant Universal qPCR mix and kit instructions (Kapa Biosystems, Wilmington, MA). All samples were individually sized and normalized to a 2nM concentration. Samples were combined in equimolar ratios to create a single pool, titrated to 9pM, and sequenced as 2 x 93 bp reads on the HiSeq 2500 instrument using the HiSeq Rapid SBS 200 cycle kit, according to the manufacturer's recommended procedure (Illumina, San Diego, CA). A total of four Rapid runs were performed to increase the mapping coverage. Targets from the two batches were mapped and identified by ENSG. Batch correction was performed using ComBat-seq (https://github.com/zhangyuqing/ComBat-seq) from the sva package to minimize experimental variance prior to subsequent analysis.

Multi-Omics Factor Analysis (MOFA)

Multi-omics factor analysis (MOFA) is a computation method that provides the characterization and visualization of multi-layered biological processes to analyze the heterogeneity between IRIS and non-IRIS conditions (39–42). In total, 8 IRIS and 12 non-IRIS patients at the pre-ART and month 1 time points with paired metabolome, transcriptome, and concentration of plasma biomarker measurements were included in the analysis. The MOFA model was employed to integrate the omics data with a series of parameters including only paired samples in all datasets, selection of factors with the removal of zero variance, and factor tolerance to establish an exploratory model (tolerance = 1). The mixture of variables with similar variance was represented as latent factors based on an unsupervised factor analysis. The MOFA model is able to automatically determine Gaussian and Poisson distributions. All pipelines and analysis are available in http://www.bioconductor.org/packages/devel/bioc/html/MOFA.html.

RESULTS

Patient Characteristics

Thirty HIV-infected ART naïve patients (22 males, 8 females) were identified in the study cohort with a median age of 37 years [interquartile range (IQR), 34-41]. Baseline demographic and clinical characteristics are shown in **Table 1**. The sex proportion was comparable and not significantly different between IRIS (female 23%) and non-IRIS (female 29%) groups (*p*-value=0.697). Prior to ART initiation, the median $CD4^+$ T cell count of all patients was 19 cells/μL (IQR, 9-42), and plasma HIV-RNA was 5.3 log_{10} copies/mL (IQR, 4.9-5.8). Thirteen patients were diagnosed with IRIS as previously described (20) with a median time between ART initiation and onset of IRIS of 30 days (IQR, 27.5-36). There were no statistically significant differences in demographics and clinical characteristics between the IRIS and non-IRIS patients. The detailed descriptions of IRIS types, co-infections, IRIS onset date, and treatment are listed in **Supplementary Table 1**. Among the 13 IRIS patients, seven were diagnosed with mycobacterial IRIS (TB or MAC). Other types of IRIS included cryptococcal, Kaposi's sarcoma, and progressive multifocal leukoencephalopathy IRIS (**Supplementary Table 1**). All patients had significant $CD4^+$ T cell count recovery as well as HIV-RNA viral load suppression after the initiation of ART (**Supplementary Figures 1A, B**). A significant increase in BMI was also observed in all patients after ART at the month 1 and month 12 time points ($p<0.001$) (**Supplementary Figure 1C**).

The Plasma Metabolite Composition Is Different Between IRIS and Non-IRIS Groups

In order to understand the major metabolic alterations associated with IRIS development, we performed an untargeted metabolomics profiling that identified over 800 metabolites in all plasma samples from a library of over 5000 metabolites composed of amino acids, peptides, carbohydrates, lipids, energy molecules, nucleotides, cofactors and vitamins, and xenobiotics. First, we sought to investigate global differences in the metabolome of patients who developed IRIS compared to those who did not at each study time point. By using a threshold of $p<0.05$, 68 differentially expressed metabolites (DEMs) were identified at the pre-ART time point (**Figure 1A**). After 1 month of ART initiation or during the IRIS event, 69 DEMs were

TABLE 1 | Baseline Demographic and Clinical Characteristics of Study Participants.

	All Patients (n = 30)	Non-IRIS (n = 17)	IRIS (n = 13)	*P*-value IRIS *vs*. Non-IRIS
Age, years median (IQR)	37 (34-41)	36 (35-41)	37 (33-43)	0.812
Female sex, No. (%)	8 (27)	5 (29)	3 (23)	0.697
Race,				
White	1	0	1	
African American	14	8	6	
Hispanic	14	8	6	
Asian	1	1	0	
BMI, kg/m^2, median (IQR)	22.7 (19.4-24.6)	22.7 (18.6-24.8)	22.7 (19.5-24.3)	0.613
$CD4^+$ T cell/μL, median (IQR)	19 (9-42)	17 (7-32)	26 (11-44)	0.502
HIV RNA, log_{10} copies/mL, median (IQR)	5.3 (4.9-5.8)	5 (4.5-5.6)	5.7 (5.1-6)	0.053

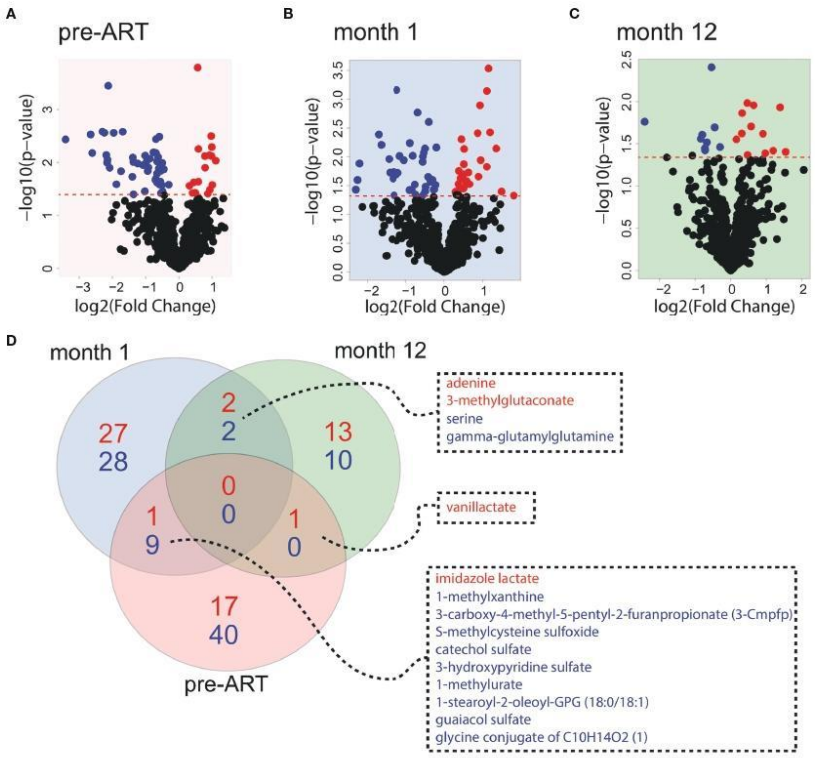

FIGURE 1 | Global metabolite expression comparing IRIS with non-IRIS patients. Volcano plots depicting differences in metabolite levels between IRIS and non-IRIS patients are shown for the pre-ART **(A)**, month 1 **(B)**, and month 12 **(C)** post-ART time points. The significance threshold (p-value=0.05) is indicated by the red dashed line. Metabolites above the significance threshold are defined as the differentially expressed metabolites (DEMs). Each point represents an identified metabolite that is significantly upregulated (red) or downregulated (blue) in the IRIS group. **(D)** Venn diagram illustrating the numbers of differentially expressed metabolites is shown. Blue color represents the number of significantly downregulated metabolites comparing IRIS and non-IRIS groups, and red color represents the number of metabolites that are upregulated.

identified (**Figure 1B**). At the month 12 time point, the number of DEMs was reduced to 28 (**Figure 1C**). Detailed DEM identities and reported values are shown in **Supplementary Table 1**. Most of the DEMs were not shared between time points suggesting that the metabolome of IRIS patients is dynamic and changes over time (**Figure 1D**).

Following the identification of individual DEMs, we found that the DEMs were also able to distinguish most of IRIS and non-IRIS patients at each time point based on principal component analysis (PCA) (**Figures 2A–C**). We extended these findings by using an unsupervised hierarchical clustering, which further confirmed the discriminatory power of the DEMs for IRIS and non-IRIS patients at each time point (**Supplementary Figures 2A–C**). These findings demonstrated that IRIS patients already exhibited a distinct metabolic profile prior to the initiation of ART that persist through the IRIS event. Additionally, alterations in metabolic profile were still detectable up to a year after ART commencement although the differences were less conspicuous.

We next attempted to identify the most informative metabolites driving the distinct metabolic signatures for IRIS development at each time point. By using a machine learning approach named decision tree, we were able to select the minimum number of metabolites that differentiated IRIS from non-IRIS groups. Notably, at the pre-ART time point, three metabolites were defined as the most informative: oxidized cysteinyl-glycine (Cys-Gly Oxidized), 1-myristoyl-2-palmitoyl-GPC (14:0/16:0), and sulfate of piperine metabolite $C_{18}H_{21}NO_3$ (**Figure 2D**). The combined result of these three metabolites could distinguish IRIS from non-IRIS group with high level of accuracy

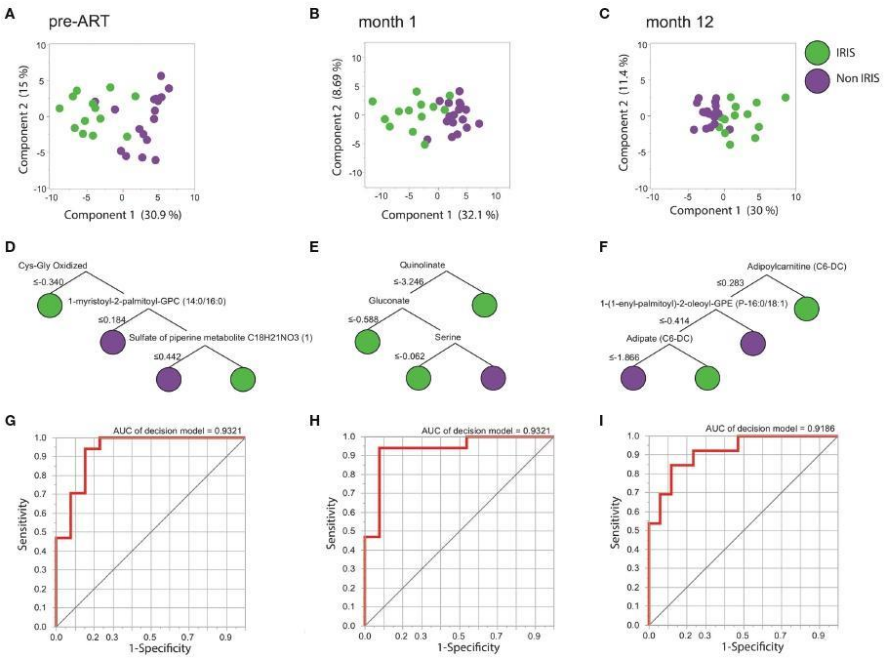

FIGURE 2 | Differentially expressed metabolites (DEMs) prediction of IRIS. Identified DEMs are analyzed using PCA for the pre-ART **(A)**, month 1 **(B)**, and month 12 **(C)** time points. Decision tree models of the predicting metabolites are shown for the pre-ART **(D)**, month 1 **(E)**, and month 12 **(F)** time points. ROC analysis illustrating the decision tree discrimination power is shown in **(G)**, **(H)**, and **(I)** for the pre-ART, month 1, and month 12 time points respectively.

[area under the curve (AUC): 0.93, p<0.0001] (**Figures 2G**). At month 1, quinolinate, gluconate, and serine were the top analytes driving the distinction (AUC: 0.93, p<0.0001) (**Figures 2E, H**), and lastly at month 12, adipoylcarnitine (C6-DC), 1-(1-enyl-palmitoyl)-2-oleoyl-GPE (P-16:0/18:1), and adipate (C6-DC) accounted for the separation of the clinical groups (AUC: 0.92, p<0.0001) (**Figures 2F, I**).

Altered Amino Acid and Lipid Metabolism Are Associated With IRIS Development

We next sought to evaluate metabolic alterations on a pathway level that could differentiate IRIS from non-IRIS condition using a co-expressed pathway modules approach as described by Russo et al. (37). Cellular processes, especially cell metabolism, are highly complex and often regulated through many interacting networks. Therefore, the co-expression analysis would extract co-regulated metabolic pathways associated with IRIS pathogenesis that may have more biological relevance. Briefly, the co-expressed pathway analysis groups metabolites with similar fold-change measurements comparing IRIS to non-IRIS groups and their respective annotated metabolic pathways based on the Metabolon reference library into modules (M). Module activity or representation distinguishing IRIS and non-IRIS condition was indicated by the computed network enrichment scores (NES). From our analysis, we identified three annotated co-expressed modules with varying levels of representation at each study time points comparing IRIS with non-IRIS groups (**Figure 3A**). At the pre-ART time point, module 4 (M4) initially had low representation in patients who developed IRIS that became upregulated at month 12 (**Figure 3A**). M3 had low representation in the IRIS group at the month 1 time point followed by an increased representation at month 12 (**Figure 3A**). M1 was only identified to be underrepresented at the month 1 time point (**Figure 3A**). Furthermore, the identified modules encompassed metabolic pathways of amino acid and lipid metabolism (**Figure 3B**). Specifically, M1 was defined by metabolic pathways for long chain fatty acids and polyunsaturated fatty acids n3 and n6 metabolism. M3 included pathways for sphingolipid and phosphatidylcholine metabolism. The final module M4 was composed of histidine and gamma glutamyl amino acid metabolism (**Figure 3B**). By using the top metabolic pathway identified in each module in an

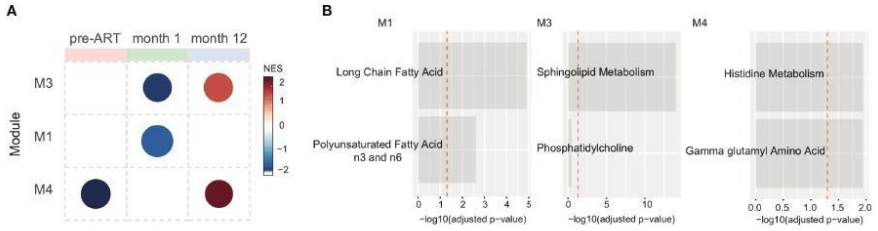

FIGURE 3 | Metabolic pathway module analysis. Co-expressed pathway modules are obtained by using metabolite fold-difference values comparing IRIS with non-IRIS groups analyzed with the *CEMiTool* R package. **(A)** Module activity for each time point is shown. Color scale reflects the network enrichment score (NES) of each module. Red color indicates a high degree of representation and blue represents low degree of representation. **(B)** Metabolic pathways that define the three identified modules are depicted. Bar graphs show the $-\log_{10}$ adjusted *p*-value of fold difference from the metabolomics dataset. The vertical dashed red line indicates an adjusted *p*-value of 0.05.

unsupervised hierarchal clustering, we found that these three pathways were unable to distinctly cluster individual samples based on time points (**Supplementary Figure 2D**). These results demonstrated that although specific metabolic pathways were differentially and dynamically represented in IRIS at each study time point, the top module pathways alone were not sufficient to characterize the nuances in metabolic changes over time.

Plasma Pro-Inflammatory Biomarkers Correlate With Metabolic Pathways in IRIS

Following the identification of DEMs and metabolic pathways unique to IRIS development, we investigated the association of metabolic pathways with plasma biomarker levels at the pre-ART and month 1 time points. At the pre-ART time point, there were no significant differences in the levels of measured plasma biomarkers between IRIS and non-IRIS patients (**Figure 4A**). After 1 month of ART initiation or during the IRIS event, biomarker measurements for soluble (s) CD14, MCP1, GMCSF, TNF, IL-8, and IL-6 were elevated in IRIS patients (**Figure 4B**).

Next, we correlated the metabolic pathway enrichment scores with plasma biomarker measurements using Spearman correlation matrices. Correlations achieving statistical significance (p-value <0.05, $-0.7 < r > 0.7$) were identified at the pre-ART and month 1 time points for both IRIS and non-IRIS groups (**Figure 4C**). We found that most of the significant correlations between plasma biomarkers and metabolic pathways occurred in the IRIS group during the IRIS event. The correlated metabolic pathways were in the lipid and amino acids metabolism families, indicating their potential regulatory involvement in IRIS pathogenesis and the implication of immune activation on lipid and amino acid metabolism disruptions. Specifically, lysophospholipid negatively correlated with TNF, and long chain fatty acids positively correlated with sCD14 and IL-2. Histidine metabolism positively correlated with sPD-1 and negatively correlated with IL-12p70. Lastly, tyrosine metabolism positively correlated with MPO and IL-8.

Metabolome Complements the Plasma Biomarker Profile and the Transcriptome in a Multi-Omics Analysis to Characterize IRIS

Given the complexity of metabolic regulations in immune responses and IRIS pathogenesis, we performed an integrative multi-omics analysis of the metabolome, transcriptome, and plasma biomarkers comparing IRIS and non-IRIS patients. In total, there were 8 IRIS patients and 12 non-IRIS patients with full pairing of the three omics datasets (**Supplementary Table 1**). Through the MOFA pipeline, we identified four latent factors that had discriminatory power to differentiate IRIS and non-IRIS conditions based on the omics data input (**Supplementary Figure 3**). Latent factor 1 (LF1) exhibited the strongest differentiating power between IRIS and non-IRIS groups, whereas latent factor 4 had the lowest differentiating potential. Within LF1, plasma biomarkers and transcriptome showed higher degree of variance compare to the metabolome. We also determined the top 10 metabolites and plasma biomarkers, and the top 20 transcriptomic pathways that contributed to the differentiating potential of LF1 (**Supplementary Figures 3B–D**). Specifically, metabolites identified in LF1 were mostly amino acids or amino acids derivatives, and the transcriptomics pathways included RNA processing and modification, B cell signaling, and antimicrobial peptides transcription.

Plasma Metabolomic Profiles Distinguish Mycobacterial IRIS From Other Types of IRIS

As co-infections may have distinct impact on IRIS pathogenesis, we further compared the metabolic profiles of patients with different types of IRIS stratified based on mycobacterial IRIS and IRIS caused by other pathogens (**Supplementary Table 1**). Among the 17 HIV-infected non-IRIS individuals, six had mycobacterial co-infection (**Supplementary Table 1**). At baseline, the overall plasma metabolome based on all identified metabolites was not affected by the different co-infections

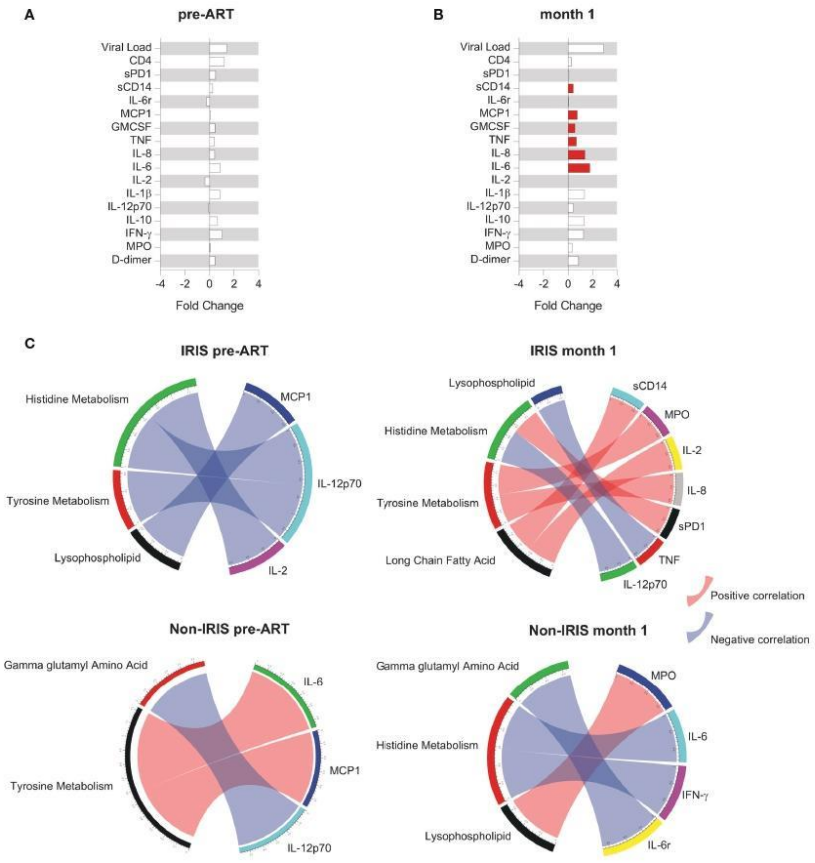

FIGURE 4 | Association between metabolic pathways and systemic inflammation in IRIS. Fold change analysis between IRIS and non-IRIS groups of HIV viral load, total $CD4^+$ T cell count, and levels of plasma biomarkers are shown for the pre-ART **(A)** and month 1 **(B)** time points. The statistically significant differences are shown in red bars. **(C)** Spearman correlations between levels of plasma biomarkers and normalized enrichment score from the co-expressed pathway modules at the pre-ART and month 1 time points for IRIS and non-IRIS groups are depicted. Blue arcs represent negative correlations, and red arcs represent positive correlations. Only statistically significant correlations with *p*-value <0.05 and correlation coefficient (r) above 0.7 or below -0.7 are portrayed.

(**Supplementary Figure 4**). Instead, the metabolic differences relied on specific metabolites and metabolic pathways. In particular, at the pre-ART time point, 58 metabolites were exclusively found in mycobacterial IRIS whereas 69 were uniquely modulated in the other types of IRIS group depicted in a Venn diagram (**Figure 5A**). Using the identified DEMs comparing mycobacterial IRIS, other types of IRIS, and non-IRIS groups, PCA and unsupervised hierarchical clustering analysis demonstrated that these three groups could be separated with minimal overlap (**Figure 5B** and **Supplementary Figures 5A–D, 6A, 6C**). The same Venn diagram and PCA analyses were repeated for the month 1 time point, and we found that DEMs were sufficient to distinguish all three groups (**Figures 5E, F** and **Supplementary Figures 5E–H, 6B, 6D**). We then employed the decision tree model and ROC analysis to select predictive metabolites at the pre-ART and month 1 time points. Results revealed that adipoylcarnitine C6 DC and eugenol sulfate could differentiate the outcome of mycobacterial IRIS, other types of IRIS, or non-IRIS conditions at the pre-ART time point (**Figures 5C, D**). At the month 1 time point, decision tree model determined succinimide, 10-nonadecenoate 19 1n9, and carotene-diol-3 exhibited discriminating power among the study groups (**Figure 5G**). ROC analysis identified an overall lower performance than that observed at the pre-ART time point, except

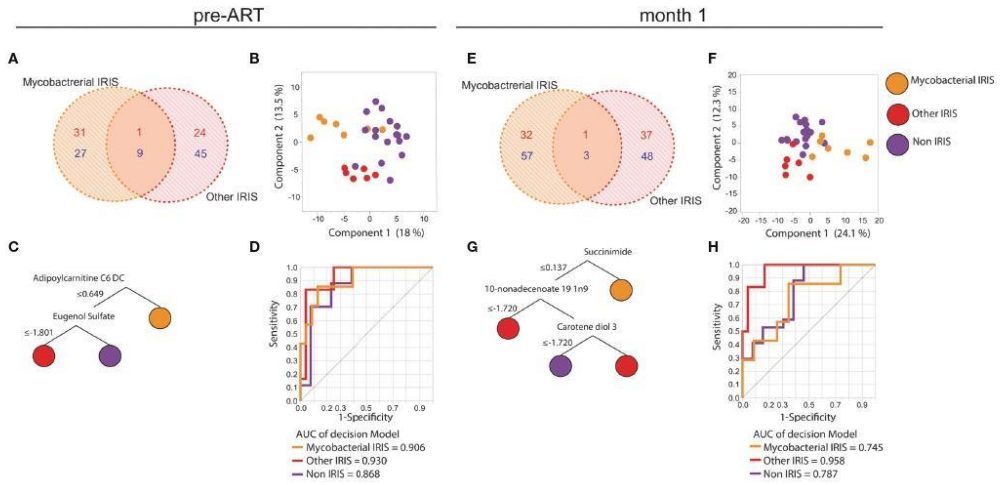

FIGURE 5 | Unique metabolic signatures in different types of IRIS. Venn diagrams illustrating the number of unique and shared DEMs comparing mycobacterial IRIS to other types of IRIS at the pre-ART **(A)** and month 1 **(E)** time points are shown. DEMs were used in a PCA plot to depict dimensionally reduced data distribution of the mycobacterial IRIS, other types of IRIS, and non-IRIS groups at the pre-ART **(B)** and month 1 **(F)** time points. Decision tree models based on the DEMs are presented for the pre-ART **(C)** and month 1 **(G)** time points. ROC analysis of the metabolites identified by the decision trees were used to test discrimination power between each study group for pre-ART **(D)** and month 1 **(H)** time points. P-values for all the AUC measures were < 0.001.

for discriminating the other IRIS group from mycobacterial IRIS or non-IRIS groups (**Figure 5H**).

Furthermore, co-expressed modules analysis was performed with same methodology used before for the comparison of mycobacterial IRIS, other types of IRIS and non-IRIS groups. There were 5 modules identified. Module representation for each group varied at different time points (**Figure 6A**). Metabolic pathways identified in each module belonged in the lipid and amino acid metabolism families, similar to those identified comparing IRIS and non-IRIS groups (**Figure 6B**). When the top pathway from each module was analyzed for each individual sample, we were unable to cluster the different group separately at the

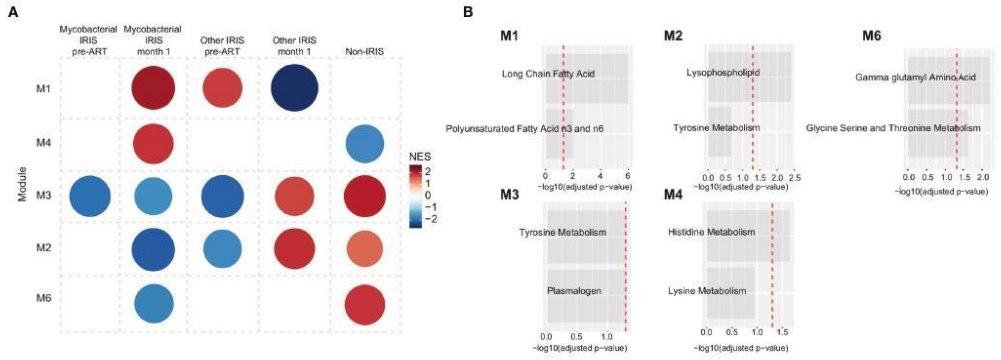

FIGURE 6 | Metabolic pathway module analysis for different types of IRIS. **(A)** Co-expressed pathway modules are obtained by CEMiTool R package using the measured metabolite levels of mycobacterial IRIS, other types of IRIS, and non-IRIS groups at the pre-ART and month 1 time points. Module representation is reflected by the network enrichment scores (NES) **(B)** Annotated metabolic pathways that define each statistically significant module are shown.

pre-ART and month 1 time points (**Supplementary Figures 6E, F**), which indicated these were not the only differentiating factors to discriminate study groups. Together, these findings revealed a perturbed host metabolism of IRIS that could potentially be associated with the underlying opportunistic pathogens and/or driven by differential gene regulation and inflammatory cytokine release.

DISCUSSION

It has been well characterized that IRIS is associated with aberrant innate and adaptive inflammatory responses to an underlying co-infection in PWH. Metabolic regulation of immune functions has gained growing attention in recent years. Here, we investigated the role of immunometabolism in IRIS pathogenesis through a comprehensive analysis of the plasma metabolome. We examined the longitudinal metabolic signatures across the pre-ART, IRIS event or 1 month post-ART equivalent, and 12 months post-ART time points. In addition, we compared various types of IRIS caused by different opportunistic infections. To our knowledge, this is the first study to present metabolomics analysis integrated with other biological parameters, such as plasma biomarkers and the transcriptome, to further decipher IRIS pathogenesis. Collectively, our findings identified potential lipid and amino acid metabolism perturbations in IRIS patients at the pre-ART and IRIS event time points, which could provide novel insight on predictors and therapeutic targets for IRIS.

We first identified more differentially expressed metabolites and correlations between metabolic pathways and inflammatory plasma biomarkers in IRIS patients prior to ART initiation and during the IRIS event. This finding not only reflected the association between cellular metabolism and the inflammatory manifestation during the IRIS event, but also revealed disrupted metabolism could be a predisposing factor for IRIS development. Following the resolution of IRIS inflammatory manifestations, metabolic differences diminished drastically by the month 12 time point between IRIS and non-IRIS groups. Although a small number of DEMs, mostly belonging to amino acid and nucleotide metabolism pathways, were still detectable at the month 12 time point, these differences could be contributed to residual inflammation, lifestyle, or medication. Furthermore, the detection of metabolic changes at the pre-ART and IRIS event in the current study was consistent with our previous findings of increased metabolic activity accompanied with higher glucose transporter expression on $CD4^+$ T cells and monocytes in IRIS patients prior to ART initiation and during the IRIS event (20). IRIS pathogenesis has been characterized by exaggerated immune activation including elevated plasma pro-inflammatory biomarkers (6, 9, 16), skewed inflammatory monocyte population (6), and robust polyfunctional antigen-specific $CD4^+$ T cell responses (3, 9, 12). In the context of metabolism and immune activation, infection by invading pathogen and T cell activation through T cell receptor ligation trigger metabolic reprogramming defined by increased glycolysis and modified mitochondria function in T-helper 1 cells, monocytes, and macrophages (22, 27, 28, 43). Metabolic reprogramming, in turn, is also essential to effector function in immune cells as blocking glycolysis and mitochondria function can inhibit immune responses (22, 27). Metabolites can also act as immunological mediators to regulate TCR activation, epigenetic modifications, and expression of transcription factors or cytokines (23, 44, 45). Consequently, disturbance of the metabolic machinery and the generation of metabolites can have a profound effect on immune activation and immune activation may also induce metabolic changes. Therefore, our observation of an altered plasma metabolite profile prior to ART initiation and during the IRIS event conform with the established connection between metabolic regulations and immune function.

The use of metabolite decision tree models, co-expressed pathway module analysis, and plasma biomarker correlations revealed amino acid and lipid metabolites as the predominant variables that differentiated IRIS from non-IRIS conditions. First, amino acids are known as the building blocks for protein synthesis and protein-mediated inflammatory signaling (46, 47). In the pre-ART decision tree, oxidized cysteinyl-glycine (cys-gly), a dipeptide composed of amino acid glycine with an attached L-cysteinyl group, was the top metabolite to distinguish IRIS from non-IRIS conditions. Cys-gly is an intermediate metabolite in the glutathione metabolism pathway that can regulate oxidative stress (48). Elevated level of cys-gly has been shown to be associated with chronic immune activation in HIV-infected individuals on ART (33). Therefore, the level of cys-gly at the pre-ART time point could be an indication for heightened immune activation and predisposes patients for the development of IRIS. In the month 1 time point decision tree, another amino acid derivative quinolinate was the first metabolite to differentiate IRIS from non-IRIS condition. The catabolism of tryptophan to kynurenine and subsequent downstream metabolites including quinolinate have been implicated to have immunoregulatory roles. Specifically, quinolinate is involved in neurodegenerative diseases associated with AIDS (49, 50). Increased activity of tryptophan metabolism, quantified by elevated plasma ratio of kynurenine to tryptophan (KT ratio), has also been observed in HIV patients and is associated HIV disease severity and higher mortality rate (51, 52). In addition, proinflammatory cytokine IFN-γ induces the activity of the rate-limiting enzyme indoleamine-2,3-deoxygenase (IDO) in tryptophan metabolism (53). Thus, the tryptophan/kynurenine pathway and associated metabolites could play a role in IRIS pathogenesis as IRIS is characterized by exaggerated immune responses and robust IFN-γ production by antigen-specific T cells.

In addition to the decision tree predictive metabolites, correlations between metabolic pathways and plasma biomarkers have revealed that amino acids histidine and tyrosine metabolism may influence the inflammatory status of IRIS. In particular, histidine metabolism was negatively correlated with pro-inflammatory cytokine IL-12p70 and positively correlated with inhibitory marker soluble PD-1. Reduced histidine metabolism has been described in chronic

inflammatory disease such as systemic lupus erythematosus (30, 31, 54). IFN-γ has also been demonstrated to upregulate the histidine catabolizing enzymes resulting in the depletion of free histidine (55). Therefore, the correlations between histidine metabolism and two plasma biomarkers essential for T cell activation emphasized the potential inhibitory effect of histidine metabolism in immune activation and IRIS pathogenesis. Tyrosine metabolism was found to positively correlate with both myeloperoxidase (MPO) and IL-8, which are essential for neutrophil responses during an infection. The induction of IL-8 facilitates innate immune responses to an infection and mediate neutrophil chemotaxis (56). Neutrophils at the inflammatory sites secrete enzyme MPO to generate antimicrobial agent hypochlorous acid and the enzymatic activity of MPO can be enhanced by free tyrosine in the extracellular space (57). As a result, the correlation of tyrosine metabolism with both IL-8 and MPO provide insight on the role of neutrophils in mediating the aberrant inflammatory responses in IRIS.

Conversely, lipid metabolism is also crucial for immune cell activation to provide both cell membrane structure and high energy fuel to maintain memory responses (58, 59). We have identified polyunsaturated fatty acids (PUFAs), long-chain fatty acids (LCFAs), sphingolipids, phosphatidylcholines (PCs), and lysophospholipids (LPLs) metabolism pathways to be differentially expressed in IRIS. Another recent TB-IRIS metabolomics study also described an altered plasma lipid metabolism signature in TB-IRIS patients and highlighted the distinct differences of PUFAs (34). PUFAs and PUFA-derived lipid mediators including prostaglandins and lipoxins exhibit immunoregulatory functions in both the innate and adaptive immune systems to modulate T cell activation, cytokine production, cell membrane permeability, and intracellular signaling (34, 60). In addition, dietary supplementation of PUFAs were found to be effective in modulating inflammatory responses in inflammatory bowel disease (IBD) animal models (61). LCFAs are also crucial to support T cell effector differentiation and function. When LCFA oxidation is irreversibly inhibited, T cell differentiation and memory T cell secondary activation were drastically hindered (62, 63). Lastly, sphingolipids, PCs, and LPLs are membrane lipids that not only provide membrane structure, but also function as signaling molecules to elicit host immune responses in autoimmune and cardiovascular diseases (64, 65). Sphingolipids have been targeted as therapeutic measures in both asthma and IBD to reduce the levels of pro-inflammatory cytokines and alleviate inflammation (66). Together, our results and previously published studies provide evidence for the intimate involvement of fatty acid metabolism in inflammation and IRIS pathogenesis.

In an attempt to further delineate the implication of metabolomics in IRIS pathogenesis, we employed the MOFA model to incorporate the metabolome, transcriptome, and plasma biomarker profile. We have demonstrated the success of this approach previously in settings such as TB, diabetes, and leishmaniasis, providing important insights into the pathogenesis of these pathological conditions (40, 41, 67). The IRIS metabolome provided complementary information that expanded our understanding of the profound immune activation observed in IRIS patients. Within MOFA, the metabolic and transcriptomic pathways variance was largely driven by amino acid metabolism and protein translation machineries, which mirrored the other findings in this study highlighting the crucial role of amino acids in immune activation. Cellular metabolism is often regulated by redundant pathways to maintain homeostasis when encountering disruptive signals. This could explain the less robust variance observed in IRIS plasma metabolome compared to the transcriptome and the plasma biomarker profile, where protein translation and concentration could be more direct cellular readouts.

Finally, several additional key features that can influence the metabolome include microbial invasion and sex (68, 69). We postulate that the unique metabolic profile of different types of IRIS are largely driven by the underlying co-infection as has been previously demonstrated in TB (32, 70, 71). In particular, human monocyte-derived macrophages infected with *M. tuberculosis* could induce a shift from oxidative phosphorylation to aerobic glycolysis (70). Another plasma metabolomics study showed significantly different levels of lipid metabolites detected in patients with active TB disease (32). Lastly, a multi-omics study integrating plasma metabolome and cell transcriptome identified signatures associated with TB progression in glutathione pathway, sphingolipid pathway, and tRNA processing (39). Thus, our findings contrasting different types of IRIS likely reflect the distinct metabolic signature influenced by the co-infection pathogen. The influence of sex on the metabolome has been explored in several previous studies. By using an untargeted metabolomics approach, differences in plasma or serum metabolite composition including lipid steroids and derivative metabolites, branched-chain amino acids used for muscle building, and short-chain fatty acids could be detected contrasting age-matched men and women groups (72–74). Findings from these studies highlight the importance of sex-matched study groups to ensure that metabolomics results are not influenced by confounding factors. In the current study, we have proportionate numbers of female study participants in the IRIS and non-IRIS groups. In addition, based on PCA analysis of all identified metabolites, although limited by a small sample size, the effect of sex on the metabolome was not different comparing IRIS and non-IRIS groups at the three study time points (**Supplementary Figure 7**).

There were several limitations in our study. First, we had a relatively small sample size especially of non-mycobacterial IRIS. In addition, we were restricted by the number of fully matched samples to perform the multi-omics analysis at each time point. Second, the plasma metabolome embodies extracellular metabolites produced from all cell types throughout the body. As a result, we cannot determine the source of metabolite production or consumption. Third, we lack extensive *in vitro* validation for the computationally identified metabolic signatures, which could serve as predictive or therapeutic targets. Lastly, we lack the inclusion of HIV uninfected healthy donors as another comparator group. Although our IRIS and non-IRIS group comparisons have been performed within a homogenous HIV infection background, an uninfected control

group with similar demographics could have provide the overall framework of the healthy plasma metabolome and a better depiction of the metabolic contributions to the pathological state of IRIS.

In conclusion, IRIS was associated with a distinct plasma metabolomics profile characterized by perturbed lipid and amino acid metabolism at the pre-ART and IRIS event time points. This study expanded our understanding for the role of cellular metabolism in IRIS pathogenesis and complemented our previously findings of glycolytic shift by FDG-PET scan and *in vitro* measurements of glucose transporter expression on monocytes and T lymphocytes (20). Thus, metabolic reprogramming could fuel the dysregulated immune activation in IRIS and metabolic pathways may serve as novel targets for preventative and therapeutic measures in inflammatory complications.

DATA AVAILABILITY STATEMENT

The RNA sequencing dataset presented in this study can be found in online repository at the GEO database GSE173697: https://www.ncbi.nlm.nih.gov/geo/query/acc.cgi?acc=GSE173697. The normalized metabolomics raw values can be found in the **Supplementary Material**.

ETHICS STATEMENT

The studies involving human participants were reviewed and approved by NIH Institutional Review Board. The patients/participants provided their written informed consent to participate in this study.

AUTHOR CONTRIBUTIONS

LP, KF, BA, and IS designed the study, contributed to data collection and analysis, and drafted the final manuscript. KF, RT, and BA processed data and generated data visualization. AR performed plasma biomarker measurements. ED performed whole blood RNA sequencing. FG, EL, MM, AL, and IS coordinated and provided clinical care. All authors contributed to the article and approved the submitted version.

FUNDING

This work is supported by the Intramural Research Program of the National Institute of Allergy and Infectious Diseases at the National Institutes of Health (NIH).

ACKNOWLEDGMENTS

The authors would like to thank all the study participants for making this study possible. The authors also would like to acknowledge all the study coordinators and clinical staff of the inpatient ward and outpatient clinics 8 at the NIH Clinical Center.

SUPPLEMENTARY MATERIAL

The Supplementary Material for this article can be found online at: https://www.frontiersin.org/articles/10.3389/fimmu.2021.693074/full#supplementary-material

REFERENCES

1. French MA. HIV/AIDS: Immune Reconstitution Inflammatory Syndrome: A Reappraisal. *Clin Infect Dis* (2009) 48(1):101–7. doi: 10.1086/595006
2. Barber DL, Andrade BB, Sereti I, Sher A. Immune Reconstitution Inflammatory Syndrome: The Trouble With Immunity When You had None. *Nat Rev Microbiol* (2012) 10(2):150–6. doi: 10.1038/nrmicro2712
3. Hsu DC, Breglio KF, Pei L, Wong CS, Andrade BB, Sheikh V, et al. Emergence of Polyfunctional Cytotoxic Cd4+ T Cells in Mycobacterium Avium Immune Reconstitution Inflammatory Syndrome in Human Immunodeficiency Virus-Infected Patients. *Clin Infect Dis* (2018) 67(3):437–46. doi: 10.1093/cid/ciy016
4. Sereti I, Sheikh V, Shaffer D, Phanuphak N, Gabriel E, Wang J, et al. Prospective International Study of Incidence and Predictors of Immune Reconstitution Inflammatory Syndrome and Death in People Living With Human Immunodeficiency Virus and Severe Lymphopenia. *Clin Infect Dis* (2020) 71(3):652–60. doi: 10.1093/cid/ciz877
5. Vinhaes CL, Araujo-Pereira M, Tiburcio R, Cubillos-Angulo JM, Demitto FO, Akrami KM, et al. Systemic Inflammation Associated With Immune Reconstitution Inflammatory Syndrome in Persons Living With HIV. *Life (Basel)* (2021) 11(1):65. doi: 10.3390/life11010065
6. Andrade BB, Singh A, Narendran G, Schechter ME, Nayak K, Subramanian S, et al. Mycobacterial Antigen Driven Activation of CD14++CD16– Monocytes Is a Predictor of Tuberculosis-Associated Immune Reconstitution Inflammatory Syndrome. *PloS Pathog* (2014) 10(10):e1004433. doi: 10.1371/journal.ppat.1004433
7. Namale PE, Abdullahi LH, Fine S, Kamkuemah M, Wilkinson RJ, Meintjes G. Paradoxical TB-IRIS in HIV-Infected Adults: A Systematic Review and Meta-Analysis. *Future Microbiol* (2015) 10(6):1077–99. doi: 10.2217/fmb.15.9
8. Meintjes G, Wilkinson RJ, Morroni C, Pepper DJ, Rebe K, Rangaka MX, et al. Randomized Placebo-Controlled Trial of Prednisone for Paradoxical Tuberculosis-Associated Immune Reconstitution Inflammatory Syndrome. *AIDS* (2010) 24(15):2381–90. doi: 10.1097/QAD.0b013e32833dfc68
9. Antonelli LR, Mahnke Y, Hodge JN, Porter BO, Barber DL, DerSimonian R, et al. Elevated Frequencies of Highly Activated CD4+ T Cells in HIV+ Patients Developing Immune Reconstitution Inflammatory Syndrome. *Blood* (2010) 116(19):3818–27. doi: 10.1182/blood-2010-05-285080
10. Barber DL, Andrade BB, McBerry C, Sereti I, Sher A. Role of IL-6 in Mycobacterium Avium–Associated Immune Reconstitution Inflammatory Syndrome. *J Immunol* (2014) 192(2):676–82. doi: 10.4049/jimmunol.1301004
11. Barber DL, Mayer-Barber KD, Antonelli LRV, Wilson MS, White S, Caspar P, et al. Th1-driven Immune Reconstitution Disease in Mycobacterium Avium–Infected Mice. *Blood* (2010) 116(18):3485–93. doi: 10.1182/blood-2010-05-286336
12. Mahnke YD, Greenwald JH, DerSimonian R, Roby G, Antonelli LR, Sher A, et al. Selective Expansion of Polyfunctional Pathogen-Specific CD4(+) T Cells in HIV-1-infected Patients With Immune Reconstitution Inflammatory Syndrome. *Blood* (2012) 119(13):3105–12. doi: 10.1182/blood-2011-09-380840
13. Ravimohan S, Tamuhla N, Nfanyana K, Steenhoff AP, Letlhogile R, Frank I, et al. Robust Reconstitution of Tuberculosis-Specific Polyfunctional CD4+ T-Cell Responses and Rising Systemic Interleukin 6 in Paradoxical Tuberculosis-Associated Immune Reconstitution Inflammatory Syndrome. *Clin Infect Dis* (2016) 62(6):795–803. doi: 10.1093/cid/civ978
14. Meintjes G, Skolimowska KH, Wilkinson KA, Matthews K, Tadokera R, Conesa-Botella A, et al. Corticosteroid-Modulated Immune Activation in the Tuberculosis Immune Reconstitution Inflammatory Syndrome. *Am J Respir Crit Care Med* (2012) 186(4):369–77. doi: 10.1164/rccm.201201-0094OC

15. Tran HT, Van den Bergh R, Vu TN, Laukens K, Worodria W, Loembe MM, et al. The Role of Monocytes in the Development of Tuberculosis-Associated Immune Reconstitution Inflammatory Syndrome. *Immunobiology* (2014) 219 (1):37–44. doi: 10.1016/j.imbio.2013.07.004
16. Grant PM, Komarow L, Lederman MM, Pahwa S, Zolopa AR, Andersen J, et al. Elevated Interleukin 8 and T-helper 1 and T-helper 17 Cytokine Levels Prior to Antiretroviral Therapy in Participants Who Developed Immune Reconstitution Inflammatory Syndrome During ACTG A5164. *J Infect Dis* (2012) 206(11):1715–23. doi: 10.1093/infdis/jis604
17. Boulware DR, Hullsiek KH, Puronen CE, Rupert A, Baker JV, French MA, et al. Higher Levels of CRP, D-Dimer, IL-6, and Hyaluronic Acid Before Initiation of Antiretroviral Therapy (ART) are Associated With Increased Risk of AIDS or Death. *J Infect Dis* (2011) 203(11):1637–46. doi: 10.1093/infdis/jir134
18. Boulware DR, Meya DB, Bergemann TL, Wiesner DL, Rhein J, Musubire A, et al. Clinical Features and Serum Biomarkers in HIV Immune Reconstitution Inflammatory Syndrome After Cryptococcal Meningitis: A Prospective Cohort Study. *PloS Med* (2010) 7(12):e1000384. doi: 10.1371/journal.pmed.1000384
19. Hsu DC, Faldetta KF, Pei L, Sheikh V, Utay NS, Roby G, et al. A Paradoxical Treatment for a Paradoxical Condition: Infliximab Use in Three Cases of Mycobacterial Iris. *Clin Infect Dis* (2016) 62(2):258–61. doi: 10.1093/cid/civ841
20. Hammoud DA, Boulougoura A, Papadakis GZ, Wang J, Dodd LE, Rupert A, et al. Increased Metabolic Activity on 18F-Fluorodeoxyglucose Positron Emission Tomography–Computed Tomography in Human Immunodeficiency Virus–Associated Immune Reconstitution Inflammatory Syndrome. *Clin Infect Dis* (2019) 68(2):229–38. doi: 10.1093/cid/ciy454
21. Akkaya B, Roesler AS, Miozzo P, Theall BP, Al Souz J, Smelkinson MG, et al. Increased Mitochondrial Biogenesis and Reactive Oxygen Species Production Accompany Prolonged Cd4(+) T Cell Activation. *J Immunol* (2018) 201 (11):3294–306. doi: 10.4049/jimmunol.1800753
22. Buck MD, O'Sullivan D, Geltink RIK, Curtis JD, Chang C-H, Sanin DE, et al. Mitochondrial Dynamics Controls T Cell Fate Through Metabolic Programming. *Cell* (2016) 166(1):63–76. doi: 10.1016/j.cell.2016.05.035
23. Macintyre AN, Gerriets VA, Nichols AG, Michalek RD, Rudolph MC, Deoliveira D, et al. The Glucose Transporter Glut1 is Selectively Essential for CD4 T Cell Activation and Effector Function. *Cell Metab* (2014) 20(1):61–72. doi: 10.1016/j.cmet.2014.05.004
24. Peng M, Yin N, Chhangawala S, Xu K, Leslie CS, Li MO. Aerobic Glycolysis Promotes T Helper 1 Cell Differentiation Through an Epigenetic Mechanism. *Science* (2016) 354(6311):481–4. doi: 10.1126/science.aaf6284
25. Ricciardi S, Manfrini N, Alfieri R, Calamita P, Crosti MC, Gallo S, et al. The Translational Machinery of Human Cd4+ T Cells Is Poised for Activation and Controls the Switch From Quiescence to Metabolic Remodeling. *Cell Metab* (2018) 28(6):895–906.e5. doi: 10.1016/j.cmet.2018.08.009
26. Sena LA, Li S, Jairaman A, Prakriya M, Ezponda T, Hildeman DA, et al. Mitochondria are Required for Antigen-Specific T Cell Activation Through Reactive Oxygen Species Signaling. *Immunity* (2013) 38(2):225–36. doi: 10.1016/j.immuni.2012.10.020
27. Chang CH, Curtis JD, Maggi LBJr., Faubert B, Villarino AV, O'Sullivan D, et al. Posttranscriptional Control of T Cell Effector Function by Aerobic Glycolysis. *Cell* (2013) 153(6):1239–51. doi: 10.1016/j.cell.2013.05.016
28. O'Neill LA, Pearce EJ. Immunometabolism Governs Dendritic Cell and Macrophage Function. *J Exp Med* (2016) 213(1):15–23. doi: 10.1084/jem.20151570
29. Al-Mubarak R, Vander Heiden J, Broeckling CD, Balagon M, Brennan PJ, Vissa VD. Serum Metabolomics Reveals Higher Levels of Polyunsaturated Fatty Acids in Lepromatous Leprosy: Potential Markers for Susceptibility and Pathogenesis. *PloS Negl Trop Dis* (2011) 5(9):e1303. doi: 10.1371/journal.pntd.0001303
30. Bengtsson AA, Trygg J, Wuttge DM, Sturfelt G, Theander E, Donten M, et al. Metabolic Profiling of Systemic Lupus Erythematosus and Comparison With Primary Sjogren's Syndrome and Systemic Sclerosis. *PloS One* (2016) 11(7):e0159384. doi: 10.1371/journal.pone.0159384
31. Perl A, Hanczko R, Lai Z-W, Oaks Z, Kelly R, Borsuk R, et al. Comprehensive Metabolome Analyses Reveal N-Acetylcysteine-Responsive Accumulation of Kynurenine in Systemic Lupus Erythematosus: Implications for Activation of the Mechanistic Target of Rapamycin. *Metabolomics* (2015) 11(5):1157–74. doi: 10.1007/s11306-015-0772-0
32. Collins JM, Walker DI, Jones DP, Tukvadze N, Liu KH, Tran VT, et al. High-Resolution Plasma Metabolomics Analysis to Detect Mycobacterium Tuberculosis-Associated Metabolites That Distinguish Active Pulmonary Tuberculosis in Humans. *PloS One* (2018) 13(10):e0205398. doi: 10.1371/journal.pone.0205398
33. Chettimada S, Lorenz DR, Misra V, Dillon ST, Reeves RK, Manickam C, et al. Exosome Markers Associated With Immune Activation and Oxidative Stress in HIV Patients on Antiretroviral Therapy. *Sci Rep* (2018) 8(1):7227. doi: 10.1038/s41598-018-25515-4
34. Silva CAM, Graham B, Webb K, Ashton LV, Harton M, Luetkemeyer AF, et al. A Pilot Metabolomics Study of Tuberculosis Immune Reconstitution Inflammatory Syndrome. *Int J Infect Dis* (2019) 84:30–8. doi: 10.1016/j.ijid.2019.04.015
35. Evans AM, DeHaven CD, Barrett T, Mitchell M, Milgram E. Integrated, Nontargeted Ultrahigh Performance Liquid Chromatography/Electrospray Ionization Tandem Mass Spectrometry Platform for the Identification and Relative Quantification of the Small-Molecule Complement of Biological Systems. *Anal Chem* (2009) 81(16):6656–67. doi: 10.1021/ac901536h
36. Espindola MS, Lima LJ, Soares LS, Cacemiro MC, Zambuzi FA, de Souza Gomes M, et al. Dysregulated Immune Activation in Second-Line Haart HIV+ Patients Is Similar to That of Untreated Patients. *PloS One* (2015) 10(12):e0145261. doi: 10.1371/journal.pone.0145261
37. Russo PST, Ferreira GR, Cardozo LE, Bürger MC, Arias-Carrasco R, Maruyama SR, et al. CemiTool: A Bioconductor Package for Performing Comprehensive Modular Co-Expression Analyses. *BMC Bioinf* (2018) 19 (1):56. doi: 10.1186/s12859-018-2053-1
38. Vinhaes CL, Oliveira-de-Souza D, Silveira-Mattos PS, Nogueira B, Shi R, Wei W, et al. Changes in Inflammatory Protein and Lipid Mediator Profiles Persist After Antitubercular Treatment of Pulmonary and Extrapulmonary Tuberculosis: A Prospective Cohort Study. *Cytokine* (2019) 123:154759. doi: 10.1016/j.cyto.2019.154759
39. Duffy FJ, Weiner J3rd, Hansen S, Tabb DL, Suliman S, Thompson E, et al. Immunometabolic Signatures Predict Risk of Progression to Active Tuberculosis and Disease Outcome. *Front Immunol* (2019) 10:527. doi: 10.3389/fimmu.2019.00527
40. Cubillos-Angulo JM, Vinhaes CL, Fukutani ER, Albuquerque VVS, Queiroz ATL, Andrade BB, et al. In Silico Transcriptional Analysis of mRNA and miRNA Reveals Unique Biosignatures That Characterizes Different Types of Diabetes. *PloS One* (2020) 15(9):e0239061. doi: 10.1371/journal.pone.0239061
41. Malta-Santos H, Fukutani KF, Sorgi CA, Queiroz ATL, Nardini V, Silva J, et al. Multi-Omic Analyses of Plasma Cytokines, Lipidomics, and Transcriptomics Distinguish Treatment Outcomes in Cutaneous Leishmaniasis. *iScience* (2020) 23(12):101840. doi: 10.1016/j.isci.2020.101840
42. Argelaguet R, Velten B, Arnol D, Dietrich S, Zenz T, Marioni JC, et al. Multi-Omics Factor Analysis-A Framework for Unsupervised Integration of Multi-Omics Data Sets. *Mol Syst Biol* (2018) 14(6):e8124. doi: 10.15252/msb.20178124
43. Cheng SC, Quintin J, Cramer RA, Shepardson KM, Saeed S, Kumar V, et al. mTOR- and HIF-1Alpha-Mediated Aerobic Glycolysis as Metabolic Basis for Trained Immunity. *Science* (2014) 345(6204):1250684. doi: 10.1126/science.1250684
44. Wang R, Dillon CP, Shi LZ, Milasta S, Carter R, Finkelstein D, et al. The Transcription Factor Myc Controls Metabolic Reprogramming Upon T Lymphocyte Activation. *Immunity* (2011) 35(6):871–82. doi: 10.1016/j.immuni.2011.09.021
45. Delgoffe GM, Powell JD. Sugar, Fat, and Protein: New Insights Into What T Cells Crave. *Curr Opin Immunol* (2015) 33:49–54. doi: 10.1016/j.coi.2015.01.015
46. Tannahill GM, Curtis AM, Adamik J, Palsson-McDermott EM, McGettrick AF, Goel G, et al. Succinate is an Inflammatory Signal That Induces IL-1beta Through HIF-1alpha. *Nature* (2013) 496(7444):238–42. doi: 10.1038/nature11986
47. Hosios AM, Hecht VC, Danai LV, Johnson MO, Rathmell JC, Steinhauser ML, et al. Amino Acids Rather Than Glucose Account for the Majority of Cell Mass in Proliferating Mammalian Cells. *Dev Cell* (2016) 36(5):540–9. doi: 10.1016/j.devcel.2016.02.012
48. Muller T, Muhlack S. Cysteinyl-Glycine Reduction as Marker for Levodopa-Induced Oxidative Stress in Parkinson's Disease Patients. *Mov Disord* (2011) 26(3):543–6. doi: 10.1002/mds.23384

49. Valle M, Price RW, Nilsson A, Heyes M, Verotta D. CSF Quinolinic Acid Levels are Determined by Local HIV Infection: Cross-Sectional Analysis and Modelling of Dynamics Following Antiretroviral Therapy. *Brain* (2004) 127 (Pt 5):1047–60. doi: 10.1093/brain/awh130
50. Moffett JR, Arun P, Puthillathu N, Vengilote R, Ives JA, Badawy AA, et al. Quinolinate as a Marker for Kynurenine Metabolite Formation and the Unresolved Question of NAD(+) Synthesis During Inflammation and Infection. *Front Immunol* (2020) 11:31. doi: 10.3389/fimmu.2020.00031
51. Byakwaga H, Boum Y, Huang Y, Muzoora C, Kembabazi A, Weiser SD, et al. The Kynurenine Pathway of Tryptophan Catabolism, CD4+ T-Cell Recovery, and Mortality Among HIV-Infected Ugandans Initiating Antiretroviral Therapy. *J Infect Dis* (2014) 210(3):383–91. doi: 10.1093/infdis/jiu115
52. Lee S, Byakwaga H, Boum Y, Burdo TH, Williams KC, Lederman MM, et al. Immunologic Pathways That Predict Mortality in HIV-Infected Ugandans Initiating Antiretroviral Therapy. *J Infect Dis* (2017) 215(8):1270–4. doi: 10.1093/infdis/jix113
53. Yap SH, Abdullah NK, McStea M, Takayama K, Chong ML, Crisci E, et al. HIV/Human Herpesvirus Co-Infections: Impact on Tryptophan-Kynurenine Pathway and Immune Reconstitution. *PloS One* (2017) 12(10):e0186000. doi: 10.1371/journal.pone.0186000
54. Perl A. Review: Metabolic Control of Immune System Activation in Rheumatic Diseases. *Arthritis Rheumatol* (2017) 69(12):2259–70. doi: 10.1002/art.40223
55. Dwivedy A, Ashraf A, Jha B, Kumar D, Agarwal N, Biswal BK. De Novo Histidine Biosynthesis Protects Mycobacterium Tuberculosis From Host IFN-Gamma Mediated Histidine Starvation. *Commun Biol* (2021) 4(1):410. doi: 10.1038/s42003-021-01926-4
56. Skov L, Beurskens FJ, Zachariae CO, Reitamo S, Teeling J, Satijn D, et al. IL-8 as Antibody Therapeutic Target in Inflammatory Diseases: Reduction of Clinical Activity in Palmoplantar Pustulosis. *J Immunol* (2008) 181(1):669–79. doi: 10.4049/jimmunol.181.1.669
57. Vlasova II, Sokolov AV, Arnhold J. The Free Amino Acid Tyrosine Enhances the Chlorinating Activity of Human Myeloperoxidase. *J Inorg Biochem* (2012) 106(1):76–83. doi: 10.1016/j.jinorgbio.2011.09.018
58. Pearce EL, Walsh MC, Cejas PJ, Harms GM, Shen H, Wang LS, et al. Enhancing CD8 T-Cell Memory by Modulating Fatty Acid Metabolism. *Nature* (2009) 460(7251):103–7. doi: 10.1038/nature08097
59. Lee J, Walsh MC, Hoehn KL, James DE, Wherry EJ, Choi Y. Regulator of Fatty Acid Metabolism, Acetyl Coenzyme a Carboxylase 1, Controls T Cell Immunity. *J Immunol* (2014) 192(7):3190–9. doi: 10.4049/jimmunol.1302985
60. McMurray DN, Jolly CA, Chapkin RS. Effects of Dietary N-3 Fatty Acids on T Cell Activation and T Cell Receptor-Mediated Signaling in a Murine Model. *J Infect Dis* (2000) 182(Suppl 1):S103–7. doi: 10.1086/315909
61. Michalak A, Mosinska P, Fichna J. Polyunsaturated Fatty Acids and Their Derivatives: Therapeutic Value for Inflammatory, Functional Gastrointestinal Disorders, and Colorectal Cancer. *Front Pharmacol* (2016) 7:459. doi: 10.3389/fphar.2016.00459
62. Raud B, Roy DG, Divakaruni AS, Tarasenko TN, Franke R, Ma EH, et al. Etomoxir Actions on Regulatory and Memory T Cells Are Independent of Cpt1a-Mediated Fatty Acid Oxidation. *Cell Metab* (2018) 28(3):504–15.e7. doi: 10.1016/j.cmet.2018.06.002
63. van der Windt GJ, O'Sullivan D, Everts B, Huang SC, Buck MD, Curtis JD, et al. CD8 Memory T Cells Have a Bioenergetic Advantage That Underlies Their Rapid Recall Ability. *Proc Natl Acad Sci USA* (2013) 110(35):14336–41. doi: 10.1073/pnas.1221740110
64. Edsfeldt A, Duner P, Stahlman M, Mollet IG, Asciutto G, Grufman H, et al. Sphingolipids Contribute to Human Atherosclerotic Plaque Inflammation. *Arterioscler Thromb Vasc Biol* (2016) 36(6):1132–40. doi: 10.1161/ATVBAHA.116.305675
65. Maceyka M, Spiegel S. Sphingolipid Metabolites in Inflammatory Disease. *Nature* (2014) 510(7503):58–67. doi: 10.1038/nature13475
66. Nixon GF. Sphingolipids in Inflammation: Pathological Implications and Potential Therapeutic Targets. *Br J Pharmacol* (2009) 158(4):982–93. doi: 10.1111/j.1476-5381.2009.00281.x
67. Dutta NK, Tornheim JA, Fukutani KF, Paradkar M, Tiburcio RT, Kinikar A, et al. Integration of Metabolomics and Transcriptomics Reveals Novel Biomarkers in the Blood for Tuberculosis Diagnosis in Children. *Sci Rep* (2020) 10(1):19527. doi: 10.1038/s41598-020-75513-8
68. Keshavarz M, Solaymani-Mohammadi F, Namdari H, Arjeini Y, Mousavi MJ, Rezaei F. Metabolic Host Response and Therapeutic Approaches to Influenza Infection. *Cell Mol Biol Lett* (2020) 25:15. doi: 10.1186/s11658-020-00211-2
69. Lovewell RR, Sassetti CM, VanderVen BC. Chewing the Fat: Lipid Metabolism and Homeostasis During M. Tuberculosis Infection. *Curr Opin Microbiol* (2016) 29:30–6. doi: 10.1016/j.mib.2015.10.002
70. Gleeson LE, Sheedy FJ, Palsson-McDermott EM, Triglia D, O'Leary SM, O'Sullivan MP, et al. Cutting Edge: Mycobacterium Tuberculosis Induces Aerobic Glycolysis in Human Alveolar Macrophages That Is Required for Control of Intracellular Bacillary Replication. *J Immunol* (2016) 196(6):2444–9. doi: 10.4049/jimmunol.1501612
71. Vrieling F, Kostidis S, Spaink HP, Haks MC, Mayboroda OA, Ottenhoff THM, et al. Analyzing the Impact of Mycobacterium Tuberculosis Infection on Primary Human Macrophages by Combined Exploratory and Targeted Metabolomics. *Sci Rep* (2020) 10(1):7085. doi: 10.1038/s41598-020-62911-1
72. Rist MJ, Roth A, Frommherz L, Weinert CH, Kruger R, Merz B, et al. Metabolite Patterns Predicting Sex and Age in Participants of the Karlsruhe Metabolomics and Nutrition (KarMeN) Study. *PloS One* (2017) 12(8):e0183228. doi: 10.1371/journal.pone.0183228
73. Darst BF, Koscik RL, Hogan KJ, Johnson SC, Engelman CD. Longitudinal Plasma Metabolomics of Aging and Sex. *Aging (Albany NY)* (2019) 11(4):1262–82. doi: 10.18632/aging.101837
74. Krumsiek J, Mittelstrass K, Do KT, Stuckler F, Ried J, Adamski J, et al. Gender-Specific Pathway Differences in the Human Serum Metabolome. *Metabolomics* (2015) 11(6):1815–33. doi: 10.1007/s11306-015-0829-0

Conflict of Interest: AR was employed by Leidos Biomedical Research, Inc.

The authors remaining declare that the research was conducted in the absence of any commercial or financial relationships that could be construed as a potential conflict of interest.

4 **PARTE 2**

4.1 HIPÓTESE

Paciente que desenvolvem SIRI associada a TB possuem reconstituição aberrante das populações de linfócitos com elevado grau de ativação imune e diferentes perfis de memória imunológica.

4.2 OBJETIVOS

4.2.1 **Objetivo geral**

Avaliar o perfil de ativação e memória imunológica em linfócitos T de pacientes que manifestaram SIRI associada a TB.

4.2.2 **Objetivos específicos**

- Avaliar a expressão de marcadores celulares associados à ativação (HLA-DR), exaustão (PD-1), proliferação (Ki-67) e citotoxicidade (Granzima B) nos compartimentos de linfócitos T $CD4^+$ e $CD8^+$ na população de estudo no período pré-TARV e durante a manifestação da SIRI;
- Correlacionar as frequências de linfócitos T $CD4^+$ e $CD8^+$ expressando marcadores de ativação com os níveis de moléculas inflamatórias no plasma dos participantes do estudo;
- Avaliar o potencial de diferentes modelos criados por aprendizado de máquinas incorporando as frequências de linfócitos T $CD4^+$ e/ou $CD8^+$ expressão moléculas relacionadas a ativação imune no prognóstico/diagnóstico de SIRI associada a TB;
- Investigar a participação de células T $CD8^+$ de memória na imunopatogênese da SIRI.
- Correlacionar os diferentes subtipos de células T $CD8^+$ de memória com as frequências de diferentes tipos de células imune expressando marcadores de ativação e com as abundancias de mediadores inflamatórios plasmáticos;
- Determinação do valor preditivo ou diagnostico dos subtipos de células T $CD8^+$ de memória na SIRI associada a TB.
-

4.3 MANUSCRITO II

DYNAMICS OF T-LYMPHOCYTE ACTIVATION RELATED TO PARADOXICAL TUBERCULOSIS-ASSOCIATED IMMUNE RECONSTITUTION INFLAMMATORY SYNDROME IN PERSONS WITH ADVANCED HIV

Este estudo avaliou o processo de ativação celular em linfócitos T CD4+ e CD8+ em indivíduos HIV-1 coinfectados com TB antes do início do tratamento e durante a manifestação de SIRI.

Resumo:
Neste estudo, avaliamos as frequências de células T CD4+ e CD8+ expressando marcadores associados com ativação (HLA-DR), exaustão celular (PD-1), proliferação (ki-67) e citotoxicidade (Granzima B). Observamos que indivíduos que desenvolveram SIRI exibem menores frequências de células T CD4+ e concomitante elevação dos níveis de células T CD8+ antes e após o início do TARV. Ademais, pacientes que desenvolveram SIRI apresentavam maiores níveis de linfócitos T CD4+ e CD8+ citotóxicos nos tempos analisados. Através de análise de redes baseada em correlações de Spearman entre as frequências de células T expressando moléculas relacionadas à dinâmica de ativação, notamos correlações negativas entre as frequências de células T CD4+ totais e CD8+ Granzima B^+, evidenciando então um possível mecanismo de compensação imunológica frente à linfopenia acentuada de células T CD4+ em episódios de SIRI. Os nossos achados demonstram diferentes perfis de correlações entre as frequências de linfócitos ativados e abundancias de mediadores solúveis no plasma, sugerindo então vias especificas estão vinculadas à ativação linfocitária no contexto de imunopatogênese da SIRI. Por fim, empregamos técnicas de aprendizado de máquinas para a criação de 3 modelos incorporando as frequências de populações linfocitárias expressando moléculas de ativação (modelo 1 = apenas células T CD4+, modelo 2 = apenas células T CD8+ e modelo 3 = ambas as populações de linfócitos T). Nossos achados sugerem que modelo 3 possui um alto potencial de distinguir pacientes que desenvolveram SIRI em comparação às suas contrapartes que não desenvolveram SIRI (AUC = 0.864). Deste modo, o nosso estudo evidencia a que ativação de linfócitos T está subjacente ao processo de deflagração da exacerbação inflamatória vista SIRI associada a TB.

Este artigo foi publicado no periódico internacional *Frontiers in immunology* (Fator de impacto = 7.5)

Publicado em 07 de outubro de 2021, doi: 10.3389/fimmu.2021.757843

frontiers in Immunology

ORIGINAL RESEARCH
published: 07 October 2021
doi: 10.3389/fimmu.2021.757843

Dynamics of T-Lymphocyte Activation Related to Paradoxical Tuberculosis-Associated Immune Reconstitution Inflammatory Syndrome in Persons With Advanced HIV

Rafael Tibúrcio[1,2,3†], Beatriz Barreto-Duarte[1,2,4,5†], Gopolan Naredren[6†], Artur T. L. Queiroz[2,7], Selvaraj Anbalagan[6], Kaustuv Nayak[6,8], Narayanan Ravichandran[9], Rajasekaran Subramani[6], Lis R. V. Antonelli[10], Kumar Satagopan[9], Komathi Anbalagan[9], Brian O. Porter[11], Alan Sher[12], Soumya Swaminathan[13], Irini Sereti[11] and Bruno B. Andrade[1,2,3,4,5,13,14,15]*

[1] Laboratório de Inflamação e Biomarcadores, Instituto Gonçalo Moniz, Fundação Oswaldo Cruz, Salvador, Brazil, [2] Multinational Organization Network Sponsoring Translational and Epidemiological Research (MONSTER) Initiative, Salvador, Brazil, [3] Faculdade de Medicina, Universidade Federal da Bahia, Salvador, Brazil, [4] Curso de Medicina, Universidade Salvador (UNIFACS), Salvador, Brazil, [5] Programa de Pós-Graduação em Clínica Médica, Universidade Federal do Rio de Janeiro, Rio de Janeiro, Brazil, [6] Department of Clinical Research, National Institute for Research in Tuberculosis, Chennai, India, [7] Center of Data and Knowledge Integration for Health (CIDACS), Instituto Gonçalo Moniz, Fundação Oswaldo Cruz, Salvador, Brazil, [8] ICGEB-Emory Vaccine Centre, International Centre for Genetic Engineering and Biotechnology, Aruna Asaf Ali Marg, India, [9] Government Hospital of Thoracic Medicine, Chennai, India, [10] Laboratório de Biologia e Imunologia de Doenças Infecciosas e Parasitárias, Instituto René Rachou, Fundação Oswaldo Cruz, Belo Horizonte, Brazil, [11] HIV Pathogenesis Section, Laboratory of Immunoregulation, National Institute of Allergy and Infectious Diseases, National Institutes of Health, Bethesda, MD, United States, [12] Immunobiology Section, Laboratory of Parasitic Diseases, National Institute of Allergy and Infectious Diseases, National Institutes of Health, Bethesda, MD, United States, [13] Wellcome Trust Centre for Infectious Disease Research in Africa, Institute of Infectious Disease and Molecular Medicine, University of Cape Town, Cape Town, South Africa, [14] Curso de medicina, Escola Bahiana de Medicina e Saúde Pública (EBMSP), Salvador, Brazil, [15] Division of Infectious Diseases, Department of Medicine, Vanderbilt University School of Medicine, Nashville, TN, United States*

OPEN ACCESS

Edited by:
Esaki M. Shankar, Central University of Tamil Nadu, India

Reviewed by:
Martyn Andrew French, University of Western Australia, Australia
Vignesh Ramachandran, University of Kuala Lumpur, Malaysia

***Correspondence:**
Bruno B. Andrade
bruno.andrade@fiocruz.br

[†]These authors share first authorship

Specialty section:
This article was submitted to Microbial Immunology, a section of the journal Frontiers in Immunology

Received: *12 August 2021*
Accepted: *22 September 2021*
Published: *07 October 2021*

Citation:
Tibúrcio R, Barreto-Duarte B, Naredren G, Queiroz ATL, Anbalagan S, Nayak K, Ravichandran N, Subramani R, Antonelli LRV, Satagopan K, Anbalagan K, Porter BO, Sher A, Swaminathan S, Sereti I and Andrade BB (2021) Dynamics of T-Lymphocyte Activation Related to Paradoxical Tuberculosis-Associated Immune Reconstitution Inflammatory Syndrome in Persons With Advanced HIV. Front. Immunol. 12:757843. doi: 10.3389/fimmu.2021.757843

Most persons living with HIV (PLWH) experience a significant restoration of their immunity associated with successful inhibition of viral replication after antiretroviral therapy (ART) initiation. Nevertheless, with the robust quantitative and qualitative restoration of $CD4^+$ T-lymphocytes, a fraction of patients co-infected with tuberculosis develop immune reconstitution inflammatory syndrome (TB-IRIS), a dysregulated inflammatory response that can be associated with significant tissue damage. Several studies underscored the role of adaptive immune cells in IRIS pathogenesis, but to what degree T lymphocyte activation contributes to TB-IRIS development remains largely elusive. Here, we sought to dissect the phenotypic landscape of T lymphocyte activation in PLWH coinfected with TB inititating ART, focusing on characterization of the profiles linked to development of TB-IRIS. We confirmed previous observations demonstrating that TB-IRIS individuals display pronounced $CD4^+$ lymphopenia prior to ART initiation. Additionally, we found an ART-induced increase in T lymphocyte activation, proliferation and cytotoxicity among TB-IRIS

patients. Importantly, we demonstrate that TB-IRIS subjects display higher frequencies of cytotoxic $CD8^+$ T lymphocytes which is not affected by ART. Moreover, These patients exhibit higher levels of activated ($HLA\text{-}DR^+$) and profilerative ($Ki\text{-}67^+$) $CD4^+$ T cells after ART commencenment than their Non-IRIS counterparts. Our network analysis reveal significant negative correlations between Total $CD4^+$ T cells counts and the frequencies of Cytotoxic $CD8^+$ T cells in our study population which could suggest the existance of compensatory mechanisms for Mtb-infected cells elimination in the face of severe $CD4^+$ T cell lymphopenia. We also investigated the correlation between T lymphocyte activation profiles and the abundance of several inflammatory molecules in plasma. We applied unsupervised machine learning techniques to predict and diagnose TB-IRIS before and during ART. Our analyses suggest that $CD4^+$ T cell activation markers are good TB-IRIS predictors, whereas the combination of $CD4^+$ and $CD8^+$ T cells markers are better at diagnosing TB-IRIS patients during IRIS events Overall, our findings contribute to a more refined understanding of immunological mechanisms in TB-IRIS pathogenesis that may assist in new diagnostic tools and more targeted patient management.

Keywords: T lymphocytes, IRIS pathogenesis, TB-HIV coinfection, inflammation, T cell activation

INTRODUCTION

The advent of antiretroviral therapy (ART) has substantially reduced the rates of morbidity and mortality associated with HIV infection. With ART, people living with HIV (PLWH) are expected to live longer and healthier lives, as treatment successfully suppresses viral replication and provides partial but substantial restoration of immunity. Although treatment mitigates the development of several opportunistic infections, tuberculosis (TB) remains a serious co-infection that can lead to long-term complications and an increased risk of death (1, 2).

A proportion of PLWH experiences a paradoxical clinical worsening or unmasking of TB within the first few weeks after ART initiation, a phenomenon known as immune reconstitution inflammatory syndrome (IRIS) (3, 4). The reported incidence of TB-related IRIS is associated with TB epidemiological settings and ranges from 8 to 54% (5, 6). Interestingly, factors such as advanced immunological deterioration coupled with high viral loads, short interval between antitubercular treatment (ATT) and ART initiation, as well as the abundance of *Mycobacterium tuberculosis* (Mtb) antigens at the time of immune restoration also play a pivotal role in IRIS pathogenesis (7). Clinical manifestations are largely variable ranging from fever and lymph node enlargement to severe and rapid worsening of respiratory symptoms, and even death (4). Since current TB-IRIS diagnostic tools remain suboptimal, newer accurate methods for early diagnosis and prediction are critical for better patient care and management.

Although TB-IRIS immunopathogenesis is both convoluted and not fully elucidated, a large number of studies suggests the contribution of dysregulated immune activation directed against Mtb antigens in the initiation of systemic inflammation (8–11). Previous reports from our group demonstrated that hyperresponsive activity from both innate and adaptive immune cells characterizes TB-IRIS (8). In fact, a rapid expansion of Mtb-specific $CD4^+$ T cells is detected among TB-IRIS patients (10). Notably, Silveira-Mattos et al. recently demonstrated that TB-IRIS individuals display profound alterations in $CD4^+$ T lymphocyte memory and effector functions prior to and after treatment (12). Additionally, as observed in previous studies involving IRIS patients with heterogenous co-infections, the frequency of T lymphocyte activation is elevated at pre-ART and is sustained during IRIS occurrence (13, 14).

In the present work, we dissected the immunophenotype of peripheral $CD4^+$ and $CD8^+$ T cells in a cohort of HIV-1 infected individuals diagnosed with pulmonary TB (PTB) before and after ART commencement. Our data showed that patients at higher risk of developing TB-IRIS exhibited more severe $CD4^+$ T cell lymphopenia then those who did not. Similarly, TB-IRIS subjects showed a higher degree of $CD4^+$ T lymphocyte activation, proliferation, and exhaustion dynamics over time with ART. Notably, these patients also displayed early and sustained expression of $CD8^+$ T cell cytotoxicity markers. Furthermore, hyperactivated T lymphocytes from IRIS patients exhibited strong positive correlations with plasma concentrations of several inflammatory biomarkers before and after ART initiation. Finally, we employed a multidimensional integrative analytical model combining T cell activation-related markers to predict and/or diagnose TB-IRIS. Collectively, the data shown in our study suggest that the patterns of T lymphocyte activation can aid in distinguishing TB-IRIS subjects from their non-IRIS counterparts before and during the IRIS occurrence.

METHODS

Ethics Statement

All clinical investigations were carried out in accordance with the principles disclosed in the Declaration of Helsinki. Of note, the pre-enrollment stage involved obtaining of written informed

consent from all participants of the present investigation. This study was approved by the Scientific Advisory Committee and Institutional Ethics Committee of the National Institute for Research in Tuberculosis (Chennai) and registered on Clinicaltrials.gov (NCT00933790).

Description of Study Population

The present study is a retrospective analysis of data collected from a previously published cohort (6). The Indian TB-IRIS cohort study comprised an observational analysis nested within a randomized controlled trial (NCT00- 933790) at the National Institute for Research in Tuberculosis (NIRT) in Chennai, India. In this retrospective investigation, HIV-1 infected patients with recent diagnosis of sputum culture-confirmed pulmonary TB were enrolled as previously reported (6). The parent randomized controlled clinical trial primarily compared outcomes of daily versus intermittent anti-TB regimens in the aforementioned group of individuals (15). Eligibility criteria were based on patient age (above 18 years old), with rifampicin-sensitive TB, and ART-naïve status. Clinical evaluation and blood samples were collected at pre-ART (baseline) and at the time of IRIS occurrence or equivalent time point (usually between 2 to 6 weeks following ART initiation). IRIS was confirmed by an independent panel of experts who were presented with the de-identified data of patients after the exclusion of drug resistance, and ruling out of endemic infections, with a thorough scrutiny for febrile episodes. IRIS was diagnosed by following a modified International Network for the study of HIV-associated IRIS (INSHI) guideline. This took into consideration both expected decreases in HIV plasma viral load (of at least 0.5 log) and sputum to assess Acid-Fast Bacillus (AFB)-negativity by culture or a decline in grade. All patients exhibited increases in $CD4^+$ T cell counts concomitantly with dramatically reduced plasma viral load. The detailed clinical, laboratory, and microbiologic description of the study participants has been previously reported (6).

Measurement of Plasma Biomarkers

Concentrations of C-reactive protein (CRP) (eBioscience, San Diego, CA), Eotaxin, Fibroblast growth factor (FGF) – basic, FMS-like tyrosine kinase 3 ligand (FLT3L), Granulocyte colony-stimulating factor (G-CSF), intestinal fatty acid binding protein (I-FABP) (Hycult Biotech, The Netherlands), Interferon (IFN) -α, IFN-β, IFN-γ, Interleukin (IL)- 1Ra, IL-1β, IL-2, IL-4, IL-5, IL-6, IL-7, IL-8, IL-9, IL-10, IL-12p40, IL-12p70, IL-13, IL-15, IL-17, Interferon-γ-induced protein 10 (IP-10/CXCL10), Monocyte chemoattractant protein-1 (MCP-1/CCL2), Macrophage inflammatory protein (MIP-1α/CCL3), MIP-1β (CCL4), Platelet-derived growth factor (PDGF), Regulated on activation normal T cell expressed and secreted (RANTES/CCL5), soluble CD14 (sCD14), soluble CD163 (sCD163), soluble Granzyme B (sGzB), soluble Programmed Cell death protein (PD) -1, soluble Tissue factor (sTF), Transforming Growth Factor (TGF)-β, Tumor Necrosis Factor (TNF)-α, and vascular endothelial growth factor (VEGF) (Bio-Plex, Bio-Rad, Hercules, CA)were assessed in cryopreserved plasma samples maintained at −80 °C.

Cell Staining and Flow Cytometry Assay

In order to dissect the immunophenotype of T lymphocytes, we evaluated markers associated with activation (HLA-DR), exhaustion (PD-1), proliferation (ki-67), and cytotoxicity (Granzyme B [GzB]). Briefly, this characterization was conducted by staining aliquots of 250 μL of whole blood with the following antibodies: CD3, CD4, CD8, HLA-DR, PD-1, Ki-67, and GzB. All antibodies were obtained from eBioscience (San Diego, CA), Biolegend (San Diego, CA), BD Biosciences (San Jose, CA) and Life Technologies (Carlsbad, CA). The antibody panel was prepared in PBS 1% BSA for 30 minutes at room temperature. Data were acquired on a BD FACS Canto II flow cytometer (BD Biosciences). All compensation and gate analysis were conducted in FlowJo 9.5.3 (TreeStar, Ashland, OR).

Network Analysis

The inferential networks were generated from Spearman correlation matrices containing values of each biomarker measured in the plasma samples and flow cytometry markers of T cell activation. All values were inputted and analyzed in *circusplot* R package. The links shown in the networks represent statistically significant Spearman rank correlations ($P<0.05$). Additionally, we dissected the structure of networks by calculating the network density. The density measure is defined as follows: density = $L/(N\ (N-1)/2)$, in which L is the number of observed edges (i.e., Spearman correlations with $P<0.05$) and N is the total number of the nodes in the network. The density is normalized, ranging between 0 (no edges in the network) and 1 (all possible edges presents). Graphics for the network analysis were customized using *circosplot* R package and Adobe Illustrator (Adobe Systems Inc.).

Data Analysis

Median values with IQR or frequencies of variables were compared using the Mann-Whitney *U* test (when two groups were compared) or the Kruskal-Wallis test with Dunn's multiple comparisons *ad hoc* analysis (when three groups were compared). Fisher's exact test or Chi-square tests were used to compare two or three groups, respectively, for proportions. Paired changes from before ART initiation to week 6 or the time of IRIS development were compared using the Wilcoxon matched-paired T test. Using JMP 10.0 software, geometric mean values (log_{10}) for each marker measured at week 0 and week 6 were calculated for the entire study population. To assess the overall pattern of expression of these markers in each clinical group and timepoint, heatmaps were built using variation from the geometric mean value calculated for each candidate biomarker. Principal component analysis was performed using the *Factorextra* R package. A hierarchical cluster analysis using the Ward's method was employed to reveal patterns of expression in plasma. Receiver operator Characteristic (ROC) curve analysis was performed on pROC package (16). Throughout the text, a p-value of <0.05 was considered statistically significant after adjustments for multiple measurements (Holm-Bonferroni's correction method). The statistical analyses were performed using GraphPad Prism 9.0

(GraphPad Software Inc., USA), the ggplot2 R package (version 3.10), and STATA 9.0 (StataCorp, TX, USA).

RESULTS

TB-IRIS Patients Display Altered CD4$^+$ and CD8$^+$ T Lymphocyte Frequencies Compared to Their Non-IRIS Counterparts

A total of 56 HIV$^+$ patients who were recently diagnosed with pulmonary TB and who were both ATT and ART-naïve were enrolled in this study. The baseline description of patients enrolled in study is presented in **Supplementary Table 1**. As demonstrated by previous studies of our group, several factors contribute to the risk of IRIS development, including low CD4$^+$ T lymphocyte counts prior to ART initiation. Therefore, we devised a flow cytometric approach to dissect the phenotype landscape of T lymphocytes in our study population at pre-ART and at 2-6 weeks after treatment initiation. We observed that baseline CD4$^+$ T cell frequencies among CD3$^+$ lymphocytes were significantly lower among TB-IRIS patients when compared to Non-IRIS individuals. Similarly, at 2-6 weeks post-treatment initiation, the amounts of CD4$^+$ T lymphocytes remained lower in the TB-IRIS group (**Figure 1A**). Of note, as an expected effect of ART, both groups displayed higher percentages of CD4$^+$ T cells at 2-6 weeks following treatment initiation when compared to baseline (**Figure 1A**). Interestingly, we also detected significantly higher CD8$^+$ T cell percentages in TB-IRIS subjects both at ART initiation and during 2-6 weeks after the start of treatment (**Figure 1B**). Next, we sought to determine the CD4$^+$/CD8$^+$ T lymphocyte ratio at both week 0 and 2-6 weeks after ART. Our analysis revealed that Non-IRIS individuals displayed higher CD4$^+$/CD8$^+$ T lymphocyte ratio when compared to their IRIS counterparts at both studied time points (**Figure 1C**). Additionally, we employed a combined measurement of both CD4$^+$ and CD8$^+$ T cell frequencies at ART initiation to further distinguish TB-IRIS from Non-IRIS individuals. Thus, we found that, when compared to the median value of the overall population, approximately 65% of TB-IRIS individuals displayed higher CD8$^+$ and lower CD4$^+$ T cell frequencies (**Figure 1D**). These results reinforce the

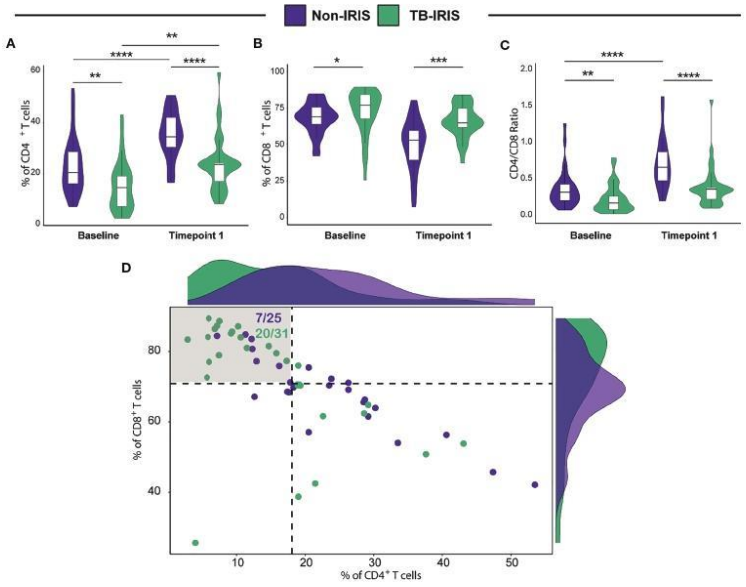

FIGURE 1 | Assessment of both CD4$^+$ and CD8$^+$ T cell frequencies in HIV-infected individuals prior to antiretroviral therapy (ART) initiation and during TB-IRIS manifestations. Comparison of CD4$^+$ **(A)** and CD8$^+$ **(B)** T cell frequencies in patients who developed TB-IRIS and those who did not at ART initiation (Baseline) and at the time of TB-IRIS manifestations (Timepoint 1), which occurred between 2 and 6 weeks after ART initiation. **(C)** CD4/CD8 T cell ratios at the aforementioned conditions. **(D)** Scatterplot displaying CD4$^+$ and CD8$^+$ T cell frequencies prior to ART initiation. Patients who developed TB-IRIS are depicted by green dots whereas those who did not experience TB-IRIS manifestations are represented by purple dots. Dotted lines on the X and Y axes represent the median value of CD4$^+$ and CD8$^+$ T cell counts within the entire study population, respectively. The shadowed quadrant represents those individuals with CD8$^+$ T cell counts above the median value and CD4$^+$ T cell frequencies below the median value for the entire population. Data were analyzed using the Mann-Whitney test or Wilcoxon matched-pairs test for paired analyses within each study group (*$p < 0.05$, **$p < 0.01$, ***$p < 0.001$, ****$p < 0.0001$).

importance of severe $CD4^+$ lymphopenia in IRIS pathogenesis, highlighting a unique profile of CD4/CD8 ratio.

Anti-Retroviral Treatment Alters Immunopathological Responses to *Mycobacterium tuberculosis*

Next, we wished to evaluate the impact of ART on T lymphocyte activation in TB-IRIS and Non-IRIS patients. We observed that the frequencies of activated $CD4^+$ T cells (measured as the percentage of $HLA\text{-}DR^+$ T cells) were similar in both groups prior to ART; however, TB-IRIS individuals displayed augmented levels of activated $CD4^+$ T cells at 2-6 weeks period in comparison to the Non-IRIS group. Additionally, we found that TB-IRIS persons exhibited higher frequencies of activated $CD4^+$ lymphocytes after ART initiation when compared to baseline levels. Interestingly, the percentages of $HLA\text{-}DR^+$ $CD8^+$ T cells were similar in the overall population regardless of ART initiation (**Figure 2A**). We then extended these findings on T cell activation to explore the effects of treatment on other characteristics of T cells such as exhaustion ($PD\text{-}1^+$ cells), proliferation ($ki\text{-}67^+$ cells), and cytotoxicity (Granzyme B^+ [GrB^+] Cells). We noticed that Non-IRIS persons had higher baseline levels of both exhausted $CD4^+$ and $CD8^+$ T cells, and that ART reduced substantially the amount of $PD\text{-}1^+$ T cells. Additionally, at ART initiation, the percentage of $PD1^+CD4^+$ cells was higher among Non-IRIS compared to TB-IRIS individuals (**Figure 2B**). We also verified that TB-IRIS persons displayed higher amounts of proliferative $CD4^+$ T cells (measured as the percentage of $Ki67^+$ cells) in comparison to the Non-IRIS group at 2-6 weeks post-ART initiation. Of note, we did not detect any significant difference in $CD8^+$ T cell proliferation status between these two groups (**Figure 2C**). Regarding cytotoxicity, we found higher frequencies of GrB^+ $CD8^+$ T cells in TB-IRIS patients, and such levels remained elevated even after ART commencement. On the other hand, we were able to detect a pronounced decline in GrB^+ $CD8^+$ levels of Non-IRIS individuals after ART. Interestingly, TB-IRIS individuals had augmented frequencies of GrB^+ $CD4^+$ at weeks 2-6 (**Figure 2D**). Our data show that TB-IRIS patients display heightened T lymphocyte activation with increased frequencies of proliferative $CD4^+$ and cytotoxic $CD8^+$ T cells during IRIS.

Network Analysis in TB-IRIS and Non-IRIS HIV-Infected Persons Reveals Nuances in T Lymphocyte Activation Patterns

We next conducted Spearman correlation-based network analysis to investigate how ART initiation and IRIS development associate with T lymphocyte activation. By employing circular layout networks to depict correlations of T cell activation markers, we observed that both IRIS and Non-IRIS patients exhibited similar correlation patterns at the pre-treatment timepoint and after ART initiation (**Figure 3A**). Nevertheless, our interactome analysis revealed that IRIS subjects displayed higher median network density (ND) before

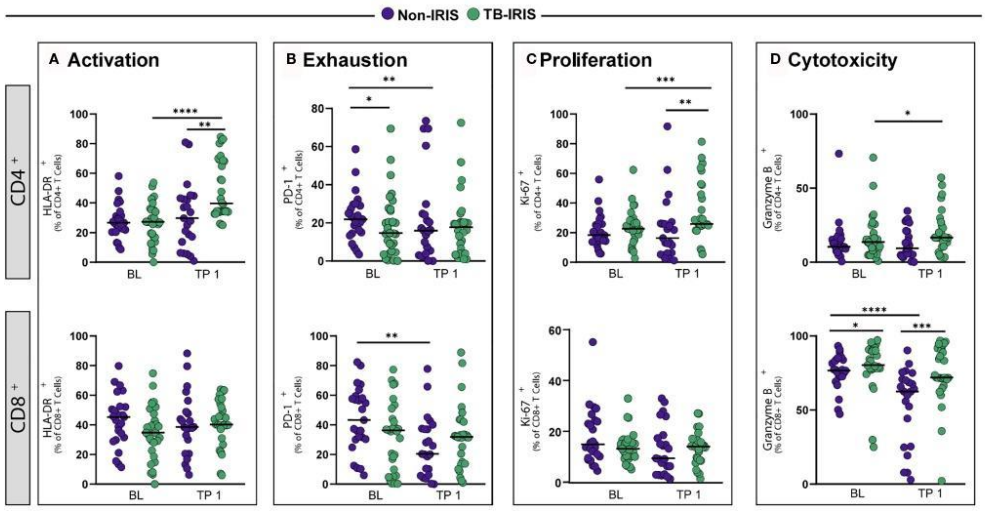

FIGURE 2 | Evaluation of T lymphocyte activation markers in TB-HIV co-infected patients prior to and following ART initiation. Expression of flow cytometry markers related to T cell activation (HLA-DR) **(A)**, exhaustion (PD-1) **(B)**, proliferation (Ki67) **(C)**, and cytotoxicity (Granzyme B) **(D)** were assessed in whole blood samples from TB-HIV co-infected individuals at baseline (BL) pre-ART and at the time of TB-IRIS manifestation (Timepoint [TP]1), which was 2-6 weeks on ART. Data were analyzed using the Mann-Whitney test or Wilcoxon matched-pairs test for paired analyses within each study group (*$p < 0.05$, **$p < 0.01$, ***$p < 0.001$, ****$p < 0.0001$).

treatment and lower ND at the 2–6-week period when compared to non-IRIS patients (**Figure 3B**). Additionally, we performed node analysis of all T cell activation-related markers that displayed statistically significant correlations in both groups. Of note, our analysis revealed that $CD4^+$ T lymphocytes ($HLA\text{-}DR^+$ cells) and cytotoxic $CD8^+$ T cells figured as top node among IRIS patients, while exhausted $CD8^+$ and proliferative $CD4^+$ T lymphocytes exhibited the highest number of correlations in the Non-IRIS group prior to ART. After 2-6 weeks of treatment, cytotoxic $CD8^+$ T cells were top nodes in the IRIS group, whereas among Non-IRIS patients, activated $CD4^+$ T lymphocytes showed the largest number of correlations (**Figure 3C**). These results argue that the identification of T lymphocyte patterns of activation may contribute to a better understanding of the immunological nuances surrounding IRIS.

T Lymphocyte Activation Correlates With Distinct Profiles of Systemic Inflammation Between TB-IRIS and Non-IRIS Patients

Considering that activated T lymphocytes play a role in systemic inflammation, we investigated how ART and IRIS development could influence the correlation between T cell activation markers and plasma levels of several inflammation-related molecules (cytokines, chemokines, and growth factors). Overall, Non-IRIS patients exhibited early and sustained negative correlations between activation markers and inflammatory molecule levels. In this group, activated $CD4^+$ T lymphocytes were negatively correlated with IL-7 as well as IFN-γ prior to treatment, and with IFN-β, sCD163, MIP1-α, and MIP1-β 2-6 weeks later. On the other hand, $HLA\text{-}DR^+CD8^+$ T cells displayed positive correlations with TGF- β, IL-4, and PDGF, while negatively associated with RANTES at the baseline timepoint. At 2-6 weeks post-treatment, these lymphocytes showed negative correlations with several markers (IFN-β, soluble Granzyme B (sGrB), Il-1Ra, IL-8, IL-15, G-CSF) (**Figure 4A**). Concerning IRIS patients, we could detect a larger number of positive correlations of markers of T cell activation with the measured inflammatory molecules. Of note, we found that activated $CD4^+$ T cells negatively correlate with FLT-3L and positively with FGF-basic only at the pre-treatment timepoint. Interestingly, activated $CD8^+$ T cells were negatively associated with IL-15, IL-17, IFN-γ, and VEGF after treatment initiation (**Figure 4B**). Among ART-naive Non-IRIS individuals, exhausted $CD4^+$ T cells were negatively correlated with IFN-β, IL-1β, IL-6, and eotaxin, whereas proliferative $CD4^+$ T cells negatively associated with

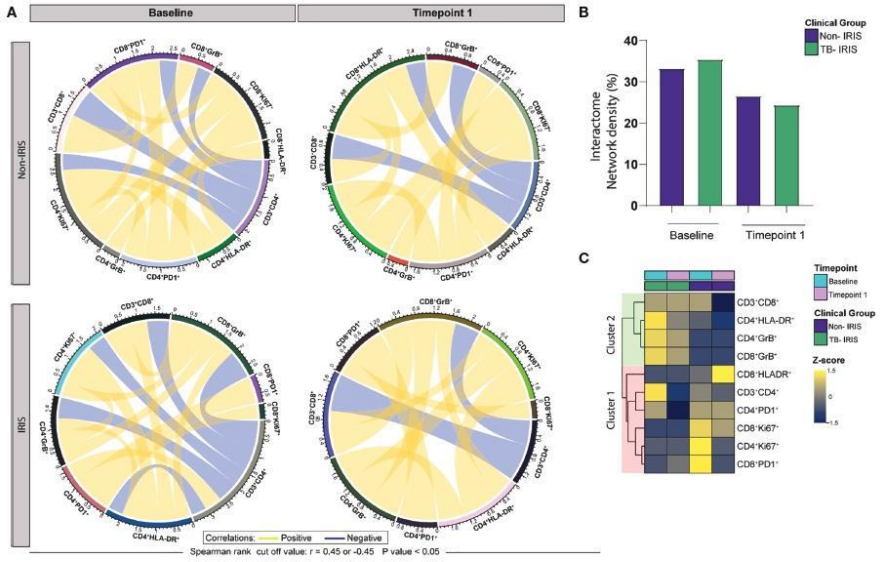

FIGURE 3 | ART initiation and TB-IRIS events are associated with coordinated alterations in the relationship between markers of T lymphocyte activation at Baseline (pre-ART) and 2-6 weeks following ART initiation. **(A)** Network analysis of T cell populations expressing activation-related markers; correlation matrices were developed with bootstrap (100 ×). **(B)** Networks depicting only significant correlations ($p < 0.05$), with Spearman rank threshold ± 0.5; graph showing interactome network density among the clinical groups. **(C)** A heatmap was employed to assess the contribution of each node based on the number of statistically significant correlations; yellow lines (edges) represent positive correlations between nodes (T cell population expressing activation-related markers), whereas blue lines depict negative correlations.

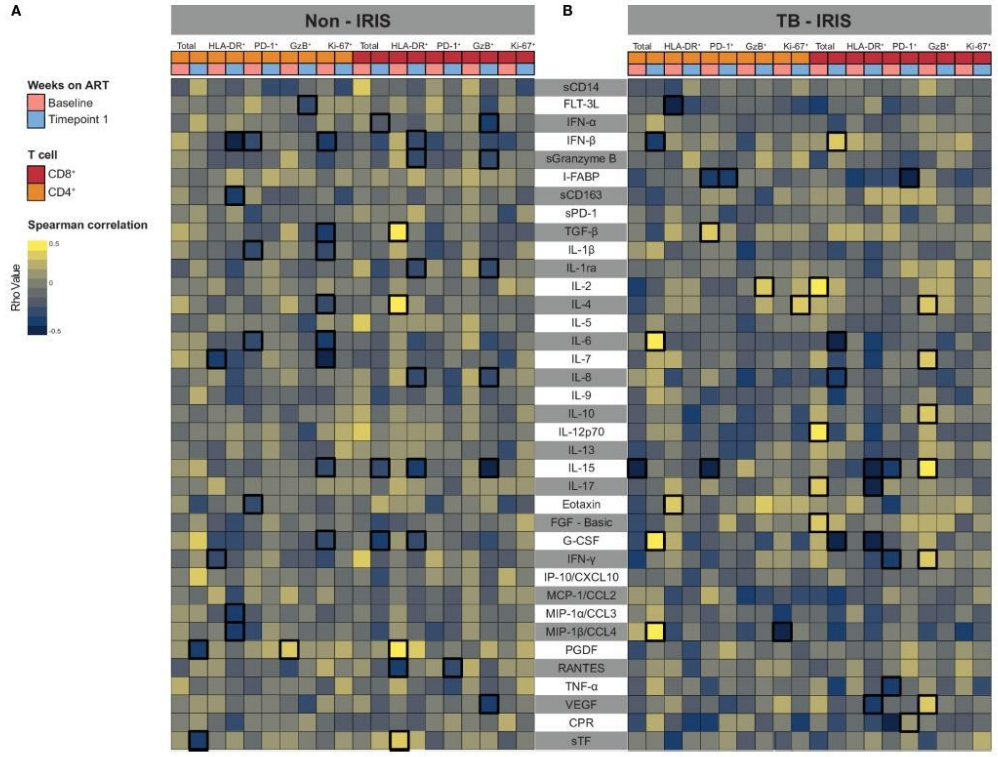

FIGURE 4 | Associations between both CD4+ and CD8+ T lymphocytes expressing activation-related biomarkers and plasma levels of several inflammatory biomarkers. A heatmap was employed to depict the strength of association between CD4+ and CD8+ T cells expressing activation-related biomarkers and the level of circulating cytokines and chemokines at Baseline (prior to ART) and after approximately 2 to 6 weeks following ART initiation (Timepoint 1) for Non-IRIS patients **(A)** and individuals who experienced TB-IRIS manifestations **(B)**. Statistically significant correlations ($P < 0.05$) after adjustment for multiple measurements are highlighted with bold squares.

IFN-β, TGF-β, IL-1β, IL-4, IL-6, IL-7, IL-15, and G-CSF. Interestingly, after 2-6 weeks of treatment, exhausted $CD8^+$ T cells correlated negatively only with RANTES, whereas cytotoxic lymphocytes with several molecules (IFN-α, sGrB, IL-1Ra, IL-8, IL-15, and VEGF). Among IRIS patients, we observed that exhausted $CD4^+$ T lymphocytes were negatively correlated with and the Intestinal Fatty acid-binding protein(I-FABP) before and after ART initiation. Conversely, we found that these lymphocytes displayed positive correlations with TGF-β, and IL-15 only in the baseline timepoint. Of note, we detected early positive correlations between cytotoxic $CD8^+$ T lymphocytes and IL-4, IL-7, IL-10, IL-15, IFN-γ, and VEGF. Altogether, these finding highlight how differential T cell activation in IRIS and Non-IRIS groups play a role in systemic inflammation upon ART initiation and IRIS pathogenesis.

Combination Models of $CD4^+$ and $CD8^+$ T Cell Activation Markers Distinguish TB-IRIS From Non-IRIS Patients

Bearing in mind the role of adaptive immunity hyperactivation in TB- IRIS pathogenesis, we aimed to estimate the predictive and diagnostic value of T cell activation-related markers in our patient cohort. Therefore, we employed unsupervised machine learning techniques with different combinations of flow cytometry markers of $CD4^+$ and $CD8^+$ T cell activation to build models with predictive and diagnostic potential. Considering T cell markers at the timepoint prior to ART initiation, our first predictive model (only composed of $CD4^+$ T cell activation markers) was better than our second (with only $CD8^+$ T cell activation markers) and third (incorporating both $CD4^+$ and $CD8^+$ T cell activation markers) models (**Figure 5**).

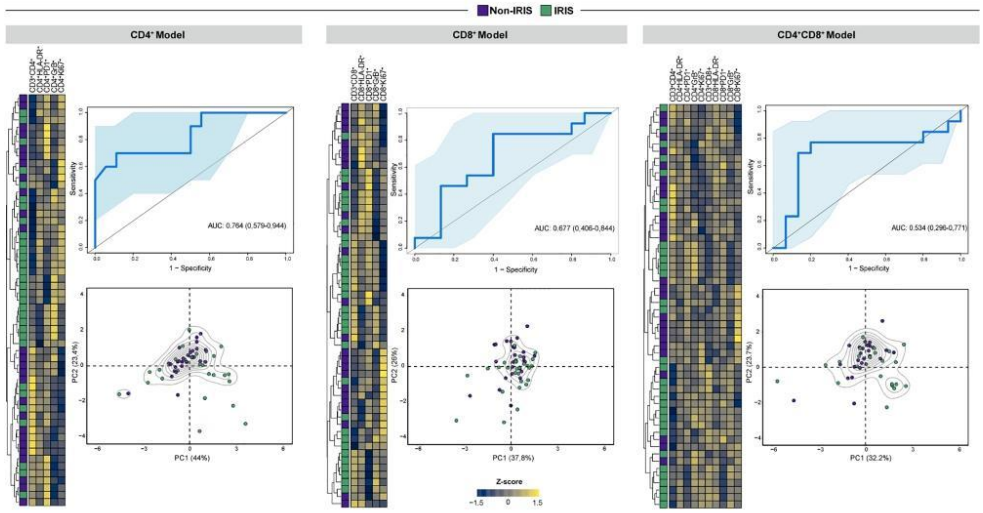

FIGURE 5 | Assessment of CD4+ and CD8+ T lymphocyte activation markers to predict TB-IRIS prior to ART. In order to create predictive models that distinguish TB-IRIS from non-IRIS patients prior to ART, unsupervised machine learning techniques were employed for either $CD4^+$ or $CD8^+$ T cell activation markers. In addition, a model encompassing both $CD4^+$ and $CD8^+$ T cell activation markers was also created. For each model, unsupervised cluster analyses (Ward's method) and principal component analyses were employed. In order to estimate the accuracy of these models in discriminating patients, a receiver-operating characteristic curve analysis was employed.

This result further suggests that activated $CD4^+$ T cells contribute more substantially to IRIS prediction than $CD8^+$ T cells. Of note, early diagnosis of TB-IRIS is critical to patient management. Thus, we employed our combinatory models considering only T cell activation dynamics after 2 to 6 weeks after ART commencement. Our first diagnostic model also displayed superior capacity to discriminate IRIS from Non-IRIS patients (AUC of 0.811 vs. 0.691). Interestingly, our third diagnostic model showed increased power of discriminating patients (AUC: 0.864) (**Figure 6**). Collectively, our results indicate $CD4^+$ T cell activation markers can serve as potential predictors of TB-IRIS, while the combination of $CD4^+$ and $CD8^+$ T cell markers is better at diagnosing TB-IRIS patients experiencing IRIS.

DISCUSSION

In the present work, we sought to evaluate the patterns of T lymphocyte activation associated with TB-IRIS development following the start of ART in PLWH displaying high $CD4^+$ T lymphocyte suppression pre-ART. Our phenotypic characterization of T cells revealed that TB-IRIS patients exhibited lower $CD4^+$ and higher $CD8^+$ T lymphocyte counts before ART in comparison to Non-IRIS individuals. These results are consistent with previous work that suggested severe $CD4^+$ T cell lymphopenia prior to ART initiation is a risk factor for IRIS development (14, 17). To better understand the role of T lymphocyte activation in IRIS, we performed immune profiling of both circulating $CD4^+$ and $CD8^+$ T cells regarding expression of activation (HLA-DR), exhaustion (PD-1), proliferation (Ki-67), and cytotoxicity (Granzyme B) markers.

Our working hypothesis was that aberrant T lymphocyte activation plays a pivotal role in exacerbating systemic inflammation as seen in TB-IRIS. We showed that TB-IRIS patients displayed higher levels of $CD4^+$ T cell activation at 2-6 weeks after ART initiation than their Non-IRIS counterparts. These findings reiterate those of Antonelli et al. that investigated a US cohort of patients with fungal, bacterial, and viral co-infections (14). Interestingly, a cross-sectional study conducted by Sangwan et al. revealed a correlation between the expression of immune activation markers and disease stage, suggesting that $CD8^+CD38^+$ T cells are associated with viral load in individuals with virological failure (18). Another striking observation of our study was the identification of enhanced levels of both exhausted and proliferative $CD4^+$ T cells, as well as Granzyme B^+CD8^+ T lymphocytes in TB-IRIS subjects. Of note, by studying a cohort of non-immunological and immunological responders, Piconi et al. showed that patients with a lower nadir $CD4^+$ exhibited inferior expansion of a $Ki67^+CD4^+$ T cell population after 7 years of ART, which was attributed to T cell hyperactivation (19). Along these lines, it is feasible that during a TB-IRIS event,

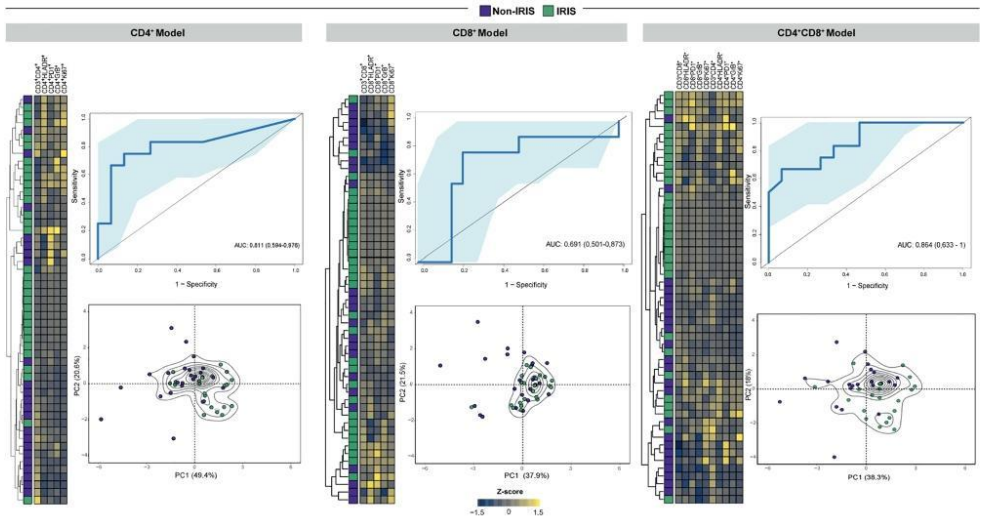

FIGURE 6 | Combination of T cell activation markers to diagnose IRIS after ART initiation. In order to create diagnostic models that distinguish TB-IRIS from non-IRIS patients after ART initiation, unsupervised machine learning techniques were employed for either $CD4^+$ or $CD8^+$ T cell activation markers. In addition, a model encompassing both $CD4^+$ and $CD8^+$ T cell activation markers was also created. For each model, unsupervised cluster analyses (Ward's method) and principal component analyses were employed. In order to estimate the accuracy of these models in discriminating patients, a receiver-operating characteristic curve analysis was employed.

patients experience an overwhelming $CD4^+$ T cell turnover (as evidenced by higher frequencies of proliferation and exhaustion markers) driven by excessive immune activation elicited by underlying TB infection. A study conducted by Massanella et al. provides compelling evidence for the association between $CD4^+$ T cell hyperactivation and increased cell turnover, culminating in cell death (20). Regarding the sustained high frequencies of cytotoxic $CD8^+$ T cells detected in TB-IRIS patients; we hypothesize that this might be a compensatory mechanism for the elimination of mycobacterium-infected cells in the face of substantial CD4 lymphopenia. Additionally, our data suggest that the sustained lower levels of activated $CD4^+$ T cells along with ART-induced decreases in cellular exhaustion indicate a more robust restoration of T lymphocyte homeostasis in Non-IRIS patients. Thus, our study extends the understanding of the diverse patterns of cellular activation and that $CD4^+$ T cells may exert a predominant role in TB-IRIS pathophysiology.

We also dissected T lymphocyte dynamics of activation in TB-IRIS patients by employing network analysis. Interestingly, we found lower values of network density in TB-IRIS patients before ART commencement, followed by a surprising increase in node connectivity during the IRIS event. In the pre-treatment timepoint, HLA-DR^+CD4^+ T cells, along with cytotoxic $CD8^+$ T cells, exhibited the highest numbers of significant correlations among IRIS patients. Of note, GrB^+CD8^+ T lymphocytes remained among the top nodes after 2-6 weeks on ART. A previous study from Wilkinson et al. underscored a substantial role of cytotoxic mediators in TB-IRIS immunopathogenesis (21). Similarly, Hsu et al. observed a role for the expansion of cytotoxic $CD4^+$ T cells in Mycobacterium avium complex-IRIS (22). In our analysis, exhausted $CD8^+$ and proliferative $Ki67^+$ $CD4^+$ T cells seemed to be central elements in network density among Non-IRIS subjects. Additionally, we aimed to investigate how differential dynamics of T cell activation were correlated with plasma markers of systemic inflammation. In the Non-IRIS group, we observed that both activated (HLA-DR^+) $CD4^+$ and $CD8^+$ T cells were negatively correlated with several inflammation-related molecules before and after ART initiation. Interestingly, in this same group of patients, we observed that HLA-DR^+ $CD8^+$ T cells were negatively correlated with IFN-β, sGZB, IL-8, IL-15, and G-CSF. These negative correlations could be part of a wider phenomenon of mycobacterium containment aided by activated $CD8^+$ T lymphocyte in parallel with a more coordinated mobilization of inflammatory molecules resulting in limited immunopathology. Conversely, in TB-IRIS patients, activated $CD4^+$ T cells displayed a substantially lower number of statistically significant correlations with plasma molecules, whereas cytotoxic $CD8^+$ T lymphocytes were positively associated with plasma levels of IL-4, IL-7, IL-10, IL-15, IFN-γ, and VEGF prior to ART. These findings argue that heightened responses of cytotoxic $CD8^+$ T lymphocytes could trigger cell

death-related signaling pathways in infected macrophages which could eventually culminate in both amplification of inflammatory responses and exacerbated pathology. Further studies are warranted to more precisely investigate the role of cytotoxic $CD8^+$ T cells in the settings of TB-IRIS immunopathogenesis. Of interest, a previous study from our group demonstrated a direct association between frequency of effector $CD4^+$ T cell subpopulations and the circulating levels of inflammatory cytokines, further suggesting the participation of T cell immune activation in augmented systemic inflammation detected in TB-IRIS (12). Collectively, these findings lend support to the notion that immune activation-driven systemic inflammation is indeed crucial to promote TB-IRIS pathogenesis."s

Notably, the overwhelming complexity of TB-IRIS immunopathogenesis impedes the attainment of accurate predictive and diagnostic methods, thus hindering appropriate patient care and disease management. Currently, a TB-IRIS diagnosis is mainly based on clinical presentation and the initial response of the underlying TB infection to ATT, with a paradoxical deterioration after ART initiation determine from both clinical assessment and imaging methods (such as chest X ray and computed tomography) (23). Therefore, major efforts have been devoted to the identification of prediction and diagnostic biomarkers to enhance TB-IRIS management strategies. In a previous retrospective study, we observed that increased baseline levels of monocyte and Th1 cell activation, alongside inflammatory markers, were independently associated with the risk of IRIS development (24). This prompted us to investigate the potential of T cell activation markers as predictive and diagnostic tools for TB-IRIS. By creating models of T cell activation patterns, we found that markers of $CD4^+$ T cell activation are better at predicting the occurrence of IRIS in our cohort. Additionally, combined CD4 and CD8 T cell activation markers were more accurate at distinguishing TB-IRIS patients from their Non-IRIS counterparts. To the best of our knowledge, this is the first work to employ flow cytometry markers of T cell activation as a possible tool for TB-IRIS diagnosis.

The main limitation of this study is the small number of patients included in our cohort. Nevertheless, the strength of the current investigation was the selection of a homogeneous cohort of individuals who were naïve to both ART and ATT and presented positive bacillar cultures, with drug-sensitive *Mycobacterium tuberculosis* strains. Moreover, the blood draws taken at the time of IRIS, before administering a single dose of anti-inflammatory medication, enhances our validity. Additionally, patients were carefully monitored since ART initiation for the identification of IRIS events, with immediate collection of blood samples at the first suspicion of an event. Collectively, our findings provide new insights to decipher fundamental events in the immune activation landscape surrounding TB-IRIS pathophysiology.

DATA AVAILABILITY STATEMENT

The raw data supporting the conclusions of this article will be made available by the authors, without undue reservation.

ETHICS STATEMENT

The studies involving human participants were reviewed and approved by Institutional Ethics Committee of the National Institute for Research in Tuberculosis (Chennai) and registered on Clinicaltrials.gov (NCT00933790). The patients/participants provided their written informed consent to participate in this study.

AUTHOR CONTRIBUTIONS

BA, IS, SS, BP, and AS conceptualized the study. BA and IS supervised the immunological study. GN and SS supervised the clinical study. IS, SS, and AS acquired funding for research. GN, RS, KS, BP, IS, and BA performed the clinical assessments. SA, KN, KA BA, and LA performed the experiments. RT, BB-D, and AQ analyzed the data. RT, BB-D, and BA drafted the first version of the manuscript. All the authors revised the manuscript. All authors contributed to the article and approved the submitted version.

FUNDING

This work received supported from the Intramural Research Program of National Institute of Allergy and Infectious Diseaes (NIAID/NIH) and by the Intramural-to-India grant from the US-India Co-operative research program. This study was also financed in part by Coordenação de Aperfeiçoamento de Pessoal de Nível Superior (CAPES) (Finance Code 001). The work of BA is supported by the Intramural Research Program of the Oswaldo Cruz Foundation (FIOCRUZ) and the National Council for Scientific and Technological Development (CNPq), Brazil. RT and BB-D were supported by PhD fellowships from CAPES. The funders had no role in study design, data collection and analysis, decision to publish, or preparation of the manuscript.

ACKNOWLEDGMENTS

The authors thank Mrs. Elze Leite (FIOCRUZ, Brazil) for logistics and administrative support. We wholeheartedly appreciate the precious scientific contributions of Dr. Sudha Subramanyam (NIRT, India) to this work. The authors also thank all the study participants.

SUPPLEMENTARY MATERIAL

The Supplementary Material for this article can be found online at: https://www.frontiersin.org/articles/10.3389/fimmu.2021.757843/full#supplementary-material

REFERENCES

1. Bruchfeld J, Correia-Neves M, Källenius G. Tuberculosis and HIV Coinfection. *Cold Spring Harb Perspect Med* (2015) 5(7):a017871. doi: 10.1101/cshperspect.a017871
2. Kwan CK, Ernst JD. HIV and Tuberculosis: A Deadly Human Syndemic. *Clin Microbiol Rev* (2011) 24(2):351–76. doi: 10.1128/CMR.00042-10
3. Cevaal PM, Bekker LG, Hermans S. TB-IRIS Pathogenesis and New Strategies for Intervention: Insights From Related Inflammatory Disorders. *Tuberculosis (Edinb)* (2019) 118:101863. doi: 10.1016/j.tube.2019.101863
4. Vinhaes CL, Araujo-Pereira M, Tibúrcio R, Cubillos-Angulo JM, Demitto FO, Akrami KM, et al. Systemic Inflammation Associated With Immune Reconstitution Inflammatory Syndrome in Persons Living With HIV. *Life (Basel)* (2021) 11(1):65. doi: 10.3390/life11010065
5. Narita M, Ashkin D, Hollender ES, Pitchenik AE. Paradoxical Worsening of Tuberculosis Following Antiretroviral Therapy in Patients With AIDS. *Am J Respir Crit Care Med* (1998) 158(1):157–61. doi: 10.1164/ajrccm.158.1.9712001
6. Narendran G, Andrade BB, Porter BO, Chandrasekhar C, Venkatesan P, Menon PA, et al. Paradoxical Tuberculosis Immune Reconstitution Inflammatory Syndrome (TB-IRIS) in HIV Patients With Culture Confirmed Pulmonary Tuberculosis in India and the Potential Role of IL-6 in Prediction. *PloS One* (2013) 8(5):e63541. doi: 10.1371/journal.pone.0063541
7. Gopalan N, Andrade BB, Swaminathan S. Tuberculosis-Immune Reconstitution Inflammatory Syndrome in HIV: From Pathogenesis to Prediction. *Expert Rev Clin Immunol* (2014) 10(5):631–45. doi: 10.1586/1744666X.2014.892828
8. Andrade BB, Singh A, Narendran G, Schechter ME, Nayak K, Subramanian S, et al. Mycobacterial Antigen Driven Activation of CD14++CD16- Monocytes Is a Predictor of Tuberculosis-Associated Immune Reconstitution Inflammatory Syndrome. *PloS Pathog* (2014) 10(10):e1004433. doi: 10.1371/journal.ppat.1004433
9. Barber DL, Andrade BB, Sereti I, Sher A. Immune Reconstitution Inflammatory Syndrome: The Trouble With Immunity When You had None. *Nat Rev Microbiol* (2012) 10(2):150–6. doi: 10.1038/nrmicro2712
10. Ravimohan S, Tamuhla N, Nfanyana K, Steenhoff AP, Letlhogile R, Frank I, et al. Robust Reconstitution of Tuberculosis-Specific Polyfunctional CD4+ T-Cell Responses and Rising Systemic Interleukin 6 in Paradoxical Tuberculosis-Associated Immune Reconstitution Inflammatory Syndrome. *Clin Infect Dis* (2016) 62(6):795–803. doi: 10.1093/cid/civ978
11. Tran HT, Van den Bergh R, Vu TN, Laukens K, Worodria W, Loembé MM, et al. The Role of Monocytes in the Development of Tuberculosis-Associated Immune Reconstitution Inflammatory Syndrome. *Immunobiology* (2014) 219(1):37–44. doi: 10.1016/j.imbio.2013.07.004
12. Silveira-Mattos PS, Narendran G, Akrami K, Fukutani KF, Anbalagan S, Nayak K, et al. Differential Expression of CXCR3 and CCR6 on $CD4^+$ T-Lymphocytes With Distinct Memory Phenotypes Characterizes Tuberculosis-Associated Immune Reconstitution Inflammatory Syndrome. *Sci Rep* (2019) 9(1):1502. doi: 10.1038/s41598-018-37846-3
13. Mahnke YD, Greenwald JH, DerSimonian R, Roby G, Antonelli LR, Sher A, et al. Selective Expansion of Polyfunctional Pathogen-Specific CD4(+) T Cells in HIV-1-Infected Patients With Immune Reconstitution Inflammatory Syndrome. *Blood* (2012) 119(13):3105–12. doi: 10.1182/blood-2011-09-380840
14. Antonelli LR, Mahnke Y, Hodge JN, Porter BO, Barber DL, DerSimonian R, et al. Elevated Frequencies of Highly Activated CD4+ T Cells in HIV+ Patients Developing Immune Reconstitution Inflammatory Syndrome. *Blood* (2010) 116(19):3818–27. doi: 10.1182/blood-2010-05-285080
15. Gopalan N, Santhanakrishnan RK, Palaniappan AN, Menon PA, Lakshman S, Chandrasekaran P, et al. Daily *vs.* Intermittent Antituberculosis Therapy for Pulmonary Tuberculosis in Patients With HIV: A Randomized Clinical Trial. *JAMA Intern Med* (2018) 178(4):485–93. doi: 10.1001/jamainternmed.2018.0141
16. Robin X, Turck N, Hainard A, Tiberti N, Lisacek F, Sanchez JC, et al. pROC: An Open-Source Package for R and S+ to Analyze and Compare ROC Curves. *BMC Bioinf* (2011) 12:77. doi: 10.1186/1471-2105-12-77
17. Luetkemeyer AF, Kendall MA, Nyirenda M, Wu X, Ive P, Benson CA, et al. Tuberculosis Immune Reconstitution Inflammatory Syndrome in A5221 STRIDE: Timing, Severity, and Implications for HIV-TB Programs. *J Acquir Immune Defic Syndr* (2014) 65(4):423–8. doi: 10.1097/QAI.0000000000000030
18. Sangwan J, Sen S, Gupta RM, Shanmuganandan K, Grewal RS. Immune Activation Markers in Individuals With HIV-1 Disease and Their Correlation With HIV-1 RNA Levels in Individuals on Antiretroviral Therapy. *Med J Armed Forces India* (2020) 76(4):402–9. doi: 10.1016/j.mjafi.2019.06.005
19. Piconi S, Trabattoni D, Gori A, Parisotto S, Magni C, Meraviglia P, et al. Immune Activation, Apoptosis, and Treg Activity Are Associated With Persistently Reduced CD4+ T-Cell Counts During Antiretroviral Therapy. *AIDS* (2010) 24(13):1991–2000. doi: 10.1097/QAD.0b013e32833c93ce
20. Massanella M, Negredo E, Pérez-Alvarez N, Puig J, Ruiz-Hernández R, Bofill M, et al. CD4 T-Cell Hyperactivation and Susceptibility to Cell Death Determine Poor CD4 T-Cell Recovery During Suppressive HAART. *AIDS* (2010) 24(7):959–68. doi: 10.1097/QAD.0b013e328337b957
21. Wilkinson KA, Walker NF, Meintjes G, Deffur A, Nicol MP, Skolimowska KH, et al. Cytotoxic Mediators in Paradoxical HIV-Tuberculosis Immune Reconstitution Inflammatory Syndrome. *J Immunol* (2015) 194(4):1748–54. doi: 10.4049/jimmunol.1402105
22. Hsu DC, Breglio KF, Pei L, Wong CS, Andrade BB, Sheikh V, et al. Emergence of Polyfunctional Cytotoxic CD4+ T Cells in Mycobacterium Avium Immune Reconstitution Inflammatory Syndrome in Human Immunodeficiency Virus-Infected Patients. *Clin Infect Dis* (2018) 67(3):437–46. doi: 10.1093/cid/ciy016
23. Quinn CM, Poplin V, Kasibante J, Yuquimpo K, Gakuru J, Cresswell FV, et al. Tuberculosis IRIS: Pathogenesis, Presentation, and Management Across the Spectrum of Disease. *Life (Basel)* (2020) 10(11):262. doi: 10.3390/life10110262
24. Musselwhite LW, Andrade BB, Ellenberg SS, Tierney A, Belaunzaran-Zamudio PF, Rupert A, et al. Vitamin D, D-Dimer, Interferon γ, and Scd14 Levels Are Independently Associated With Immune Reconstitution Inflammatory Syndrome: A Prospective, International Study. *EBioMedicine* (2016) 4:115–23. doi: 10.1016/j.ebiom.2016.01.016

Conflict of Interest: The authors declare that the research was conducted in the absence of any commercial or financial relationships that could be construed as a potential conflict of interest.

4.4 MANUSCRITO III

FREQUENCY OF CXCR3^{+} CD8+ T LYMPHOCYTE SUBSETS IN PERIPHERAL BLOOD IS ASSOCIATED WITH THE RISK OF PARADOXICAL TUBERCULOSIS-ASSOCIATED IMMUNE RECONSTITUION SYNDROME DEVELOPMENT IN ADVANCED HIV DISEASE

Este trabalho avaliou a relevância das células T CD8+ de memória no desenvolvimento da SIRI em indivíduos HIV-1 coinfectados com TB antes do início do tratamento e durante a manifestação de SIRI.

Resumo:
Neste estudo, determinamos as frequências dos subtipos de células T CD8+ no contexto de desenvolvimento da SIRI. Observamos que indivíduos que desenvolveram SIRI exibem maiores frequências de células T CD8+ de memória durante a manifestação da SIRI. Ademais, notamos que as frequências de células T CD8+ de memória foram correlacionadas positivamente com a carga bacilar no período pré-tratamento entre indivíduos que viriam desenvolver SIRI. Observamos também que pacientes que desenvolveram SIRI apresentavam maiores níveis de linfócitos CD8+ de memória efetora e menores frequências de linfócitos CD8+ naïve após o início do tratamento. A comparação do Δ (frequência após início da TARV subtraída pela frequência pré-TARV) revelou uma menor magnitude na expansão de células T CD8+ naïve em pacientes que manifestaram SIRI. Além disso, analises de rede baseadas em correlações de Spearman revela diferentes padrões correlação entre o Δ dos subtipos de linfócitos de memória e moléculas inflamatórias plasmáticas, sugerindo então que a reconstituição destas células nos grupos clínicos em questão está vinculada a diferentes processos de ativação celular e inflamação. Posteriormente, investigamos a expressão de CXCR3 (receptor de citocinas relacionado com a migração de células T CD8+ para tecidos inflamados) no compartimento de memória dos linfócitos na nossa população de estudo. Nossos achados sugerem diminuídas frequências de linfócitos CD8+ expressando CXCR3 em indivíduos que desenvolveram SIRI, sugerindo possivelmente a retenção destas populações celulares em tecidos persistentemente inflamados. Por fim, aplicamos técnicas de regressão logística e análise de curva ROC para avaliar a competência das frequências destas populações de linfócitos em discernir pacientes SIRI dos que não desenvolveram tal síndrome antes e após o início do tratamento. Observamos que as frequências de células T CD8+ naïve expressando CXCR3 estão independentemente associadas com uma menor probabilidade de desenvolvimento de SIRI associada a TB. Assim, o nosso estudo contribuiu para o esclarecimento de nuances da participação de células T CD8+ de memória na SIRI.

Este artigo foi publicado no periódico internacional *Frontiers in immunology* (Fator de impacto = 7.5)

frontiers | Frontiers in Immunology

ORIGINAL RESEARCH
published: 01 April 2022
doi: 10.3389/fimmu.2022.873985

Frequency of CXCR3$^+$ CD8$^+$ T-Lymphocyte Subsets in Peripheral Blood Is Associated With the Risk of Paradoxical Tuberculosis-Associated Immune Reconstitution Inflammatory Syndrome Development in Advanced HIV Disease

Rafael Tibúrcio[1,2,3†], Gopalan Narendran[4†], Beatriz Barreto-Duarte[1,2,5,6], Artur T. L. Queiroz[2,7], Mariana Araújo-Pereira[1,2,3], Selvaraj Anbalagan[4], Kaustuv Nayak[4,8], Narayanan Ravichandran[9], Rajasekaran Subramani[4], Lis R. V. Antonelli[10], Kumar Satagopan[9], Komathi Anbalagan[9], Brian O. Porter[11], Alan Sher[12], Soumya Swaminathan[4], Irini Sereti[11] and Bruno B. Andrade[1,2,3,5,6,13,14,15]*

[1] Laboratório de Inflamação e Biomarcadores, Instituto Gonçalo Moniz, Fundação Oswaldo Cruz, Salvador, Brazil, [2] Multinational Organization Network Sponsoring Translational and Epidemiological Research (MONSTER) Initiative, Salvador, Brazil, [3] Faculdade de Medicina, Universidade Federal da Bahia, Salvador, Brazil, [4] Department of Clinical Research, National Institute for Research in Tuberculosis, Chennai, India, [5] Curso de Medicina, Universidade Salvador (UNIFACS), Salvador, Brazil, [6] Programa de Pós-Graduação em Clínica Médica, Universidade Federal do Rio de Janeiro, Rio de Janeiro, Brazil, [7] Center of Data and Knowledge Integration for Health (CIDACS), Instituto Gonçalo Moniz, Fundação Oswaldo Cruz, Salvador, Brazil, [8] ICGEB-Emory Vaccine Centre, International Centre for Genetic Engineering and Biotechnology, New Delhi, India, [9] Government Hospital of Thoracic Medicine, Chennai, India, [10] Laboratório de Biologia e Imunologia de Doenças Infecciosas e Parasitárias, Instituto René Rachou, Fundação Oswaldo Cruz, Belo Horizonte, Brazil, [11] HIV Pathogenesis Section, Laboratory of Immunoregulation, National Institute of Allergy and Infectious Diseases, National Institutes of Health, Bethesda, MD, United States, [12] Immunobiology Section, Laboratory of Parasitic Diseases, National Institute of Allergy and Infectious Diseases, National Institutes of Health, Bethesda, MD, United States, [13] Wellcome Trust Centre for Infectious Disease Research in Africa, Institute of Infectious Disease and Molecular Medicine, University of Cape Town, Cape Town, South Africa, [14] Curso de Medicina, Escola Bahiana de Medicina e Saúde Pública (EBMSP), Salvador, Brazil, [15] Division of Infectious Diseases, Department of Medicine, Vanderbilt University School of Medicine, Nashville, TN, United States

Background: Tuberculosis-associated immune reconstitution inflammatory syndrome (TB-IRIS) is a clinical aggravation of TB symptoms observed among a fraction of HIV coinfected patients shortly after the start of antiretroviral therapy (ART). Of note, TB-IRIS is characterized by exacerbated inflammation and tissue damage that occurs in response to the elevated production of CD4$^+$ T cell-derived IFN-γ. Nevertheless, the possible participation of CD8$^+$ T cells in TB-IRIS development remains unclear.

Methods: We performed a comprehensive assessment of the composition of CD8$^+$ T cell memory subsets and their association with circulating inflammation-related molecules in TB-HIV coinfected patients initiating ART.

Results: We found that TB-IRIS individuals display higher frequencies of Antigen-experienced CD8$^+$ T cells during the onset of IRIS and that the levels of these cells

OPEN ACCESS

Edited by:
Daniel Scott-Algara, Institut Pasteur, France

Reviewed by:
Enrique Espinosa, Instituto Nacional de Enfermedades Respiratorias-México (INER), Mexico
Simone Gonçalves Fonseca, Universidade Federal de Goiás, Brazil

***Correspondence:**
Bruno B. Andrade
bruno.andrade@fiocruz.br

†*These authors share first authorship*

Specialty section:
This article was submitted to Inflammation, a section of the journal Frontiers in Immunology

Received: *11 February 2022*
Accepted: *14 March 2022*
Published: *01 April 2022*

Citation:
Tibúrcio R, Narendran G, Barreto-Duarte B, Queiroz ATL, Araújo-Pereira M, Anbalagan S, Nayak K, Ravichandran N, Subramani R, Antonelli LRV, Satagopan K, Anbalagan K, Porter BO, Sher A, Swaminathan S, Sereti I and Andrade BB (2022) Frequency of CXCR3$^+$ CD8$^+$ T-Lymphocyte Subsets in Peripheral Blood Is Associated With the Risk of Paradoxical Tuberculosis-Associated Immune Reconstitution Inflammatory Syndrome Development in Advanced HIV Disease. Front. Immunol. 13:873985. doi: 10.3389/fimmu.2022.873985

positively correlate with baseline mycobacterial smear grade. TB-IRIS individuals exhibited higher frequencies of effector memory and lower percentages of naïve CD8$^+$ T cells than their Non-IRIS counterparts. In both TB-IRIS and Non-IRIS patients, ART commencement was associated with fewer significant correlations among memory CD8$^+$ T cells and cells from other immune compartments. Networks analysis revealed distinct patterns of correlation between each memory subset with inflammatory cytokines suggesting different dynamics of CD8$^+$ T cell memory subsets reconstitution. TB-IRIS patients displayed lower levels of memory cells positive for CXCR3 (a chemokine receptor that plays a role in trafficking activated CD8$^+$ T cells to the tissues) than Non-IRIS individuals before and after ART. Furthermore, we found that CXCR3$^+$ naïve CD8$^+$ T cells were inversely associated with the risk of TB-IRIS development. On the other hand, we noticed that the frequencies of CXCR3$^+$ effector CD8$^+$ T cells were positively associated with the probability of TB-IRIS development.

Conclusion: Our data suggest that TB-IRIS individuals display a distinct profile of memory CD8$^+$ T cell subsets reconstitution after ART initiation. Moreover, our data point to a differential association between the frequencies of CXCR3$^+$ CD8$^+$ T cells and the risk of TB-IRIS development. Collectively, our findings lend insights into the potential role of memory CD8$^+$ T cells in TB-IRIS pathophysiology.

Keywords: TB-IRIS, immunologic memory, CD8$^+$ T cells, naïve lymphocytes, *M. tuberculosis* infection

INTRODUCTION

Mycobacterium spp infection-related diseases remain as major threats to human health, being associated with substantially high rates of morbidity and mortality worldwide, especially in developing countries (1). Noticeably, it is very well documented that humans exhibit a wide range of immune responses against *Mycobacterium tuberculosis* (Mtb) which produces a spectrum of manifestations including latent infection, subclinical disease, and both active pulmonary and extrapulmonary tuberculosis (TB) (2). Interestingly, only a fraction of individuals latently infected with Mtb will ever progress to active TB during the course of their lives. As immunity against Mtb infection occurs in a CD4$^+$ T cell-dependent fashion, Human Immunodeficiency Virus (HIV) infection considerably tips the balance towards the mitigation of host protective responses (3). Of note, HIV infection is a major risk factor for active TB development, despite the introduction and overwhelming success of combination antiretroviral therapy (ART) in recent decades (3).

Shortly after the commencement of ART, a fraction of TB-coinfected people with HIV (PWH) may manifest a paradoxical or unmasking worsening of TB symptoms associated with a considerable clinical deterioration in a reaction known as immune reconstitution inflammatory syndrome (IRIS) (4). Clinical features associated with TB-IRIS are diverse and range from mild symptoms (such as fever and lymph node enlargement) to severe respiratory, central nervous system, hematologic, and mesenteric complications, and even death (4). Mechanistically, IRIS occurs when ART-promoted reconstitution of CD4$^+$ T cells results in full activation of previously primed Mtb-harboring macrophages. This ultimately leads to an uncoordinated production of pro-inflammatory molecules and considerable inflammation-driven tissue damage (5). Identifiable risk factors for IRIS development include a high pre-ART HIV viral load, advanced immunosuppression associated with severe CD4$^+$ lymphopenia, as well as a short interval between antitubercular treatment (ATT) and ART (6).

Several reports suggest that cellular immunity mediated by both innate immune cells and CD4$^+$ T cells plays a pivotal role in TB-IRIS immunopathogenesis (7). Previous work from our group demonstrated that hyperactivation of classical (CD14^{++}CD16$^+$) monocytes before ART is associated with an increased risk of IRIS development (8). Additionally, a comprehensive assessment of functional and memory compartments of CD4$^+$ T lymphocytes also revealed distinct patterns of reconstitution during TB-IRIS onset (9). Others have suggested the possible participation of CD8$^+$ T cells in the pathogenesis of TB-IRIS, by demonstrating that activation of these cells was associated with robust protective immune responses concomitant to limited immunopathology in the context of TB-IRIS (10). Consistent with this, we have recently identified increased frequencies of cytotoxic Granzyme B-expressing (GzB$^+$) CD8$^+$ T cells in TB-IRIS patients that arguably could be a compensatory mechanism in the face of severe CD4$^+$ lymphopenia (11). Nevertheless, few reports contemplate the impact of ART-mediated reconstitution of memory CD8$^+$ T lymphocyte subsets and whether this could significantly result in an augmented risk for TB-IRIS development.

Here we sought to perform a comprehensive assessment of the memory CD8$^+$ T lymphocyte compartment in TB-IRIS. Our findings suggest an enrichment of Antigen-experienced CD8$^+$ T

cells that positively correlated to Mtb smear grades (or antigen burden) in TB-IRIS patients. Further dissection of the memory compartment revealed that these patients displayed augmented levels of effector memory cells. Of interest, by devising a Spearman correlation-based approach, we noticed differential patterns of correlation between the $CD8^+$ T cell memory compartment and surrogate markers of cellular activation and inflammation in our study population. Additionally, the magnitude of naïve $CD8^+$ T cell reconstitution after ART was substantially higher among Non-IRIS individuals when contrasted to the TB-IRIS arm of our study. Furthermore, we found that the frequencies of a subpopulation naïve $CD8^+$ T cells expressing $CXCR3^+$ were independently associated with a decreased probability of TB-IRIS development. Our findings provide insights into the potential role of $CD8^+$ T cell memory subset reconstitution in the pathogenesis of TB-IRIS.

METHODS

Ethics Statement

All clinical investigations were carried out following the principles disclosed in the Declaration of Helsinki. Written informed consent was obtained from all participants before any study procedures. This study was approved by the Scientific Advisory Committee and Institutional Ethics Committee of the National Institute for Research in Tuberculosis (Chennai) and registered on Clinicaltrials.gov (NCT00933790).

Description of the Study Population

The present study is a retrospective analysis of clinical, laboratory, and microbiologic data collected from a previously published cohort (12). The Indian TB-IRIS cohort study comprised of an observational analysis nested within a randomized controlled trial (NCT00933790) at the National Institute for Research in Tuberculosis (NIRT) in Chennai, India. HIV-1 infected patients with a recent diagnosis of sputum culture-confirmed pulmonary TB were enrolled as previously reported (12). The parent randomized controlled clinical trial primarily compared outcomes of daily versus intermittent anti-TB regimens in the aforementioned group of individuals (13). Eligibility criteria were based on patient age (above 18 years old), confirmation of rifampicin-sensitive TB, and ART-naïve status.

Clinical evaluation and blood samples were collected at pre-ART (baseline) and at the time of IRIS occurrence or equivalent time point (usually between 2 to 6 weeks following ART initiation, hereafter mentioned as timepoint 1). IRIS was diagnosed by following a modified International Network for the study of HIV-associated IRIS (INSHI) guidelines as previously described (12). This took into consideration both expected decreases in HIV plasma viral load (of at least 0.5 logs) and sputum to assess Acid-Fast Bacillus (AFB)-negativity by culture or a decline in Mtb smear grade. The baseline description of patients enrolled in the study is presented in **Supplementary Table 1**.

Measurement of Plasma Biomarkers

Concentrations of C-reactive protein (CRP) (eBioscience, San Diego, CA), Eotaxin, Fibroblast growth factor (FGF) – basic, FMS-like tyrosine kinase 3 ligand (FLT3L), Granulocyte colony-stimulating factor (G-CSF), intestinal fatty acid binding protein (I-FABP) (Hycult Biotech, The Netherlands), Interferon (IFN)-α, IFN-β, IFN-γ, Interleukin (IL)-1Ra, IL-1β, IL-2, IL-4, IL-5, IL-6, IL-7, IL-8, IL-9, IL-10, IL-12p40, IL-12p70, IL-13, IL-15, IL-17, Interferon-γ-induced protein 10 (IP-10), Monocyte chemoattractant protein (MCP)-1, Macrophage inflammatory protein (MIP)-1, MIP-1α, MIP-1β, Platelet-derived growth factor (PDGF), Regulated on activation normal T cell expressed and secreted (RANTES), soluble CD14 (sCD14), soluble CD163 (sCD163), soluble GzB, soluble Programmed cell death protein (PD) -1, soluble Tissue factor (sTF), Transforming Growth Factor (TGF)-β, Tumor Necrosis Factor (TNF)-α, and vascular endothelial growth factor (VEGF) were assessed using Luminex assay technology (Bio-Plex, Bio-Rad, Hercules, CA) were assessed in cryopreserved plasma samples maintained at −80°C.

Cell Staining and Flow Cytometry Assays

In order to dissect the immunophenotype of T cells, we evaluated markers associated with activation (HLA-DR), exhaustion (PD-1), proliferation (Ki-67), and cytotoxicity (GzB). Phenotypic identification of memory subsets was based on the expression of CD45 and CCR7 [central memory ($CD27^+CD45RO^+$), naïve ($CD27^+CD45RO^-$), effector ($CD27^-CD45RO^-$), and effector memory ($CD27^-CD45RO^+$]. Functional identification of $CD4^+$ T cells was based on the expression of CCR6 and CXCR3 receptors [Th1 ($CXCR3^+CCR6^-$), Th2 ($CXCR3^-CCR6^-$), and Th17 ($CXCR3^-CCR6^+$). Briefly, this characterization was conducted by staining aliquots of 250 µL of whole blood on the day of the participant's visit with the following antibodies: CXCR3, CD3, CD4, CD8, HLA-DR, PD-1, Ki-67, and GzB. All antibodies were obtained from eBioscience (San Diego, CA), Biolegend (San Diego, CA), BD Biosciences (San Jose, CA), and Life Technologies (Carlsbad, CA). The antibody panel was prepared in PBS with 1% BSA for 30 minutes at room temperature. Data were acquired on a BD FACS Canto II flow cytometer (BD Biosciences). All compensation and gate analyses were conducted in FlowJo 9.5.3 (TreeStar, Ashland, OR).

Network Analysis

The inferential networks were generated from Spearman correlation matrices containing values of each biomarker measured in the plasma samples and flow cytometry markers of T cell activation. All values were inputted and analyzed in the *circusplot* R package. The links shown in the networks represent statistically significant Spearman rank correlations ($P<0.05$). Additionally, we dissected the structure of networks by calculating the network density. The density measure is defined as follows: density = $L/(N\ (N-1)/2)$, in which L is the number of observed edges (i.e., Spearman correlations with $P<0.05$) and N is the total number of the nodes in the network. The density is normalized, ranging between 0 (no edges in the network) and 1

(all possible edges present). Graphics for the network analysis were customized using Adobe Illustrator 21 (Adobe Systems Inc.).

Data Analysis

Median values with IQR or frequencies of variables were compared using the Mann-Whitney *U* test (when two groups were compared) or the Kruskal-Wallis test with Dunn's multiple comparisons *ad hoc* analysis (when three groups were compared). Fisher's exact test or Chi-square tests were used to compare two or three groups, respectively, for proportions. Paired changes from before ART initiation to week 6 or the time of IRIS development were compared using the Wilcoxon matched-paired T-test. Using JMP 10.0 software, geometric mean values (log_{10}) for each marker measured at week 0 and week 6 were calculated for the entire study population. To assess the overall pattern of expression of these markers in each clinical group and timepoint, heatmaps were built using variation from the geometric mean value calculated for each candidate biomarker. Unsupervised principal component analysis was performed using the *Factorextra* R package. Unsupervised hierarchical cluster analysis using Ward's method was employed to reveal patterns of expression in plasma. Receiver operator characteristic (ROC) curve analysis was performed using the pROC package [16]. Throughout the text, a p-value of <0.05 was considered statistically significant after adjustments for multiple comparisons (Holm-Bonferroni's correction method). The statistical analyses were performed using GraphPad Prism 9.0 (GraphPad Software Inc., USA), the *ggplot2* R package (version 3.10), and STATA 9.0 (StataCorp, TX, USA).

RESULTS

TB-Iris Patients Display Higher Frequencies of Antigen-Experienced CD8$^+$ T Cells Than Non-Iris Individuals After Art Commencement

It has been demonstrated that ART-mediated immune reconstitution is associated with a robust increase in CD4$^+$ T lymphocyte frequencies in the peripheral blood following treatment initiation (9). However, whether TB co-infection impacts how quickly peripheral memory and naïve lymphocyte counts will rise after ART initiation remains unclear. In addition, little is known about the effects of immune reconstitution in the CD8$^+$ T lymphocyte memory compartment, especially in the setting of TB. Here, we sought to investigate whether ART initiation was associated with quantitative changes in the frequencies of naïve and Antigen-experienced (memory) CD8$^+$ T cells in individuals who developed TB-IRIS or not. We tested this by employing a flow cytometric approach that considered the expression of CD45RO and CCR7 to identify the following: naïve cells (CD27$^+$CD45RO$^-$) and Antigen (Ag)-experienced cells (combination of all central memory, effector, and effector memory cells). During IRIS onset, TB-IRIS participants displayed higher percentages of memory and lower percentages of naïve CD8$^+$ T cells when contrasted to Non-IRIS individuals (**Figure 1A**). Next, we assessed how Ag-experienced CD8$^+$ T cells correlate with several clinical measurements. Of note, we observed that, among IRIS patients, Ag-experienced CD8$^+$ T cells positively correlated with Mtb smear grade before ART (**Figure 1B**). Collectively, our data suggest an enrichment of memory CD8$^+$ T cells during TB-IRIS onset that correlated with antigen burden.

TB-IRIS Is Associated With Increased Percentages of Effector Memory CD8$^+$ T Cells

Next, we sought to dissect the changes in the CD8$^+$ T cell memory compartment during immune reconstitution. To compare differences in memory CD8$^+$ T cells, we employed an unsupervised hierarchical cluster analysis to depict the overall profile of each memory lymphocyte subset associated with TB-IRIS or Non-IRIS patients before and after the ART initiation. Additionally, we also applied a principal component analysis (PCA) to assess how efficiently memory CD8$^+$ T cell subsets could distinguish our study participants at each timepoint (**Figures 2A, B**). Although our PCA and hierarchical clustering revealed the existence of different profiles of CD8$^+$ T cell memory subsets in both timepoints of our study, we noticed a better separation of the patient groups at the time of IRIS occurrence. Of interest, we also noticed that these subsets were also associated with different levels of Mtb smear grade. Particularly, at both timepoints, central memory and naïve subsets were associated with lower Mtb smear grade, while effector cells were associated with higher bacillary loads. Noticeably, while we were not able to observe significant differences in the CD8$^+$ T cell memory compartment before ART, we noticed that TB-IRIS patients displayed lower rates of naïve cells and higher rates of effector memory CD8$^+$ T cells after treatment (**Figure 2C**). Altogether, our data suggest the immunopathogenesis of TB-IRIS could be associated with a predominance of effector memory CD8$^+$ T cells and concomitant lower naïve cells after ART in co-infected patients.

CD8$^+$ T Lymphocyte Memory Subsets Correlate With Distinct Profiles of Cellular Activation in Non-Iris And TB-Iris Participants

It is well known that immune activation plays a deleterious role in chronic untreated HIV infection which can lead to aberrant reconstitution of the memory lymphocyte compartment and an augmented risk for IRIS development (14). Bearing this in mind, we sought to investigate the patterns of correlation between memory CD8$^+$ T cell subsets and other innate and adaptive immune cells in our cohort of TB/HIV co-infected individuals before and after ART commencement. We noticed that, in both studied groups, memory CD8$^+$ T cells displayed a high number of correlations with other immune cells before treatment initiation (**Figure 3**).

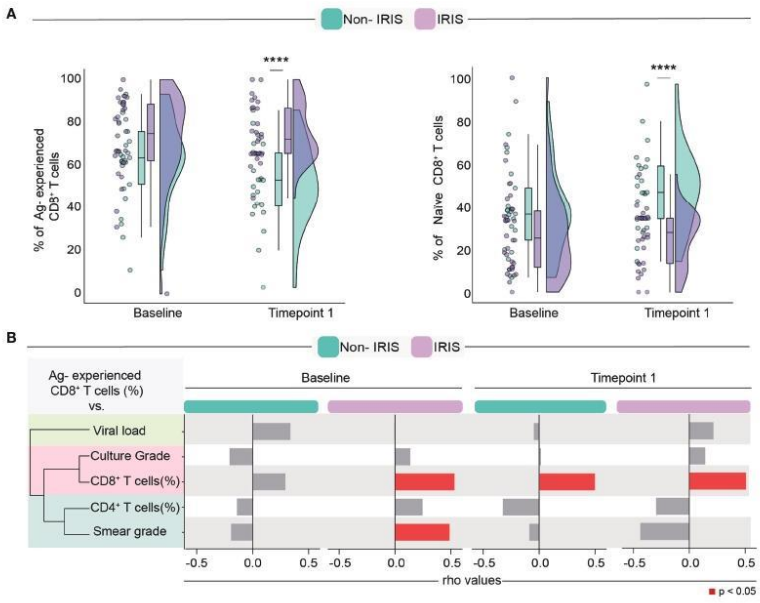

FIGURE 1 | Assessment of Antigen-experienced CD8$^+$ T cells before and after ART commencement. **(A)** Comparison of frequencies of Antigen-experienced and naïve CD8 T cells. **(B)** Spearman correlation analysis between Antigen-experienced CD8$^+$ T cell frequencies and surrogate clinical parameters at both timepoints. Data were analyzed using the Mann-Whitney test or Wilcoxon matched-pairs test for paired analyses within each study group (****p < 0.0001).

Before ART, Non-IRIS participants exhibited a higher number of correlations between memory CD8$^+$ T cells and other immune cells than their TB-IRIS counterparts. Specifically, Ag-experienced CD8$^+$ T cells showed strong correlations with proliferating (Ki-67$^+$) CD8$^+$ and CD4$^+$ T cells, cytotoxic (GzB$^+$) CD4$^+$ T cells, Th1 and Th2 CD4$^+$ T cells, central memory CD4$^+$ T cells, as well as total and PD-1$^+$ T regulatory (T reg) cells, and effector CD4$^+$ T cells.

In the TB-IRIS group, pre-ART frequencies of Ag-experienced CD8$^+$ T cells displayed fewer correlations with other immune cells. Ag-experienced cells were correlated with central memory and effector memory CD4$^+$ T cells, and PD-1$^+$ Tregs. Conversely, naïve CD8$^+$ T cells from TB-IRIS patients showed a high number of significant correlations. Naïve CD8$^+$ T cells negatively correlated with the total number of CD8$^+$ T cells, GzB$^+$ CD8$^+$ and CD4$^+$ lymphocytes, activated and Ki67$^+$ CD4$^+$ and effector memory CD4$^+$ T cells, while positively correlated with the frequencies of naïve CD4$^+$ T cells.

After treatment initiation, Non-IRIS individuals exhibited positive correlations between central memory CD8$^+$ T cells and PD-1$^+$ CD8$^+$, activated CD4$^+$, and Th17 T cells. In this same group, naïve CD8$^+$ T cells were negatively correlated with the total number of CD8$^+$ and GzB$^+$ T lymphocytes as well as central memory CD4$^+$ T cells. Among TB-IRIS individuals, naïve CD8$^+$ T cells displayed several negative associations with total frequency of CD8$^+$ T cells, GzB$^+$ CD8$^+$ T cells, activated and proliferating CD4$^+$ T cells, and effector memory CD4$^+$ T cells. Effector memory CD8$^+$ T cells showed strong positive correlations with the total frequency of CD8$^+$ T cells, Tregs, and activated Tregs. Conversely, we were able to detect negative correlations between these cells and PD-1$^+$ T regs in this same group of patients. In summary, our observations suggest substantial differences in associations among CD8$^+$ T cell memory subsets and markers of cellular activation during immune reconstitution in our study population.

The Magnitude of Memory Subset Variation Differently Correlates With Inflammatory Molecules in Non-Iris And TB-Iris Patients

Next, we wished to examine the variation of memory CD8$^+$ T lymphocyte subsets following treatment initiation in our study population. We found that the degree of variation (Δ [the absolute number of cells at timepoint 1 minus the baseline counts]) of naïve CD8$^+$ T cells was higher in Non-IRIS patients compared with TB-IRIS (**Figure 4A**). We could not detect significant variations when examining the other subsets of memory CD8$^+$ T cells. These results prompted us to

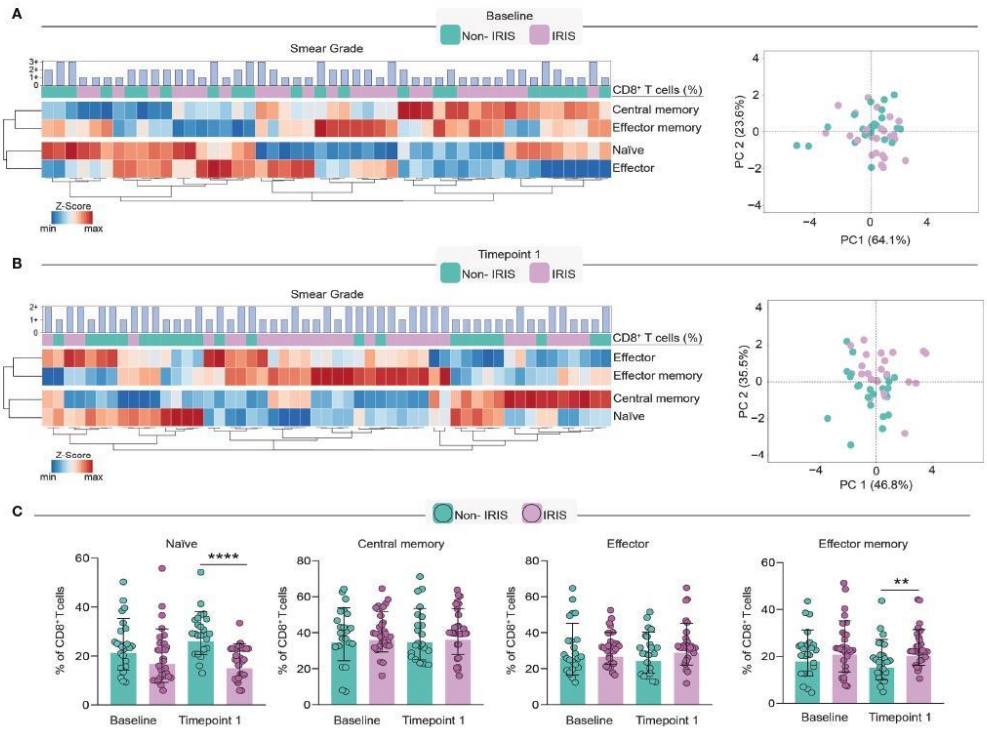

FIGURE 2 | Evaluation of CD8$^+$ T cell memory subsets in TB-IRIS pathogenesis. In order to dissect the memory subset of CD8$^+$ T cells, we employed a heatmap coupled with hierarchical cluster analysis (Ward's method) and principal component analysis at baseline **(A)** and timepoint 1 **(B)**. Principal component analysis was performed considering the frequencies of CD8$^+$ T cell memory subsets at the aforementioned time points. Scatterplots depict the frequencies of each memory subset within total CD8$^+$ T cell counts. **(C)** Comparison of frequencies of memory subsets in TB-IRIS and Non-IRIS patients. Data were analyzed using the Mann-Whitney test or Wilcoxon matched-pairs test for paired analyses within each study group (**p < 0.01, ****p < 0.0001).

investigate whether the magnitude of this variation of memory subsets correlated with the pre-ART abundance of several inflammatory mediators.

Among Non-IRIS patients, we observed that the Δ of naïve CD8$^+$ T cells positively correlated with the level of FGF basic and negatively correlated with soluble Tissue factor (sTF) (**Figure 4B**). Additionally, we observed that Δ of central memory cells displayed negative correlations with RANTES and positive correlations with both TGF-β and sTF. Interestingly, the Δ of effector CD8$^+$ T cells from Non-IRIS participants correlated negatively with TGF-β, sTF, IFN-β, IL-1β, IL-4, and PDGF levels, while exhibiting a positive correlation with RANTES. Of note, in this same group, the Δ of effector memory cells correlated positively with sTF and TGF-β.

Concerning TB-IRIS participants, we detected that the Δ of naïve CD8$^+$ T cells correlated positively with intestinal fatty acid-binding protein (IFABP). Of note, we noticed that the variation of central memory T cells was positively correlated with IFN-α and IP-10, while negatively associated with IL-2, IL-5, and IL-13. Additionally, we found that the Δ of effector memory cells were correlated with sCD163, MIP-1a, and MIP-1b, whereas the variation of effector cells displayed correlations with IFN-α, IL-2, IL-5, IL-13, IP-10, and IFN-β.

Collectively, our observations suggest that the magnitude of memory CD8$^+$ T lymphocyte subset reconstitution displays different correlation patterns with inflammatory mediators in TB-IRIS patients, which may have implications for the pathology of TB-IRIS.

Non-Iris Patients Display Sustained Higher Frequencies of CXCR3$^+$CD8$^+$ T Cells Than Their TB-Iris Counterparts

We next ascertained whether the distinct composition of the CD8$^+$ T cell memory compartment seen between TB-IRIS and Non-IRIS

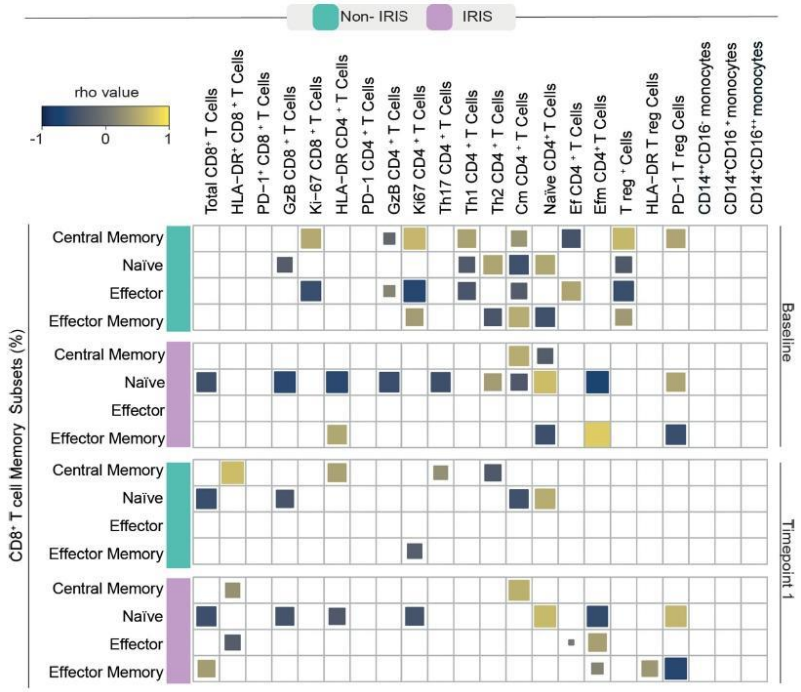

FIGURE 3 | Spearman correlations between CD8+ T cell memory subsets and activated adaptive and innate immune cells. A Spearman-based correlation matrix was employed to depict the strength of association among percentages of the memory subsets of CD8+ T cells and the frequency of other activated immune cells at Baseline (before ART) and after approximately 2 to 6 weeks following ART initiation (timepoint 1) for Non-IRIS and TB-IRIS subjects. Statistically significant correlations ($P < 0.05$) after adjustment for multiple measurements are highlighted as yellow squares (positive correlations) or blue squares (negative correlations).

groups was related to a differential commitment to an effector fate during IRIS onset. To evaluate this possibility, we employed a flow cytometric approach to measuring the expression of CXCR3+ in the memory subsets of CD8+ T cells. Of note, CXCR3 is a chemokine receptor that plays a role in trafficking activated CD8+ T cells to peripheral tissues (15). We observed that Non-IRIS individuals displayed higher levels of total CD8+ T cells expressing CXCR3+ before and after ART commencement (**Figure 5A**). A similar pattern of CXCR3+ expression was seen in naïve CD8+ T cells. Furthermore, the start of ART was associated with an increase in CXCR3+ expression in both groups. Interestingly, we also noted higher frequencies of CXCR3+ central memory CD8+ T cells in Non-IRIS patients than in TB-IRIS patients.

Subsequently, we sought to correlate the expression of CXCR3+ memory subsets with circulating levels of several cytokines and chemokines (**Figure 5B**). Preceding ART, CXCR3+ central memory cells displayed strong positive correlations with TGF-β, IL-4, IL-17, PDGF, and sTF levels in Non-IRIS individuals. This same correlation pattern was seen in TB-IRIS; however, the magnitudes of the Spearman correlations were considerably lower. Of interest, the number of CXCR3+ naïve T cells correlated positively with IFN-β, TGF-β, IL-4, and PDGF levels, while correlating negatively with RANTES. We could not detect any significant correlation between CXCR3+ effector T cells and the measured inflammatory molecules. Conspicuously, after the start of ART, the number and magnitude of correlations among CXCR3+ memory T cells and inflammatory mediators were considerably reduced in both groups. Particularly, we noticed that the number of CXCR3+ naïve T cells negatively correlated with sGzB and TNF-α levels in Non-IRIS patients. Among TB-IRIS patients, CXCR3+ central memory cells negatively correlated with PDGF levels. Together, these findings suggest strong associations between CXCR3+ memory CD8+ T cells and inflammation-related biomarkers, which could comprise important immunologic networks that play a crucial role in TB-IRIS development.

We also wished to evaluate whether delayed ART following ATT initiation could impact the frequencies of CXCR3+ memory CD8+ T cells. We noted that, in the entire study population, time to ART was positively correlated with pre-ART frequencies of

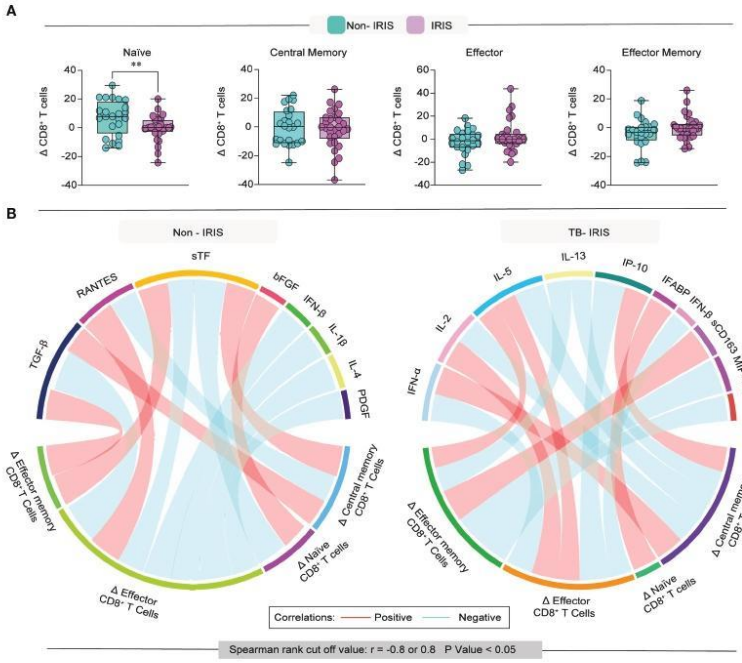

FIGURE 4 | Evaluation of the degree of immune reconstitution in memory CD8⁺ T cells. **(A)** Boxplot depicts the delta (frequency timepoint 1 – frequency baseline) of each memory subset in our study population. **(B)** Network analysis of CD8 T cell memory subsets and association with inflammation-related molecules; correlation matrices were developed with bootstrap (100 ×). Networks depicting only significant correlations ($p < 0.05$). Data were analyzed using the T-test (**$p < 0.01$).

naïve and central memory CD8⁺ T cells expressing CXCR3 (**Supplementary Figure 1**). Remarkably, time to ART was positively correlated with the frequency of CXCR3⁺ central memory CD8+ T cells in the Non-IRIS group at timepoint 1. Additionally, we also observed that patients who initiated ART more than 4 weeks after ATT initiation showed augmented frequencies of all memory CD8⁺ subsets expressing CXCR3 after up at timepoint 1 (**Supplementary Figure 1**). In summary, our results highlight that delayed ART initiation is associated with an enrichment of CXCR3⁺ CD8⁺ T cells with possible implications in TB-IRIS pathogenesis.

The Frequencies of CXCR3⁺ Memory CD8⁺ T Cell Subsets Are Differently Associated With the Risk of TB-Iris Development

Next, we broadened the scope of our analysis to evaluate whether the frequency of CXCR3⁺ memory CD8⁺ T lymphocyte subsets could predict and/or diagnose TB-IRIS in our study population. We first employed ROC curve analysis to assess the power of discrimination based on CXCR3⁺ expression at baseline and timepoint 1 (approximately 2 to 6 weeks after ART start) (**Figure 6A**). Of note, we found that the total frequency of CXCR3⁺ CD8⁺ T cells could discriminate TB-IRIS from Non-IRIS subjects at both timepoints. Importantly, our ROC curves analysis obtained high AUC values for CXCR3⁺ central memory cell frequency at timepoint 1, further highlighting its potential diagnostic potential. Additionally, the frequencies of naïve CD8⁺ T cells expressing CXCR3⁺ were also statistically significant at distinguishing our patients at both timepoints.

Next, we applied a multivariate regression model using the pre-ART frequencies of CXCR3⁺ memory CD8⁺ T cells to predict TB-IRIS (**Figure 6B**). After adjustment for pre-ART CD4⁺ T cell counts, viral load, smear grade, and the time between ATT and ART, we found that baseline frequencies of CXCR3⁺ naïve CD8⁺ T cells were independently associated with a lower odds ratio of TB-IRIS development (OR, 0.885 [95% CI (0.795 – 0.985)]). On the other hand, the pre-ART percentages of CXCR3⁺ effector CD8⁺ T cells were associated with a higher risk of TB-IRIS (OR, 1.381 [95% CI (1.044 – 1.826)]).

Additionally, by applying the same model to the frequencies of CXCR3⁺ memory CD8⁺ T cells at timepoint 1, we noted that increased frequencies of CXCR3⁺ naïve CD8⁺ T cells were associated with reduced risk of TB-IRIS development (OR, 0.860 [95% CI (0.758 – 0.976)]). Conversely, we found that

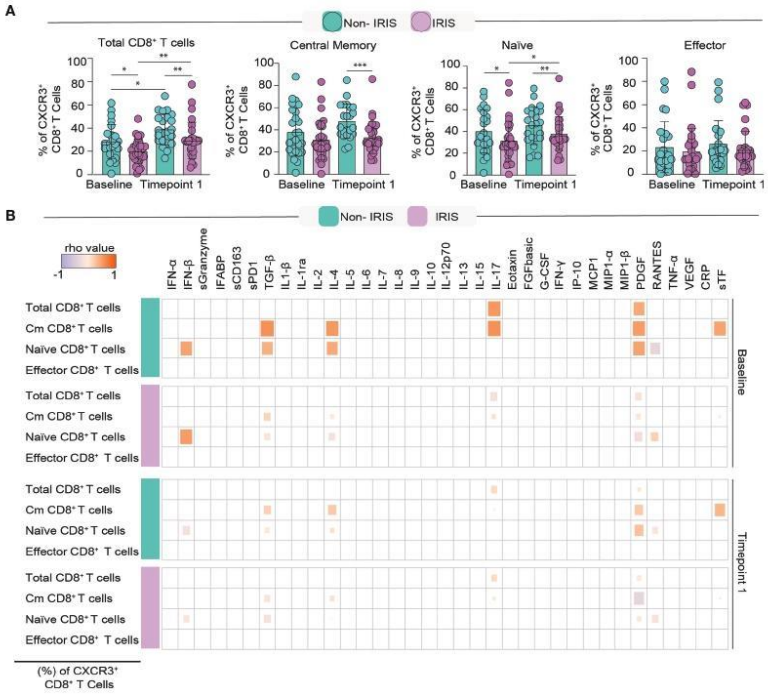

FIGURE 5 | Assessment of CXCR3$^+$ memory CD8$^+$ T cells in TB-IRIS and Non-IRIS individuals. **(A)** Frequencies of CXCR3$^+$ in each memory compartment of CD8$^+$ T cells. **(B)** A Spearman-based correlation matrix was employed to depict the strength of association among percentages of the memory subsets of CD8$^+$ T cells and the concentration of pre-ART inflammatory molecules in Non-IRIS and TB-IRIS subjects. Statistically significant correlations ($P < 0.05$) after adjustment for multiple measurements are highlighted as orange squares (positive correlations) or purple squares (negative correlations). $^*p < 0.05$, $^{**}p < 0.01$, $^{***}p < 0.001$.

higher percentages of CXCR3$^+$ effector CD8$^+$ T cells were independently associated with a higher risk of TB-IRIS (OR, 1.116 [95% CI (1.028 – 1.213)]). Collectively, our data suggest that the abundance of CXCR3$^+$ subpopulations of naïve and memory CD8$^+$ T cells could be employed to assess the risk of TB-IRIS development.

DISCUSSION

In our current investigation, we sought to examine the alterations in the CD8$^+$ T lymphocyte memory compartment in the face of ART-mediated immune reconstitution in highly immunosuppressed TB-HIV coinfected individuals. Here, we report an inverse association between the frequencies of naïve CXCR3$^+$ CD8$^+$ T cells and the probability of TB-associated IRIS occurrence. Conversely, we also detected that the frequencies of the CXCR3$^+$ effector CD8$^+$ T cell subset were associated with an increased risk of TB-IRIS. There is robust evidence on the contributions of CD8$^+$ T cells in the mobilization of appropriate immune responses in several infectious diseases, including HIV infection and TB (16–18). A previous study by our group addressed the nuances of T lymphocyte activation in TB-IRIS development and outlined the participation of cytotoxic CD8$^+$ T cells during ART-promoted immune reconstitution (11).

It has been demonstrated that immunological memory, a distinguishing feature of the immune system in eliciting more robust responses upon antigen re-encounter, plays a role in the immunopathogenesis of several diseases and vaccination (19–22). Our working hypothesis is that TB-IRIS patients experience an aberrant reconstitution of CD8$^+$ T cell memory subsets after ART, which arguably could contribute to the amplification of uncontrolled lung inflammation and tissue damage. We noticed that TB-IRIS patients displayed a higher prevalence of these cells that were correlated with higher Mtb bacillary burden before ART and these individuals also exhibited lower rates of naïve CD8$^+$ T cells. These findings are in agreement with those previously found by our group when investigating the memory compartment of CD4$^+$ T cells (9). More specifically, our findings suggest an enrichment of effector

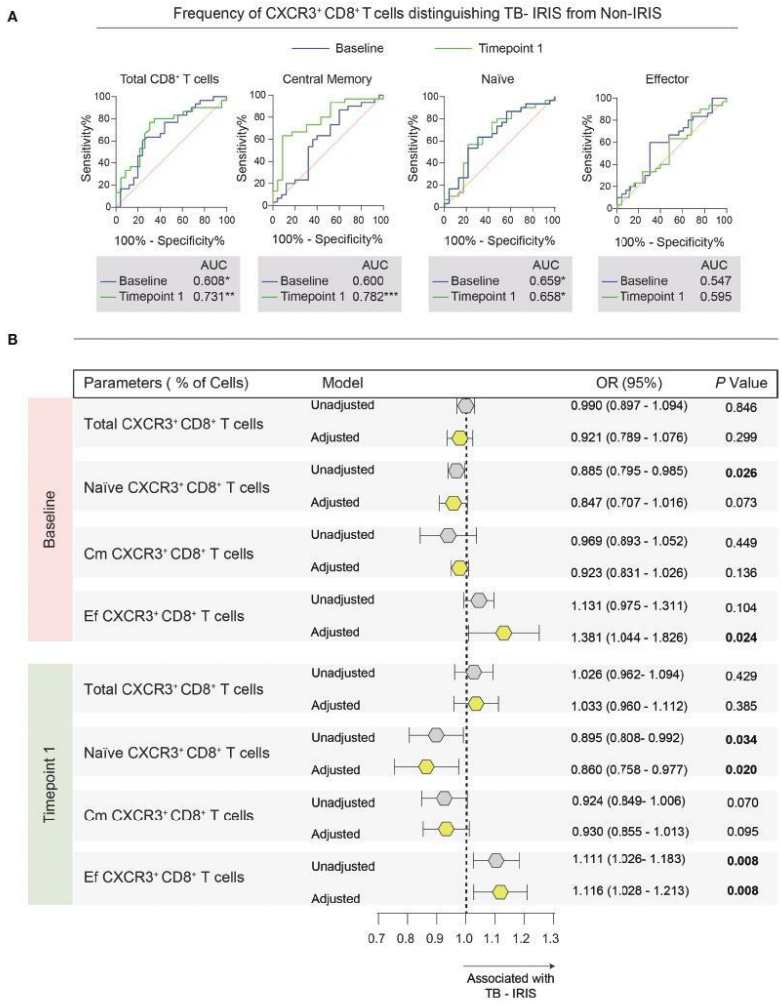

FIGURE 6 | Association between memory CD8+ T cell subsets expressing CXCR3 and the risk of TB-IRIS development. **(A)** Receiver operator characteristic (ROC) curves were employed to discriminate TB-IRIS from Non-IRIS patients at both timepoints taking into account the frequency of each flow cytometric population. **(B)** Multivariate regression analysis to evaluate the association between the frequencies of CXCR3+ memory CD8+ T cells and *Mycobacterium tuberculosis* immune reconstitution inflammatory syndrome (TB-IRIS). The multivariate model included the following variables: CD4+ T cell counts, viral load, smear grade, and the number of days between ATT and ART initiation. Odds ratios (OR) represent the 95% confidence interval increase in the frequency of each lymphocyte population. P values are shown in bold. Gray polygons represent unadjusted models, while yellow ones represent adjusted models.

memory CD8+ T cells in TB-IRIS patients during the occurrence of IRIS, which may represent the presence of clonally expanded CD8+ T cells that are specific for Mtb antigens. Further studies to assess whether these populations of effector memory CD8+ T cells exhibit a more cytotoxic phenotype are warranted.

Our group has previously demonstrated that pre-ART cellular activation predisposes individuals to TB-IRIS (8, 11). Notably, TB-IRIS and Non-IRIS patients differed substantially in the number of correlations found before ART initiation. This could be explained by CD8+ T cells playing a pivotal role in

orchestrating different immunologic responses in these distinct settings of severe immunosuppression. Likewise, this could be interpreted as a compensatory mechanism in which $CD8^+$ memory T cells take a central stage in maintaining homeostasis during the processes of immune reconstitution. Particularly, central memory T cells correlated positively with cycling $CD4^+$ and $CD8^+$ T cells as well as total and exhausted Tregs among Non-IRIS individuals. Conversely, at timepoint 1, TB-IRIS patients displayed more significant correlations, especially with memory $CD4^+$ T cells and T regs.

Spearman correlation analysis revealed that the magnitude of memory subset variation between TB-IRIS and Non-IRIS patients displayed different correlational patterns with inflammatory mediators. On one hand, we find that the immune reconstitution of memory T cell compartments in the Non-IRIS group was more heterogeneous, displaying correlations with the pre-ART abundance of both anti- and pro-inflammatory molecules (especially TGF- β, IL-4, sTF, and IFN-β). On the other hand, among TB-IRIS the variation in memory T cell subsets exhibited a higher number of correlations with inflammatory mediators. These results seem in good agreement with previous reports of increases of Th1 inflammatory mediators (namely IL-2, IFNs, TNF-α) in TB-IRIS (23, 24). One could argue that aberrant reconstitution of memory $CD8^+$ T lymphocyte compartment in the face of persistently high bacillary burden is coupled with both detrimental inflammation and clinical deterioration seen in TB-IRIS patients.

We also wished to ascribe whether the observed heterogeneity in memory compartment reconstitution between our study groups was due to *de novo* differentiation of naïve T cells in the face of $CD4^+$ T cell rise or to a redistribution of previously differentiated memory $CD8^+$ T cells from lymphoid tissues to the hematogenous compartment. Regarding the quantitative recovery of $CD4^+$ T cells, it has been to occur in two main phases. The first phase, which happens from 1 to up to 6 months after treatment initiation, is characterized by the redistribution of memory T cells that were trapped in lymphoid organs to the periphery, coupled with a substantial reduction in viral load, whereas the other phase can last many years and is characterized by a slow and gradual increase of $CD4^+$ cells (25). Along these lines, it has been suggested that the levels of $CD8^+$ T cells also rise in the circulation after treatment due to non-specific redistribution (23). Our analysis of $CD8^+$ T cells expressing $CXCR3^+$, a chemokine receptor largely recognized for directing cells to sites of inflammation, revealed that Non-IRIS patients display higher rates of $CXCR3^+$ cells in the periphery before and after treatment. One could speculate that the lower degree of $CXCR3^+$ circulating $CD8^+$ T cells among TB-IRIS patients reflects retention of these cells in persistently inflamed lymphoid tissues. More specifically, one could hypothesize that Mtb- harboring cells, more predominant in TB-IRIS patients at IRIS onset, could produce higher amounts of $CXCR3^+$ ligands (ie. CXCL9, C XCL10, CXCL-11), therefore increasing the trafficking of $CXCR3^+$ $CD8^+$ T cells into sites of inflammation. The abundance of $CXCR3^+$ ligands in the settings of TB-IRIS and the identification of cell populations that secrete them are warranted to be conducted.

The limitations of our study include the small number of patients included in our study cohort with a large number of comparisons and the lack of functional assays to assess cells. Another important limitation is the lack of tissue, to evaluate T-cells in areas of infection and inflammation. The strengths of our study include the selection of a well-described cohort of patients who were not previously treated for either HIV infection or TB, had close clinical follow up along with detailed microbiologic evaluation and same day flow cytometric analysis before the administration of anti-inflammatory medications at the IRIS timepoint. Taken together, our findings provide significant insight into the role of immunological memory of $CD8^+$ T cells in the immunopathogenesis of TB-IRIS.

DATA AVAILABILITY STATEMENT

The raw data supporting the conclusions of this article will be made available by the authors, without undue reservation.

ETHICS STATEMENT

The studies involving human participants were reviewed and approved by Scientific Advisory Committee and Institutional Ethics Committee of the National Institute for Research in Tuberculosis (Chennai) and registered on Clinicaltrials.gov (NCT00933790). The patients/participants provided their written informed consent to participate in this study.

AUTHOR CONTRIBUTIONS

BA, IS, SS, BP, and AS conceptualized the study. BA and IS supervised the immunological study. GN and SS supervised the clinical study. IS, SS, and AS acquired funding for research. GN, RS, KS, BP, IS, and BA performed the clinical assessments. SA, KN, KA, BA, and LA performed the experiments. RT, BB-D, MA-P, and AQ analyzed the data. RT and BA drafted the first version of the manuscript. All the authors revised the manuscript.

FUNDING

This work received support from the Intramural Research Program of the National Institute of Allergy and Infectious Diseases (NIAID/NIH) and by the Intramural-to-India grant from the US-India Co-operative research program. This study was also financed in part by Coordenação de Aperfeiçoamento de Pessoal de Nível Superior (CAPES) (Finance Code 001). The work of BA is supported by the Intramural Research Program of the Oswaldo Cruz Foundation (FIOCRUZ) and the National Council for Scientific and Technological Development (CNPq), Brazil. RT, MA-P and BB-D were supported by Ph.D. fellowships from CAPES.

ACKNOWLEDGMENTS

The authors thank Mrs. Elze Leite (FIOCRUZ, Brazil) for logistics and administrative support. We wholeheartedly appreciate the precious scientific contributions of Dr. Sudha Subramanyam (NIRT, India) to this work. The authors also thank all the study participants.

SUPPLEMENTARY MATERIAL

The Supplementary Material for this article can be found online at: https://www.frontiersin.org/articles/10.3389/fimmu.2022.873985/full#supplementary-material

Supplementary Figure 1 | Expression of CXCR3$^+$ in memory CD8$^+$ T cells from patients that initiated ART with more or less than 4 weeks difference from ATT initiation. We employed a hierarchical cluster analysis of z-score normalized values of CXCR3$^+$ memory CD8$^+$ T lymphocytes at Baseline **(A)** and at timepoint 1 **(B)**. The right panel depicts Spearman correlation coefficient values between time from ATT to ART initiation vs. the frequency of indicated parameters. **(C)** Violin plots represent the frequencies of each CXCR3$^+$ memory CD8$^+$ T cell in our study groups. Data were analyzed using the Mann-Whitney test or Wilcoxon matched-pairs test for paired analyses within each study group (**$p < 0.01$, ****$p < 0.0001$). Data were analyzed using the Mann-Whitney test or Wilcoxon matched-pairs test for paired analyses within each study group (* $p < 0.05$, **$p < 0.01$, ***$p < 0.001$, ****$p < 0.0001$).

Supplementary Table 1 | Characteristics of the study participants.

Supplementary Table 2 | Antibody Panel used to assess CD8$^+$ T lymphocyte memory subset.

REFERENCES

1. World Health Organization. *Global Tuberculosis Report 2015*. Paris, France: WHO (2015).
2. Pai M, Behr MA, Dowdy D, Dheda K, Divangahi M, Boehme CC, et al. Tuberculosis. *Nat Rev Dis Primers* (2016) 2:16076. doi: 10.1038/nrdp.2016.76
3. Havlir DV, Getahun H, Sanne I, Nunn P. Opportunities and Challenges for HIV Care in Overlapping HIV and TB Epidemics. *JAMA* (2008) 300:423–30. doi: 10.1001/jama.300.4.423
4. Vinhaes CL, Araujo-Pereira M, Tibúrcio R, Cubillos-Angulo JM, Demitto FO, Akrami KM, et al. Systemic Inflammation Associated With Immune Reconstitution Inflammatory Syndrome in Persons Living With HIV. *Life (Basel)* (2021) 11(1):65. doi: 10.3390/life11010065
5. Barber DL, Andrade BB, Sereti I, Sher A. Immune Reconstitution Inflammatory Syndrome: The Trouble With Immunity When You Had None. *Nat Rev Microbiol* (2012) 10(2):150–6. doi: 10.1038/nrmicro2712
6. Gopalan N, Andrade BB, Swaminathan S. Tuberculosis-Immune Reconstitution Inflammatory Syndrome in HIV: From Pathogenesis to Prediction. *Expert Rev Clin Immunol* (2014) 10(5):631–45. doi: 10.1586/1744666X.2014.892828
7. Esmail H, Riou C, Bruyn ED, Lai RP, Harley Y, Meintjes G, et al. The Immune Response to Mycobacterium Tuberculosis in HIV-1-Coinfected Persons. *Annu Rev Immunol* (2018) 36:603–38. doi: 10.1146/annurev-immunol-042617-053420
8. Andrade BB, Singh A, Narendran G, Schechter ME, Nayak K, Subramanian S, et al. Mycobacterial Antigen-Driven Activation of CD14++CD16- Monocytes Is a Predictor of Tuberculosis-Associated Immune Reconstitution Inflammatory Syndrome. *PloS Pathog* (2014) 10(10):e1004433. doi: 10.1371/journal.ppat.1004433
9. Silveira-Mattos PS, Narendran G, Akrami K, Fukutani KF, Anbalagan S, Nayak K, et al. Differential Expression of CXCR3 and CCR6 on CD4$^+$ T-Cells With Distinct Memory Phenotypes Characterizes Tuberculosis-Associated Immune Reconstitution Inflammatory Syndrome. *Sci Rep* (2019) 9(1):1502. doi: 10.1038/s41598-018-37846-3
10. Espinosa E, Romero-Rodríguez DP, Cantoral-Díaz MT, Reyes-Terán G. Transient Expansion of Activated CD8(+) T Cells Characterizes Tuberculosis-Associated Immune Reconstitution Inflammatory Syndrome in Patients With HIV: A Case-Control Study. *J Inflamm (Lond)* (2013) 10:21. doi: 10.1186/1476-9255-10-21
11. Tibúrcio R, Barreto-Duarte B, Naredren G, Queiroz ATL, Anbalagan S, Nayak K, et al. Dynamics of T-Lymphocyte Activation Related to Paradoxical Tuberculosis-Associated Immune Reconstitution Inflammatory Syndrome in Persons With Advanced HIV. *Front Immunol* (2021) 12:757843. doi: 10.3389/fimmu.2021.757843
12. Narendran G, Andrade BB, Porter BO, Chandrasekhar C, Venkatesan P, Menon PA, et al. Paradoxical Tuberculosis Immune Reconstitution Inflammatory Syndrome (TB-IRIS) in HIV Patients With Culture Confirmed Pulmonary Tuberculosis in India and the Potential Role of IL-6 in Prediction. *PloS One* (2013) 8(5):e63541. doi: 10.1371/journal.pone.0063541
13. Gopalan N, Santhanakrishnan RK, Palaniappan AN, Menon PA, Lakshman S, Chandrasekaran P, et al. Daily *vs.* Intermittent Antituberculosis Therapy for Pulmonary Tuberculosis in Patients With HIV: A Randomized Clinical Trial. *JAMA Intern Med* (2018) 178(4):485–93. doi: 10.1001/jamainternmed.2018.0141
14. Boulougoura A, Sereti I. HIV Infection and Immune Activation: The Role of Coinfections. *Curr Opin HIV AIDS* (2016) 11(2):191–200. doi: 10.1097/COH.0000000000000241
15. Groom JR, Luster AD. CXCR3 in T Cell Function. *Exp Cell Res* (2011) 317(5):620–31. doi: 10.1016/j.yexcr.2010.12.017
16. Collins DR, Gaiha GD, Walker BD. CD8$^+$ T Cells in HIV Control, Cure, and Prevention. *Nat Rev Immunol* (2020) 20(8):471–82. doi: 10.1038/s41577-020-0274-9
17. Lin PL, Flynn JL. CD8 T Cells and Mycobacterium Tuberculosis Infection. *Semin Immunopathol* (2015) 37(3):239–49. doi: 10.1007/s00281-015-0490-8
18. Prezzemolo T, Guggino G, La Manna MP, Di Liberto D, Dieli F, Caccamo N. Functional Signatures of Human CD4 and CD8 T Cell Responses to Mycobacterium Tuberculosis. *Front Immunol* (2014) 5:2014.00180. doi: 10.3389/fimmu.2014.00180
19. Ratajczak W, Niedźwiedzka-Rystwej P, Tokarz-Deptuła B, Deptuła W. Immunological Memory Cells. *Central-European J Immunol* (2018) 43(2):194–203. doi: 10.5114/ceji.2018.77390
20. Principe N, Kidman J, Goh S, Tilsed CM, Fisher SA, Fear VS, et al. Tumor-Infiltrating Effector Memory Antigen-Specific CD8$^+$ T Cells Predict Response to Immune Checkpoint Therapy. *Front Immunol* (2020) 11:2020.584423. doi: 10.3389/fimmu.2020.584423
21. Ribeiro SP, Milush JM, Cunha-Neto E, Kallas EG, Kalil J , Somsouk M, et al. The CD8$^+$Memory Stem T Cell (T(SCM)) Subset Is Associated With Improved Prognosis in Chronic HIV-1 Infection. *J Virol* (2014) 88(23):13836–44. doi: 10.1128/JVI.01948-14
22. Jung JH, Rha MS, Sa M, Choi HK, Jeon JH, Seok H, et al. SARS-CoV-2-Specific T Cell Memory Is Sustained in COVID-19 Convalescent Patients for 10 Months With the Successful Development of Stem Cell-Like Memory T Cells. *Nat Commun* (2021) 12(1):4043. doi: 10.1038/s41467-021-243771
23. Bourgarit A, Carcelain G, Martinez V, Lascoux C, Delcey V, Gicquel B, et al. Explosion of Tuberculin-Specific Th1-Responses Induces Immune Restoration Syndrome in Tuberculosis and HIV Co-Infected Patients. *AIDS (Lond Engl)* (2006) 20(2):F1–7. doi: 10.1097/01.aids.0000202648.18526.bf
24. Guihot A, Bourgarit A, Carcelain G, Autran B. Immune Reconstitution After a Decade of Combined Antiretroviral Therapies for Human Immunodeficiency Virus. *Trends Immunol* (2011) 32(3):131–7. doi: 10.1016/j.it.2010.12.002
25. Meintjes G, Wilkinson KA, Rangaka MX, Skolimowska K, van Veen K, Abrahams M, et al. Type 1 Helper T Cells and FoxP3-Positive T Cells in HIV-Tuberculosis-Associated Immune Reconstitution Inflammatory Syndrome. *Am J Respir Crit Care Med* (2008) 178(10):1083–9. doi: 10.1164/rccm.200806-858OC

Conflict of Interest: The authors declare that the research was conducted in the absence of any commercial or financial relationships that could be construed as a potential conflict of interest.

Publisher's Note: All claims expressed in this article are solely those of the authors and do not necessarily represent those of their affiliated organizations, or those of the publisher, the editors and the reviewers. Any product that may be evaluated in this article, or claim that may be made by its manufacturer, is not guaranteed or endorsed by the publisher.

5 **DISCUSSÃO**

A compreensão dos fenômenos imunopatogênicos da SIRI associa à tuberculose é essencial para o desenvolvimento de ferramentas prognósticas e diagnósticas mais eficientes, assim como para melhorar o manejo de pacientes infectados pelo HIV-1 durante o início do TARV. Sabe-se que perturbações metabólicas são subjacentes às alterações qualitativas das funções de diversas células imunológicas, culminando na exacerbação da inflamação sistêmica e hiperativação celular. No cerne dos processos patológicos da SIRI, encontram-se os linfócitos T que elicitam respostas imunológicas robustas contra patógenos oportunistas durante o evento de reconstituição numérica e funcional das populações linfocitárias. Neste contexto, o presente estudo buscou investigar fatores que influenciam a deflagração de distúrbio inflamatórios sistêmicos e a relevância do processo de ativação e formação de memória imunológica de linfócitos T em pacientes com SIRI associada a TB. Conjuntamente, os três trabalhos apresentados apontam nuances patológicas da SIRI com potencial relevância em intervenções clínicas.

Uma das quintessências imunológicas da infecção pelo HIV-1 é a progressiva depleção de células T $CD4^+$ acoplada à gradual elevação do estado de ativação do sistema imunológico. Sabe-se que o estado de ativação celular crônica e a sustentada inflamação sistêmica estão associados com a mitigação de respostas imunológicas contra patógenos oportunistas (SERETI; ALTFRED, 2016). Sabe-se que apesar de eficaz na supressão viral e restauração parcial da imunidade, o TARV não é capaz de cessar completamente o processo inflamatório. Além disso, o início do tratamento está associado, em uma fração de indivíduos co-infectados por *Mtb*, com desenvolvimento da síndrome inflamatória da reconstituição imune. Neste contexto patológico, respostas celulares mediadas pela reconstituição de linfócitos T $CD4^+$ são direcionadas contra antígenos de *Mtb* acarretando a ativação completa de células mieloides e secreção de fatores pro-inflamatórios (BARBER et al, 2012)

Diversos estudos sugerem a participação substancial do metabolismo energético em diversos processos de manutenção da homeostase celular (O'Neill et al, 2016). Desta maneira, frente a estímulos promovidos por infecções, as células imunológicas alteram suas vias metabólicas a fim de suprir suas demandas catabólicas e anabólicas necessárias para a eficiente eliminação dos patógenos (KLEIN et al; 2018). **Hammoud et al. (2019) demonstraram através da utilização tomografia por emissão de pósitrons (PET-SCAN) que pacientes que desenvolveram SIRI após o início do TARV possuíam maiores níveis de metabolismo glicolítico. Ademais, neste mesmo estudo também foi sugerida a maior expressão do**

transportador relacionado com a importação glicose (Glut-1) na superfície de linfócitos T CD4+ e monócitos de pacientes SIRI. Aqui investigamos longitudinalmente o efeito do TARV no status do metabolismo de pacientes HIV-1^{+} através de uma abordagem de identificação e determinação da abundância de metabolitos plasmáticos. Desta maneira, foi possível identificar possíveis alvos de perturbações imunometabólicas associadas com a patogênese da SIRI.

Nossos dados indicam que o início do TARV está relacionado com alterações substanciais em vias de metabolismo de lipídios e aminoácidos em pacientes que desenvolveram SIRI. Os aminoácidos constituem um grupo de monômeros necessários para a síntese de proteínas, que por sua vez, são moléculas multifuncionais, incluindo a participação na propagação de sinais inflamatórios. Por outro lado, os lipídios são macromoléculas importantes para a síntese e manutenção de membranas celulares e de diversas organelas assim como a geração de energia. A utilização de ferramentas de aprendizado de máquinas nos permitiu desenvolver modelos capazes de distinguir pacientes que desenvolveram SIRI do grupo controle deste estudo. Para tal, foram levadas em consideração as abundâncias dos metabolitos diferencialmente presente no plasma da população de estudo. O nosso modelo de árvore de decisão revelou que a cisteinil-glicina oxidado (um dipeptídeo composto de glicina conjugado à um grupo L-cisteinil) era capaz de distinguir os pacientes com bastante eficácia no período pré-TARV. Importante intermediário do metabolismo da glutatinona, a cisteinil-glicinal está intrinsecamente relacionada com processos de regulação do estresse oxidativo no meio intracelular. Chettimada et al. (2018) demonstraram a associação entre a abundância de cisteinil-glicina oxidado e níveis de ativação celular em pacientes infectados por HIV-1. Desta maneira, este estudo sugere a existência de um sistema de compensação frente à elevados distúrbios oxidativos promovidos pela hiperativação celular no contexto de infecção pelo HIV. Assim, propormos que esta molécula possa ser utilizada como um biomarcador de elevação do processo de ativação imune e de predisposição para o desenvolvimento de SIRI associada a micobactérias.

O modelo de árvore de decisão referente ao período de um mês após o início do tratamento apontou o quinolinato com o metabolito com maior potencial de discriminação dos pacientes com SIRI. Este aminoácido é um intermediário da via de catabolismo do triptofano a quinurenina, com diversas implicações no imunometabolismo celular. É importante ressaltar a participação da enzima indoleamina 2,3 – dioxigenase (IDO) na via de conversão do triptofano a quinolinato. Foi demonstrado que células da imunidade inata, como células dendríticas e monócitos, possuem elevada expressão e atividade de IDO que refletem o seu grau de ativação (Hwang et al, 2005). **Ademais, os achados do estudo conduzido por Byakwaga et al. (2014)**

corroboram com a associação existente entre altos níveis de metabolismo da quinurenina, níveis de reconstituição de linfócitos T CD4+ e mortalidade em uma coorte de pacientes infectados com HIV em Uganda. Trabalhos seminais também ratificam a posição central da atividade de IDO e do metabolismo de quinurenina na inibição da profiliferação linfocitária, sustentação da ativação imune e complicações neurológicas associadas a AIDS (BOASSO et al., 2007; GUILLEMIN; KERR; BREW, 2005; GRANT et al., 2000). Nossos dados também salientam que as perturbações metabólicas em pacientes com SIRI persistem mesmo após 12 meses de tratamento. Este fato é evidenciado por nosso modelo de arvore de decisão no 12º mês que sugere alterações no metabolismo do lipídio adipolicartinina.

Os dados deste trabalho também mostram que há distintos padrões de correlação entre as vias metabólicas e biomarcadores inflamatórios circulantes. Notamos que a histidina se correlaciona negativamente com a abundância de IL-12p70 (uma citocina pró-inflamatória produzida principalmente por DCs), ao passo que este mesmo aminoácido exibiu correlações positivas com PD-1 solúvel (marcador de exaustão celular). Detectamos também correlações positivas significativas entre outro aminoácido essencial, o triptofano, e moléculas relacionadas com a atividade de neutrófilos, como a IL-8 e MPO. A IL-8 é uma potente citocina relacionada com o recrutamento (quimiotaxia) de neutrófilos, ao passo que a MPO é uma molécula presente nos grânulos neutrófilos e são secretadas mediante ativação destas células (num processo conhecido como degranulação). Assim, nossos dados apontam uma possível associação entre o metabolismo do triptofano e atividade e recrutamento de neutrófilos na SIRI. Estes achados estão em consonância com o estudo conduzido por NAKIWALA et al. (2018), em que se pode observar elevação da ativação neutrofilica e liberação de grânulos em pacientes durante a manifestação da SIRI.

Sabe-se que em períodos de homeostase imunológica, os linfócitos encontram-se em um estado de latência funcional. O encontro destas células com antígenos cognatos de seus receptores, desencadeia um profundo remodelamento do seu programa transcricional, culminando na ativação de genes associados com a proliferação (caracterizando o fenômeno de expansão clonal). Uma vez que a razão eficiente célula: antígeno tenha sido alcançada e o patógeno eliminado, a população linfocitária passa por um processo de contração. Contudo, uma fração destes linfócitos permanece como células de memória capaz de elicitar uma resposta mais robusta frente ao reencontro com o patógeno em questão. Neste sentido, avaliamos a dinâmica de ativação de linfócitos T CD4+ e CD8+ em uma coorte de pacientes HIV^+ no início do tratamento. **Trabalhos seminais de French et al. (2000) pavimentaram o entendimento de como a linfopenia acentuada de células T CD4+ predispõe pacientes em início de**

tratamento à ocorrência de SIRI. Nossos achados corroboram com estes estudos, uma vez que observamos que pacientes SIRI possuem menores frequências de células T CD4+ nos períodos pré-TARV e mesmo após o início do tratamento. Além disso, uma grande fração dos indivíduos que desenvolveram SIRI possuíam frequências de linfócitos T CD4+ inferiores à mediana da população total estudada, ao passo que possuíam maiores percentagem de células T CD8+. A coletânea desses achados sustenta a ideia da linfopenia de CD4+como um fator de risco para o desenvolvimento de SIRI.

Para investigar a relevância dos linfócitos no processo imunopatogênicos da SIRI associada a TB, realizamos a dissecção fenotípica dos linfócitos CD4+ e CD8+ quanto à expressão de marcadores associados à ativação, proliferação, citotoxicidade e exaustão celular**.** Os episódios de SIRI foram associados à maiores frequências de linfócitos T CD4+ expressando HLA-DR. Concomitantemente, observamos a expansão de células T CD4+ e CD8+ com perfil citotóxico em pacientes com SIRI**. Nossos achados reiteram aqueles de Antonelli et al. (2010) que demonstraram a proliferação de linfócitos T CD4+ com aberrações no perfil de ativação durante a manifestação de SIRI associada à uma gama de patógenos. Nesta mesma linha, HSU et al. (2018) constaram a emergência de linfócitos T CD4+ citotóxicos com elevado potencial de produção de citocinas em pacientes com SIRI associada a *M. avium***. Sabe-se que o sistema imunológico dispõe de diferentes mecanismos redundantes cuja ações se sobrepõe frente a processos que põe a integridade homeostática em risco. Desta maneira, não podemos descartar a possibilidade da existência de sistemas de compensação em pacientes com alto grau de imunossupressão. Assim, detectamos correlações negativas entre as porcentagens de células T CD4+ totais e as frequências de células T CD8+ citotóxicas. Este dado remete a importância de linfócitos citotóxicos no contexto de SIRI.

Os achados do segundo manuscrito permitiram o delineamento da participação de linfócitos T ativados em uma população de estudo mais clinicamente homogênea, onde a ocorrência de SIRI associada a outros patógenos além da *Mtb* foi descartada. Assim, nós testamos se modelos que levam em consideração o perfil de ativação de linfócitos T poderiam predizer ou diagnosticar a ocorrência de SIRI. O modelo composto apenas por células T CD4+ foi superior na predição de SIRI, ao passo que o modelo conjunto de CD4+ e CD8+ foi mais eficiente no diagnóstico de SIRI. No nosso entendimento, este é o primeiro estudo a aplicar algoritmos de aprendizado de máquinas que levem em consideração marcadores de ativação linfocitária para a determinação de SIRI.

Diversos estudos demonstraram que o estabelecimento da memória imunológica é primordial para a mobilização de respostas protetoras contra reinfecções e reduzem os níveis de dano tecidual e inflamação crônica nos casos de infecções persistentes (Ratajczak etl al 2018; Principe et al, 2020; Ribeiro et al,2014). Portanto, o terceiro manuscrito explorou a importância do compartimento de memória imunológica de células T CD8+ no contexto de desenvolvimento da SIRI. No nosso estudo, detectamos um predomínio de linfócitos que já tiveram contato prévio com antígenos (células de memória) em pacientes que desenvolveram SIRI. Estas células de memória foram correlacionadas positivamente com a carga bacilar no período pré-TARV. **Silveira et al. (2019) demonstraram que a reconstituição do compartimento de memória de células T CD4+ é caracterizada pela expansão de linfócitos de memória efetora e redução de linfócitos naïve**. Em consonância com estes achados, encontramos frequências superiores de células T CD8+ de memória efetora em pacientes com SIRI**. Espinosa et al. (2013) demonstraram que essa se trata de uma expansão transiente deste perfil de célula de memória, com normalização do compartimento de memória por volta de 40 semanas após o início do TARV**.

Pode-se aventar a possibilidade da expansão de células CD8+ de memória efetora ser um fenômeno secundário ao processo de ativação celular generalizado visto na SIRI. A investigação das possíveis associações entre o compartimento de memória das células T CD8+ de revelou que o início do tratamento reduz o número de correlações entre os linfócitos T CD8+ de memória e outras células imunológicas expressando marcadores de ativação. No período pré-TARV controles que não desenvolveram SIRI exibiam correlações negativas entre linfócitos T regulatórios (Treg) e linfócitos $CD8^{+}$ efetores e de memória efetora. Esses resultados sugerem um potencial papel das células Treg em restringir os efeitos da ativação de células T CD8+ efetoras. **Shankar et al. (2008) levantaram a hipótese que indivíduos que não desenvolvem SIRI possuem maior frequência de células precursoras de linfócitos Treg que suprimem a geração de moléculas pro-inflamatórias em via contato direto, e independentemente de IL-10 com as células T CD4+ convencionais**. De maneira similar, pode-se sugerir que os linfócitos t-reg engajam em contato com células CD8+ de memória efetora para limitar sua participação nos processos imunopatológicos da SIRI.

Sabe-se que a reconstituição linfocitária promovida pela TARV ocorre de maneira multifásica. Dentro de poucas semanas após o início da TARV, o aumento na abundância de células T CD4+ ocorre devido a recirculação de células retidas em tecidos linfoides onde ocorria a replicação viral e intenso processo inflamatório. As etapas subsequentes, que podem levar de meses a anos, são caracterizadas pela síntese *de novo* de linfócitos T naïve. Nossos dados

corroboram com a ideia de reconstituição diferencial do compartimento de linfócitos CD8+ de memória em pacientes com SIRI que apresentaram uma menor magnitude na reconstituição de linfócitos naïve.

Além disso, fez-se importante a determinação da abundância de células CD8+ recirculantes. Sabe-se que o CXCR3 é um importante receptor de quimiocinas associado com o direcionamento de linfócitos para sítios de inflamação. Observamos que pacientes que desenvolveram SIRI possuem menor frequência de células CD8+ expressando CXCR3. Isso poderia eventualmente ser explicada pela retenção destas células em sítios persistentemente inflamados. Além disso, em no grupo controle, as células cxcr3 foram correlacionadas positivamente com citocinas anti-inflamatórias como IL-4 e TGF-b. Loise et al. (2019) demonstraram o acúmulo de células T CD8+ CXCR3+ e intenso recrutamento de células th1 na mucosa intestinal de pacientes sob TARV, evidenciando uma participação de células CXCR3+ na amplificação de processo patológicos. Considerando os nossos dados sobre a relevância de células CD8+ de memória expressando CXCR3 no contexto de SIRI, investigamos a capacidade dessas subpopulações celulares em distinguir pacientes que desenvolveram SIRI. Nossos resultados apontam o potencial dessas subpopulações em diagnosticar e predizer a ocorrência de SIRI.

6 **PRINCIPAIS ACHADOS DA TESE**

1. O metabolismo de lipídios e aminoácidos é capaz de diferenciar pacientes que desenvolveram antes da TARV e durante o evento SIRI, implicando a associação entre estresse oxidativo, via do triptofano e sinalização mediada por lipídios e o desenvolvimento de SIRI.

2. Pacientes que desenvolvem SIRI possuem uma linfopenia de células T CD4+ acentuada antes do início da TARV e possuem elevadas frequências de células T CD8+.

3. Os episódios de SIRI são associados a disfunções da dinâmica de ativação linfocitária, com elevação de linfócitos T CD4+ HLA-DR+ e células T CD4+ e CD8+ expressando Granzima B.

4. A linfopenia de células CD4+ está associada à um aumento das frequências de células CD8+ citotóxicas (mecanismo de compensação).

5. Modelos baseados em algoritmos de aprendizado de máquinas são capazes de predizer e diagnosticar SIRI levando em consideração as frequências de linfócitos expressando moléculas associadas a ativação celular.

6. Pacientes que desenvolveram SIRI possuem maiores níveis de células T CD8+ de memória previamente a introdução do TARV, e estas células estão correlacionadas positivamente com a carga bacilar.
7. A reconstituição do compartimento de células T CD8+ de memória é predominada por células de memória efetora em pacientes que desenvolvem SIRI. Por sua vez, a magnitude da variação das frequências dessas células esta correlacionada positivamente com as abundancias de citocinas pro-inflamatórias.
8. Em pacientes que manifestaram SIRI associada a TB, ocorre retenção de células T CD8+ expressando CXCR3 em sítios persistentemente inflamados.

9. As frequências de células CD8+ de memória expressando CXCR3 são capazes de distinguir pacientes que desenvolvem SIRI de suas contrapartes que não manifestam tal síndrome após o início do TARV.

7 **CONCLUSÃO GERAL**

Os resultados apresentados neste conjunto de manuscritos sugerem a influência de fatores imunometabólicos e de ativação linfocitária na imunopatogênese da SIRI, destacando-se a hiperativação de linfócitos T $CD4^+$ e $CD8^+$ no cerne do desenvolvimento de tal síndrome.

REFERÊNCIAS

ABRAHEM, Rachel et al. The Role of Dendritic Cells in TB and HIV Infection. **Journal of Clinical Medicine**, v. 9, n. 8, p. 2661, 2020.

ACHTMAN, M. Evolution, population structure, and phylogeography of genetically monomorphic bacterial pathogens. *Annu. Rev. Microbiol.* **62**, 53–70 (2008).

ALTFELD, M., & GALE, M., JR (2015). Innate immunity against HIV-1 infection. Nature immunology, 16(6), 554–562.

AMULIC, Borko et al. Neutrophil function: from mechanisms to disease. **Annual review of immunology**, v. 30, p. 459-489, 2012.

ANTONELLI, Lis RV et al. Elevated frequencies of highly activated CD4+ T cells in HIV+ patients developing immune reconstitution inflammatory syndrome. **Blood, The Journal of the American Society of Hematology**, v. 116, n. 19, p. 3818-3827, 2010.

BADRI, M. et al. Association between tuberculosis and HIV disease progression in a high tuberculosis prevalence area. **The International Journal of Tuberculosis and Lung Disease**, v. 5, n. 3, p. 225-232, 2001.

BARBER, D. L. et al. Immune reconstitution inflammatory syndrome: the trouble with immunity when you had none. **Microbiology**, v. 10, n. 2, 150–156, 2012.

BARBER, D. L. e tal. Th1-driven immune reconstitution disease in Mycobacterium avium-infected mice. **Blood**, v. 116, n. 18, p. 3485–3493, 2010.

BARBERIS, I et al. The history of tuberculosis: from the first historical records to the isolation of Koch's bacillus. **J Prev Med Hyg**., v. 58, n. 1, 2017.

BOILY, M. C. et al. Heterosexual risk of HIV-1 infection per sexual act: systematic review and meta-analysis of observational studies. **The Lancet. Infectious diseases**, v. 9, n. 2, 118–129, 2009.

BRASIL. MINISTÉRIO DA SAÚDE DO BRASIL. **Manual de Recomendações para o controle da tuberculose no Brasil**. 2. ed. Brasília: MS, 2019. Disponível em: <http://antigo.aids.gov.br/pt-br/pub/2019/manual-de-recomendacoes-para-o-controle-da-tuberculose-no-brasil>.

BRENNAN, P. J. Structure, function, and biogenesis of the cell wall of Mycobacterium tuberculosis. **Tuberculosis**, v. 83, p. 91–7 2003.

BRITES D, Gagneux S. Old and new selective pressures on mycobacterium tuberculosis. **Infect Genet Evol**., v. 12. N. 4, p. 678-85, 2012. doi: 10.1016/j.meegid.2011.08.010.

BRITES, D.; Gagneux, S. Old and new selective pressures on Mycobacterium tuberculosis. **Infect. Genet. Evol**., v. 12, p. 678–685, 2012.

BROWN, Lawrason. **The story of clinical pulmonary tuberculosis**. 1941.

BRUCHFELD, Judith; CORREIA-NEVES, Margarida; KÄLLENIUS, Gunilla. Tuberculosis and HIV coinfection. **Cold Spring Harbor perspectives in medicine**, v. 5, n. 7, p. a017871, 2015.

BUZON, V. et al. Crystal structure of HIV-1 gp41 including both fusion peptide and membrane proximal external regions. **Plos Pathogens**, v. 6, n. 5, .2010.

BYAKWAGA, H. et al. The kynurenine pathway of tryptophan catabolism, CD4+ T-cell recovery, and mortality among HIV-infected Ugandans initiating antiretroviral therapy. **The Journal of infectious diseases**, 210 (3), 383–391, 2014.

CARDONA, Paula; CARDONA, Pere-Joan. Regulatory T cells in Mycobacterium tuberculosis infection. **Frontiers in immunology**, v. 10, p. 2139, 2019.

CASTRO, Kenneth G. et al. **Updated guidelines for using interferon gamma release assays to detect Mycobacterium tuberculosis infection**. United States, 2010.

CAVE, A. J. E.; DEMONSTRATOR, Arnott. The evidence for the incidence of tuberculosis in ancient Egypt. **British Journal of Tuberculosis**, v. 33, n. 3, p. 142-152, 1939.

CHETTIMADA, S. et al. Exosome markers associated with immune activation and oxidative stress in HIV patients on antiretroviral therapy. **Scientific reports**, v. 8, n.1, p.7227, 2018.

CHURCHYARD, G. et al. What We Know About Tuberculosis Transmission: An Overview**.** **J. Infect. Dis**., v. 216, (suppl - 6), 2017.

DAVIS, J. L. et al. Diagnostic accuracy of same-day microscopy versus standard microscopy for pulmonary tuberculosis: a systematic review and meta-analysis. **Lancet Infect Dis**, v. 13, n. 2, p. 147-154, Feb 2013.

DAVIS, J. L. et al. Diagnostic accuracy of same-day microscopy versus standard microscopy for pulmonary tuberculosis: a systematic review and meta-analysis. **Lancet Infect Dis**, 13, n. 2, p. 147-154, Feb 2013.

DAVIS, J. Lucian et al. Diagnostic accuracy of same-day microscopy versus standard microscopy for pulmonary tuberculosis: a systematic review and meta-analysis. **The Lancet infectious diseases**, v. 13, n. 2, p. 147-154, 2013.

DEEKS, Steven G. et al. HIV infection. **Nature reviews Disease primers**, v. 1, n. 1, p. 1-22, 2015.

ESMAIL, Hanif et al. The immune response to Mycobacterium tuberculosis in HIV-1-coinfected persons. **Annual review of immunology**, v. 36, p. 603-638, 2018.

ESPINOSA, E. et al. Transient expansion of activated CD8+ (+) T cells characterize tuberculosis-associated immune reconstitution inflammatory syndrome in patients with HIV: a case control study. **Journal of inflammation**, London, v. 10, n. 21, 2013.

FARHAT, M1 et al. False-positive tuberculin skin tests: what is the absolute effect of BCG and non-tuberculous mycobacteria?. **The International Journal of Tuberculosis and Lung Disease**, v. 10, n. 11, p. 1192-1204, 2006.

Fisher, R. D. et al. Structural and biochemical studies of ALIX/AIP1 and its role in retrovirus budding. **Cell,** v. 128, n. 5, p. 841–852, 2007.

FLYNN, Joanne L.; CHAN, J.; LIN, P. L. Macrophages and control of granulomatous inflammation in tuberculosis. **Mucosal immunology**, v. 4, n. 3, p. 271-278, 2011.

FOREMAN, Taylor W. et al. CD4 T cells are rapidly depleted from tuberculosis granulomas following acute SIV co-infection. **Cell Reports**, v. 39, n. 9, p. 110896, 2022.

French, M. A. et al. Immune restoration disease after the treatment of immunodeficient HIV-infected patients with highly active antiretroviral therapy. **HIV Medicine**, v., 1, n. 2, p. 107–115, 2000.

FRITH, J. History of tuberculosis Part 1: pthisis, consumption and the white plague**. Journal of Military and Veterans' Health,** v. 22, n. 2, 2014.

GAGNEUX, S. Ecology and evolution of Mycobacterium tuberculosis. **Nat Rev Microbiol**, v. 16, p. 202–213, 2018.

GELDMACHER, C. et al. Preferential infection and depletion of Mycobacterium tuberculosis-specific CD4 T cells after HIV-1 infection**. J Exp Med**., v. 207, n. 13, 2869-81, 2010.

Giovanetti, M. et al. Molecular epidemiology of hiv-1 in african countries: a comprehensive overview**. Pathogens**, Switzerland, v. 9, n. 12, p. 1072, 2020.

GREENE, Joseph T. et al. Regulation of myeloid-cell activation. **Current Opinion in Immunology**, v. 73, p. 34-42, 2021.

GROSSMAN, Zvi et al. Pathogenesis of HIV infection: what the virus spares is as important as what it destroys. **Nature medicine**, v. 12, n. 3, p. 289-295, 2006.

Gurunathan S. et al. 2009. Use of predictive markers of HIV disease progression in vaccine trials. **Vaccine**, v. 27, p.199, 2015

HAHN, B. H. et al. AIDS as a zoonosis: scientific and public health implications**. Science**, New York, v. 287, n. 5453, p. 607–614, 2000.

HAMMOUD, D. A. et al. Increased Metabolic Activity on 18F-Fluorodeoxyglucose Positron Emission Tomography-Computed Tomography in Human Immunodeficiency Virus-Associated Immune Reconstitution Inflammatory Syndrome. **Clinical infectious diseases: an official publication of the Infectious Diseases Society of America**, v. 68, n. 2, p. 229–238, 2019.

HSU, D. C. et al. Emergence of polyfunctional cytotoxic CD4+ T cells in mycobacterium avium immune reconstitution inflammatory syndrome in human immunodeficiency virus-infected

patients. **Clinical infectious diseases: an official publication of the Infectious Diseases Society of America**, v. 67, n. 3, p. 437–446, 2018.

HUNTER, Robert L. Pathology of post primary tuberculosis of the lung: an illustrated critical review. **Tuberculosis**, v. 91, n. 6, p. 497-509, 2011.

HUNTER, Robert L.; JAGANNATH, Chinnaswamy; ACTOR, Jeffrey K. Pathology of postprimary tuberculosis in humans and mice: contradiction of long-held beliefs. **Tuberculosis**, v. 87, n. 4, p. 267-278, 2007.

HUSSELL, T.; BELL, T. J. Alveolar macrophages: Plasticity in a tissue-specific context**. Nat. Rev. Immuno**l., v.14, p. 81–93, 2014.

HWANG, S. L. et al. Indoleamine 2, 3-dioxygenase (IDO) is essential for dendritic cell activation and chemotactic responsiveness to chemokines. **Cell research**, v. 15, n. 3, p. 167–175, 2005.

JANG, J.O. Horizontally acquired genomic islands in the tubercle bacilli. **Trends Microbiol**., v .16, p. 303–308, 2008.

JANSSEN, Saskia et al. Mortality in severe human immunodeficiency virus-tuberculosis associates with innate immune activation and dysfunction of monocytes. **Clinical Infectious Diseases**, v. 65, n. 1, p. 73-82, 2017.

JASENOSKY, Luke D. et al. T cells and adaptive immunity to Mycobacterium tuberculosis in humans. **Immunological reviews**, v. 264, n. 1, p. 74-87, 2015.

JONES, Brenda E. et al. Relationship of the manifestations of tuberculosis to CD4 cell counts in patients with human immunodeficiency virus infection. **American Journal of Respiratory and Critical Care Medicine**, v. 148, n. 5, p. 1292-1297, 1993.

JOSHI, N; WALTER J. M; MISHARIN, A. V. Alveolar macrophages. **Cell Immunol**., v. 330, p. 86–90, 2018.

KESTENS, Luc et al. Expression of activation antigens, HLA-DR and CD38, on CD8 lymphocytes during HIV-1 infection. **Aids**, v. 6, n. 8, p. 793-797, 1992.

KLEIN, Geltink, R. I. et al. Unraveling the Complex Interplay Between T Cell Metabolism and Function. **Annual Review of Immunology**, v. 36, n.1, p.461–488, 2018.

KWAN, Candice K.; ERNST, Joel D. HIV and tuberculosis: a deadly human syndemic. **Clinical microbiology reviews**, v. 24, n. 2, p. 351-376, 2011.

KWONG, P. D. et al. Structure of an HIV gp120 envelope glycoprotein in complex with the CD4 receptor and a neutralizing human antibody**. Nature**, v. 393, n. 6686, p. 648–659, 1998.

LAWN, S. D.; NICOL, M. P. Xpert (R) MTB/RIF assay: development, evaluation and implementation of a new rapid molecular diagnostic for tuberculosis and rifampicin resistance. **Future Microbiol**, 6, n. 9, p. 1067-1082, Sep 2011.

LAWN, S. D.; ZUMLA, A. I. Tuberculosis. **Lancet**, v. 378, p. 57–72, 2012.

LEWINSOHN, Deborah A. et al. Tuberculosis immunology in children: diagnostic and therapeutic challenges and opportunities. **The International Journal of Tuberculosis and Lung Disease**, v. 8, n. 5, p. 658-674, 2004.

LI W. et al. Roles of Mucosal Immunity against Mycobacterium tuberculosis Infection. **Tuberc Res Treat**., p. 791728, 2012.

LIU, J. et al. Molecular architecture of native HIV-1 gp120 trimers. **Nature**, v. 455, n. 7209, p. 109–113, 2008.

LODDENKEMPER, Robert; LIPMAN, Marc; ZUMLA, Alimuddin. Clinical aspects of adult tuberculosis. **Cold Spring Harbor perspectives in medicine**, v. 6, n. 1, p. a017848, 2016.

LOHMANN, E, et al. Grading of a positive sputum smear and the risk of mycobacterium tuberculosis transmission. **Int J Tuberculosis and Lung Disease**, v. 16, n. 11, p. 477–84, 2012.

LOISEAU, C. et al. Increased CXCR3+ T cells impairs recruitment of t-helper type 17 cells via interferon γ and interleukin 18 in the small intestine mucosa during treated HIV-1 infection. **The Journal of Infectious Diseases**, v. 220, n. 5, p.830–840, 2019.

MAHNKE, Y. D. Selective expansion of polyfunctional pathogen-specific CD4+(+) T cells in HIV-1-infected patients with immune reconstitution inflammatory syndrome. **Blood,** v. 119, n. 13, p. 3105–3112, 2012.

MANAS, E. et al. Impact of tuberculosis on the course of HIV-infected patients with a high initial CD4 lymphocyte count. **The International Journal of Tuberculosis and Lung Disease**, v. 8, n. 4, p. 451-457, 2004.

MARIMANI, M; AHMAD, A; DUSE, A. The role of epigenetics, bacterial and host factors in progression of Mycobacterium tuberculosis infection. **Tuberculosis,** v. 113, p. 200-214, 2018.

MEINTJES, G.; BRUST, J. C. M.; NUTTALL, J.; MAARTENS, G. Management of active tuberculosis in adults with HIV. **Lancet HIV**, v. 6, 2019.

MEINTJES, Graeme et al. Prednisone for the prevention of paradoxical tuberculosis-associated IRIS. **New England Journal of Medicine**, v. 379, n. 20, p. 1915-1925, 2018.

MOIR, S.; CHUN, T.; W.; FAUCI, A. S. Pathogenic mechanisms of HIV disease. **Annual review of pathology**, v. 6, p. 223–248, 2011.

MOREIRA-TEIXEIRA, Lúcia et al. Type I IFN exacerbates disease in tuberculosis-susceptible mice by inducing neutrophil-mediated lung inflammation and NETosis. **Nature communications**, v. 11, n. 1, p. 1-18, 2020.

MORRISON, W. J.; OFFNER, H.; VANDENBARK, A. A. Understanding the CD4 molecule: surface expression and function. **Journal of neuroscience research**, v. 38, n. 1, 1–5, 1994.

MÜLLER, M. et al. Southern and Central Africa: immune reconstitution inflammatory syndrome in patients starting antiretroviral therapy for HIV infection: a systematic review and meta-analysis. **The Lancet. Infectious Diseases**, v. 10, n. 40, p. 251–261, 2010.

NAIDOO, K. et al. The immune reconstitution inflammatory syndrome after antiretroviral therapy initiation in patients with tuberculosis: Findings from the SAPiT trial. **Ann. Intern. Med.** , v. 157, p. 313–324, 2012.

NAING, Cho et al. Meta-analysis: the association between HIV infection and extrapulmonary tuberculosis. **Lung**, v. 191, n. 1, p. 27-34, 2013.

NAKIWALA, J. K. et al. Neutrophil Activation and Enhanced Release of Granule Products in HIV-TB Immune Reconstitution Inflammatory Syndrome. **Journal of Acquired Immune Deficiency Syndromes**, v. 77n. 2, 221–229, 2018.

Narendran G, Andrade BB, Porter BO, Chandrasekhar C, Venkatesan P, Menon PA, et al. Paradoxical Tuberculosis Immune Reconstitution Inflammatory Syndrome (TB-SIRI) in HIV Patients With Culture Confirmed Pulmonary Tuberculosis in India and the Potential Role of IL-6 in Prediction. PloS One (2013) 8(5):e63541.

Narita M, Ashkin D, Hollender ES, Pitchenik AE. Paradoxical Worsening of Tuberculosis Following Antiretroviral Therapy in Patients With AIDS. Am J Respir Crit Care Med (1998) 158(1):157–61.

O'GARRA, Anne et al. The immune response in tuberculosis. **Annual review of immunology**, v. 31, p. 475-527, 2013.

O'NEILL, L. A.; KISHTON, R. J.; RATHMELL, J. A guide to immunometabolism for immunologists. **Nature reviews. Immunology,** v. 16, n. 9, p. 553–565, 2016.

PAI, Madhukar; ZWERLING, Alice; MENZIES, Dick. Systematic review: T-cell–based assays for the diagnosis of latent tuberculosis infection: an update. **Annals of internal medicine**, v. 149, n. 3, p. 177-184, 2008.

PATEL, Dhavalkumar D.; KUCHROO, Vijay K. Th17 cell pathway in human immunity: lessons from genetics and therapeutic interventions. **Immunity**, v. 43, n. 6, p. 1040-1051, 2015.

Paulson, T. Epidemiology: a mortal foe. **Nature**, v. 502, 2013.

PHILIPS, Jennifer A.; ERNST, Joel D. Tuberculosis pathogenesis and immunity. **Annual Review of Pathology: Mechanisms of Disease**, v. 7, n. 1, p. 353-384, 2012.

Piguet, V., & Steinman, R. M. (2007). The interaction of HIV with dendritic cells: outcomes and pathways. Trends in immunology, 28(11), 503–510.

PODINOVSKAIA, M; LEE, W.; CALDWELL, S.; RUSSELL, D. G. Infection of macrophages with Mycobacterium tuberculosis induces global modifications to phagosomal function. **Cell Microbiol**. v. 15, n. 6, p. 843-59, 2013. doi: 10.1111/cmi.12092.

Principe N, Kidman J, Goh S, Tilsed CM, Fisher SA, Fear VS, et al. Tumor-Infiltrating Effector Memory Antigen-Specific CD8+ T Cells Predict Response to Immune Checkpoint Therapy. Front Immunol (2020).

QUINN, C. M. et al. Tuberculosis SIRI: pathogenesis, presentation, and management across the spectrum of disease. **Life,** Switzerland), v.10, n. 11, 262, 2020.

RAMAKRISHNAN, Lalita. Revisiting the role of the granuloma in tuberculosis. **Nature Reviews Immunology**, v. 12, n. 5, p. 352-366, 2012.

RATAJCZAK, W. et al. Immunological Memory Cells. **Central-European J. Immunol.,** v. 43, n. 2, 194–203, 2018.

RAVIMOHAN, Shruthi et al. Tuberculosis and lung damage: from epidemiology to pathophysiology. **European Respiratory Review**, v. 27, n. 147, 2018.

RIBEIRO, S. P.et al. The CD8+Memory Stem T Cell (T(SCM)) subset is associated with improved prognosis in chronic hiv-1 infection. J. Virol., v. 88, n. 23, p. 3836–44, 2014.

RILEY, R. L. et al. Aerial dissemination of pulmonary tuberculosis. A two-year study of contagion in a tuberculosis ward. 1959. **Am J Epidemiol**., v. 42, n. 1, p. 3-14, 1995.

RIZZUTO, C. D. et al. A conserved HIV gp120 glycoprotein structure involved in chemokine receptor binding. **Science.** New York, v. 280, n. 5371, p. 1949–1953, 1998.

RUSSELL, D. G.; BARRY, C.E; FLYNN, J. L. Tuberculosis: what we don't know can, and does, hurt us. **Science, v.** 328, n. 5980, p. 852–856, 2010.

SARAVIA, Jordy; CHAPMAN, Nicole M.; CHI, Hongbo. Helper T cell differentiation. **Cellular & molecular immunology**, v. 16, n. 7, p. 634-643, 2019.

SERETI, I.; ALTFELD, M. Immune activation and HIV: an enduring relationship. **Current opinion in HIV and AIDS**, v. 11, n. 2, p. 129–130, 2016.

SHANKAR, E. M. et al. Does CD4+CD25+foxp3+ cell (Treg) and IL-10 profile determine susceptibility to immune reconstitution inflammatory syndrome (SIRI) in HIV disease?. **Journal of inflammation**. London, v. 5, n. 2, 2008.

SHARP, P. M.; HAHN, B. H. Origins of HIV and the AIDS pandemic. Cold Spring Harbor perspectives in medicine, 1(1), 2011.

Sharp, P. M. et al. Origins and evolution of AIDS viruses: estimating the timescale. **Biochemical Society transactions**, v. 28, n. 2, p. 275–282, 2000.

SHARPE, Arlene H.; PAUKEN, Kristen E. The diverse functions of the PD1 inhibitory pathway. **Nature Reviews Immunology**, v. 18, n. 3, p. 153-167, 2018.

SIERRA, S.; KUPFER, B.; KAISER, R. Basics of the virology of HIV-1 and its replication. **J. Clin. Virol., v**. 34, n. 4, p. 233–44, 2005.

SILVEIRA-MATTOS, P. S. et al. Differential expression of CXCR3 and CCR6 on CD4+ T-lymphocytes with distinct memory phenotypes characterizes tuberculosis-associated immune reconstitution inflammatory syndrome. **Scientific reports**, v. 9, n. 1, p. 1502, 2019.

SONG, Liang et al. The function of dendritic cells in modulating the host response. **Molecular oral microbiology**, v. 33, n. 1, p. 13-21, 2018.

STORLA, D. G.; YIMER, S.; BJUNE, G. A. A systematic review of delay in the diagnosis and treatment of tuberculosis. **BMC Public Health**, 8, p. 15, Jan 14 2008.

SZABO, Susanne J. et al. A novel transcription factor, T-bet, directs Th1 lineage commitment. **Cell**, v. 100, n. 6, p. 655-669, 2000.

TĂBĂRAN, A. F. et al. Silver Nanoparticles for the Therapy of Tuberculosis. **Int J Nanomedicine**, v. 5, p. 2231-2258, 2020.

TAHIROV, T. H. et al. Crystal structure of HIV-1 Tat complexed with human P-TEFb. **Nature**, v. 465, n.7299, p. 747–751, 2010.

TANIUCHI, Ichiro. CD4 helper and CD8 cytotoxic T cell differentiation. **Annual review of Immunology**, v. 36, p. 579-601, 2018.

TEITELBAUM, R.; SCHUBERT, W.; GUNTHER, L. The M cell as a portal of entry to the lung for the bacterial pathogen Mycobacterium tuberculosis. **Immunity**., v. 10, n. 6, p. 641–650, 1999.

UPADHYAY, S.; MITTAL, E.; PHILIPS, J. A. Tuberculosis and the art of macrophage manipulation. **Pathog Dis.,** v. 76, n. 4 ,2018.

VALIN, N. et al. Risk factors for "unmasking immune reconstitution inflammatory syndrome" presentation of tuberculosis following combination antiretroviral therapy initiation in HIV-infected patients. **Aids**. London, v. 24, p. 1519–1525, 2010.

VON SCHWEDLER, U. K. et al. The protein network of HIV budding**. Cell,** v.114, n. 6, 701–713, 2013.

WALKER, Naomi F. et al. Matrix degradation in human immunodeficiency virus type 1–Associated tuberculosis and tuberculosis immune reconstitution inflammatory syndrome: a prospective observational study. **Clinical Infectious Diseases**, v. 65, n. 1, p. 121-132, 2017.

WANG, C. C. et al. Airborne transmission of respiratory viruses**. Science**, v. 373, n. 6558, 2021.

WEISSENHORN, W. Atomic structure of the ectodomain from HIV-1 gp41. **Nature**, v. 387, n. 6631, p. 426–430, 1997.

World Health Organization. **Global tuberculosis report**. 22nd ed Geneva: WHO, 2017.

World Health Organization. 2013a. **Global TB report**. Geneva: WHO, 2013.

ZANETTI, G. et al. Cryo-electron tomographic structure of an immunodeficiency virus envelope complex in situ. **Plos Pathogens**, v. 2, n. 8, 2006.

ZHU, P. et al. Distribution and three-dimensional structure of AIDS virus envelope spikes. **Nature,** v. 441, n. 7095, 847–852, 2006.

ZIMMERMAN, M. R; BULL, N. Y. Pulmonary and osseous tuberculosis in an Egyptian mummy. **Acad Med.**, v. 55, n. 6, p. 604–608, 1979.

Anexo A - artigos produzidos em colaboração durante o período do doutorado

Integration of metabolomics and transcriptomics reveal novel biomarkers in the blood for tuberculosis diagnosis in children.

www.nature.com/scientificreports

scientific reports

OPEN

Integration of metabolomics and transcriptomics reveals novel biomarkers in the blood for tuberculosis diagnosis in children

Noton K. Dutta[1,12✉], Jeffrey A. Tornheim[1,2,12], Kiyoshi F. Fukutani[3,4,5,12], Mandar Paradkar[6,12], Rafael T. Tiburcio[4,5], Aarti Kinikar[7], Chhaya Valvi[7], Vandana Kulkarni[6], Neeta Pradhan[6], Shri Vijay Bala Yogendra Shivakumar[8], Anju Kagal[7], Akshay Gupte[2], Nikhil Gupte[2,6], Vidya Mave[2,6], Amita Gupta[1,2,6,11], Bruno B. Andrade[4,5,8,9,10,12] & Petros C. Karakousis[1,11,12✉]

Pediatric tuberculosis (TB) remains a major global health problem. Improved pediatric diagnostics using readily available biosources are urgently needed. We used liquid chromatography-mass spectrometry to analyze plasma metabolite profiles of Indian children with active TB (n = 16) and age- and sex-matched, *Mycobacterium tuberculosis*-exposed but uninfected household contacts (n = 32). Metabolomic data were integrated with whole blood transcriptomic data for each participant at diagnosis and throughout treatment for drug-susceptible TB. A decision tree algorithm identified 3 metabolites that correctly identified TB status at distinct times during treatment. N-acetylneuraminate achieved an area under the receiver operating characteristic curve (AUC) of 0.66 at diagnosis. Quinolinate achieved an AUC of 0.77 after 1 month of treatment, and pyridoxate achieved an AUC of 0.87 after successful treatment completion. A set of 4 metabolites (gamma-glutamylalanine, gamma-glutamylglycine, glutamine, and pyridoxate) identified treatment response with an AUC of 0.86. Pathway enrichment analyses of these metabolites and corresponding transcriptional data correlated N-acetylneuraminate with immunoregulatory interactions between lymphoid and non-lymphoid cells, and correlated pyridoxate with p53-regulated metabolic genes and mitochondrial translation. Our findings shed new light on metabolic dysregulation in children with TB and pave the way for new diagnostic and treatment response markers in pediatric TB.

The World Health Organization estimates incident tuberculosis (TB) occurs in 1.1 million children annually, representing > 200,000 deaths and 11% of global burden[1]. India ranks first in pediatric TB cases among 22 high-burden countries[2]. Since young children with pulmonary TB generally cannot cough effectively, microbiological confirmation of *Mycobacterium tuberculosis* (MTB) infection is established in only 15–50% of cases[3,4], and often only after invasive sample collection[4]. Although rapid molecular tests have improved sensitivity over smear

[1]Center for Tuberculosis Research, Department of Medicine, Johns Hopkins University School of Medicine, 1551 East Jefferson Street, Room 110, Baltimore, MD 21287, USA. [2]Center for Clinical Global Health Education, Department of Medicine, Johns Hopkins University School of Medicine, Baltimore, MD, USA. [3]Laboratório de Inflamação E Biomarcadores, Instituto Gonçalo Moniz, Fundação Oswaldo Cruz, Salvador, Brazil. [4]Multinational Organization Network Sponsoring Translational and Epidemiological Research (MONSTER) Initiative, Salvador, Brazil. [5]Curso de Medicina, Faculdade de Tecnologia E Ciências, Salvador, Brazil. [6]Byramjee Jeejeebhoy Government Medical College, Johns Hopkins University Clinical Research Site, Pune, Maharashtra, India. [7]Byramjee Jeejeebhoy Government Medical College, Pune, Maharashtra, India. [8]Johns Hopkins University - India Office (CCGHE), Pune, Maharashtra, India. [9]Universidade Salvador (UNIFACS), Laureate Universities, Salvador, Brazil. [10]Escola Bahiana de Medicina E Saúde Pública (EBMSP), Salvador, Brazil. [11]Department of International Health, Johns Hopkins Bloomberg School of Public Health, Baltimore, MD, USA. [12]These authors contributed equally: Noton K. Dutta, Jeffrey A. Tornheim, Kiyoshi F. Fukutani, Mandar Paradkar, Bruno B. Andrade and Petros C. Karakousis. ✉email: notonkumardutta@gmail.com; petros@jhmi.edu

Inflammatory profile of patients with tuberculosis with or without HIV-1 co-infection: a prospective cohort study and immunological network analysis

Published in final edited form as:
Lancet Microbe. 2021 August ; 2(8): e371–e385. doi:10.1016/s2666-5247(21)00037-9.

Inflammatory profile of patients with tuberculosis with or without HIV-1 co-infection: a prospective cohort study and immunological network analysis

Elsa Du Bruyn[#], **Kiyoshi F Fukutani**[#], **Neesha Rockwood**[#], **Charlotte Schutz**, **Graeme Meintjes**, **Maria B Arriaga**, **Juan M Cubillos-Angulo**, **Rafael Tibúrcio**, **Alan Sher**, **Catherine Riou**, **Katalin A Wilkinson**, **Bruno B Andrade**[†], **Robert J Wilkinson**[†]

Wellcome Centre for Infectious Disease Research in Africa, Institute of Infectious Disease and Molecular Medicine (E Du Bruyn MD, N Rockwood PhD, C Schutz MD, G Meintjes PhD, C Riou PhD, K A Wilkinson PhD, B B Andrade MD, Prof R J Wilkinson FMedSci) and Department of Medicine (E Du Bruyn, C Schutz, G Meintjes, Prof R J Wilkinson), University of Cape Town, Observatory, South Africa; Instituto Gonçalo Moniz, Fundação Oswaldo Cruz, Salvador, Brazil (K F Fukutani PhD, M B Arriaga MSc, J M Cubillos-Angulo MSc, R Tibúrcio MSc, B B Andrade); Multinational Organization Network Sponsoring Translational and Epidemiological Research Initiative, Salvador, Brazil (K F Fukutani, M B Arriaga, J M Cubillos-Angulo, R Tibúrcio, B B Andrade); Curso de Medicina, Faculdade de Tecnologia e Ciências, Salvador, Brazil (K F Fukutani); Department of Infectious Diseases, Imperial College London, London, UK (N Rockwood, Prof R J Wilkinson); Department of Microbiology, Faculty of Medicine, University of Colombo, Colombo, Sri Lanka (N Rockwood); Laboratory of Parasitic Diseases, National Institute of Allergy and Infectious Diseases, National Institutes of Health, Bethesda, MD, USA (A Sher PhD); The Francis Crick Institute, London, UK (K A Wilkinson, Prof R J Wilkinson); Universidade Salvador, Laureate Universities, Salvador, Brazil (B B Andrade); Escola Bahiana de Medicina e Saúde Pública, Salvador, Brazil (B B Andrade); Division of Infectious Diseases, Department of Medicine, Vanderbilt University School of Medicine, Nashville, TN, USA (B B Andrade)

[#] These authors contributed equally to this work.

Summary

Background—HIV-1 mediated dysregulation of the immune response to tuberculosis and its effect on the response to antitubercular therapy (ATT) is incompletely understood. We aimed to analyse the inflammatory profile of patients with tuberculosis with or without HIV-1 co-infection

Correspondence to: Prof Robert J Wilkinson, Wellcome Centre for Infectious Disease Research in Africa, Institute of Infectious Disease and Molecular Medicine, University of Cape Town, Observatory 7925, South Africa robert.wilkinson@uct.ac.za.
[†] These senior authors contributed equally

Contributors

EDB, NR, CS, KAW, and BBA did experiments. EDB, NR, KAW, CS, GM, CR, RJW, and BBA designed experiments. EDB, NR, KFF, CR, and BBA analysed the data. NR and CS did the clinical recruitment, administered the projects, and curated the respective datasets. KAW, GM, and RJW provided materials and infrastructural support. EDB, KFF, NR, JMC-A, MBA, RT, CR, KAW, CS, GM, AS, RJW, and BBA wrote the manuscript. NR, CS, and BBA verified the data. All authors had full access to all the data in the study and had final responsibility for the decision to submit for publication.

Data sharing

Detailed description of network analysis methodology and the full clinical protocol are available in appendix 1 (pp 6–7, 27). All raw Luminex immunoassay data are available in appendix 2.

Hydroxyurea treatment is associated with reduced degree of oxidative perturbation in children and adolescents with sickle cell anemia

www.nature.com/scientificreports

scientific reports

OPEN

Hydroxyurea treatment is associated with reduced degree of oxidative perturbation in children and adolescents with sickle cell anemia

Caian L. Vinhaes[1,2,3,8], Rozana S. Teixeira[4,5,8], Jay A. S. Monteiro-Júnior[4,8], Rafael Tibúrcio[1,2,3,8], Juan M. Cubillos-Angulo[1,2,3], María B. Arriaga[1,2,3], Adrielle G. Sabarin[4], Amâncio J. de Souza[4], Jacqueline J. Silva[1,4], Isa M. Lyra[6], Ana Marice Ladeia[4,7,8] & Bruno B. Andrade[1,2,3,4,5,8,9]

Sickle cell anemia (SCA) is the most common inherited hemolytic anemia worldwide. Here, we performed an exploratory study to investigate the systemic oxidative stress in children and adolescents with SCA. Additionally, we evaluated the potential impact of hydroxyurea therapy on the status of oxidative stress in a case–control study from Brazil. To do so, a panel containing 9 oxidative stress markers was measured in plasma samples from a cohort of 47 SCA cases and 40 healthy children and adolescents. Among the SCA patients, 42.5% were undertaking hydroxyurea. Multidimensional analysis was employed to describe disease phenotypes. Our results demonstrated that SCA is associated with increased levels of oxidative stress markers, suggesting the existence of an unbalanced inflammatory response in peripheral blood. Subsequent analyses revealed that hydroxyurea therapy was associated with diminished oxidative imbalance in SCA patients. Our findings reinforce the idea that SCA is associated with a substantial dysregulation of oxidative responses which may be dampened by treatment with hydroxyurea. If validated by larger prospective studies, our observations argue that reduction of oxidative stress may be a main mechanism through which hydroxyurea therapy attenuates the tissue damage and can contribute to improved clinical outcomes in SCA.

Sickle cell anemia (SCA) is the most common monogenic hemoglobinopathy disease in the world[1,2]. This disease is characterized by altered hemoglobin synthesis (sickle hemoglobin [HbS]), which leads to several pathological effects, including hemolysis, vaso-occlusive crises, progressive organic damage, and eventual early death[3]. Notably, such hereditary hemolytic anemia exhibits a high prevalence in Brazil, especially in the state of Bahia[4]. Due to the scarcity of an effective pharmacological treatment, understanding of fundamental mechanisms underlying SCA may lead to development of novel therapies and optimized patient care[3,5,6].

Numerous aspects are long proposed to influence the pathogenesis of SCA[7,8]. Notably, a large number of studies investigating oxidative stress in SCA patients have indicated that several types of reactive oxygen species (ROS) affect red blood cells (RBCs), resulting in metabolic dysfunction of these cells and alteration of their biochemical properties[9,10]. There is also evidence supporting the idea that oxidative damage mediates cytoskeleton

[1]Instituto Gonçalo Moniz, Fundação Oswaldo Cruz (FIOCRUZ), Salvador 40296-710, Brazil. [2]Multinational Organization Network Sponsoring Translational and Epidemiological Research (MONSTER) Initiative, Salvador 41810-710, Brazil. [3]School of Medicine, Faculdade de Tecnologia E Ciências (UniFTC), Salvador 41741-590, Brazil. [4]Bahiana School of Medicine and Public Health, Bahia Foundation for the Development of Sciences, Salvador 40290-000, Brazil. [5]School of Medicine, Federal University of Bahia, Salvador 40110-100, Brazil. [6]University Salvador (UNIFACS), Laureate International Universities, Salvador 41720-200, Brazil. [7]Catholic University of Salvador, Salvador 41740-090, Brazil. [8]These authors contributed equally: Caian L. Vinhaes, Rozana S. Teixeira, Jay A. S. Monteiro-Júnior and Rafael Tibúrcio. [9]These authors jointly supervised this work: Ana Marice Ladeia and Bruno B. Andrade. ✉email: bruno.andrade@fiocruz.br

Immunomodulatory And Anti-Fibrotic Effects Following The Infusion Of Umbilical Cord Mesenchymal Stromal Cells In A Critically Ill Patient With Covid-19 Presenting Lung Fibrosis: A Case Report

frontiers in Medicine

CASE REPORT

Immunomodulatory and Anti-fibrotic Effects Following the Infusion of Umbilical Cord Mesenchymal Stromal Cells in a Critically Ill Patient With COVID-19 Presenting Lung Fibrosis: A Case Report

Kátia Nunes da Silva[1,2,3], Priscila Carvalho Guedes Pinheiro[2], André Luiz Nunes Gobatto[3], Rogério da Hora Passos[4], Bruno Diaz Paradas[1,5], Luciana Souza de Aragão França[1,5], Carolina Kymie Vasques Nonaka[3,6], Beatriz Barreto-Duarte[3,6,7], Mariana Araújo-Pereira[3,7,8], Rafael Tibúrcio[9], Fernanda Ferreira Cruz[8,10,11,12], Gabriela Louise Soares Martins[1,5], Bruno B. Andrade[3,6,8,13], Hugo Caire de Castro-Faria-Neto[10,11,12], Patrícia Risken Macêdo Rocco[8,10,11,12]* and Bruno Solano de Freitas Souza[1,3,5]*

[1] Center for Biotechnology and Cell Therapy, São Rafael Hospital, Salvador, Brazil, [2] D'Or Institute for Research and Education (IDOR), Salvador, Brazil, [3] Gonçalo Moniz Institute, Oswaldo Cruz Foundation (FIOCRUZ), Salvador, Brazil, [4] Critical Care Unit, São Rafael Hospital, Salvador, Brazil, [5] Curso de Medicina, Universidade Salvador (UNIFACS), Laureate International Universities, Salvador, Brazil, [6] Programa de Pós-Graduação em Ciência Médica, Universidade Federal do Rio de Janeiro, Rio de Janeiro, Brazil, [7] Multinational Organization Network Sponsoring Translational and Epidemiological Research (MONSTER) Initiative, Salvador, Brazil, [8] Faculdade de Medicina, Universidade Federal da Bahia, Salvador, Brazil, [9] Laboratory of Pulmonary Investigation, Carlos Chagas Filho Institute of Biophysics, Federal University of Rio de Janeiro, Rio de Janeiro, Brazil, [10] COVID-19 Virus Network from Brazilian Council for Scientific and Technological Development, Brasília, Brazil, [11] COVID-19 Virus Network from Foundation Carlos Chagas Filho Research Support of the State of Rio de Janeiro, Rio de Janeiro, Brazil, [12] National Institute of Science and Technology for Regenerative Medicine, Rio de Janeiro, Brazil, [13] Laboratory of Immunopharmacology, Oswaldo Cruz Institute, Oswaldo Cruz Foundation (FIOCRUZ), Rio de Janeiro, Brazil

Background: The patients with coronavirus disease 2019 (COVID-19) associated with severe acute respiratory distress syndrome (ARDS) may require prolonged mechanical ventilation which often results in lung fibrosis, thus worsening the prognosis and increasing fatality rates. A mesenchymal stromal cell (MSC) therapy may decrease lung inflammation and accelerate recovery in COVID-19. In this context, some studies have reported the effects of MSC therapy for patients not requiring invasive ventilation or during the first hours of tracheal intubation. However, this is the first case report presenting the reduction of not only lung inflammation but also lung fibrosis in a critically ill long-term mechanically ventilated patient with COVID-19.

Case Presentation: This is a case report of a 30-year-old male patient with COVID-19 under invasive mechanical ventilation for 14 days in the intensive care unit (ICU), who presented progressive clinical deterioration associated with lung fibrosis. The symptoms onset was 35 days before MSC therapy. The patient was treated with allogenic human umbilical-cord derived MSCs [5 x 10^7 (2 doses 2 days interval)]. No serious adverse events were observed during and after MSC administration. After MSC

OPEN ACCESS

Edited by:
Zlatko Kopitarić,
International Agency for Research on Cancer (IARC), France

Reviewed by:
Chuan Zhang,
6th Medical Center of the PLA General Hospital, China
Alireza Shafiei,
Tehran University of Medical Sciences, Iran

*Correspondence:
Bruno Solano de Freitas Souza
bruno.solano@fiocruz.br
Patrícia Risken Macêdo Rocco
prmrocco@biof.ufrj.br

Specialty section:
This article was submitted to Infectious Diseases – Surveillance, Prevention and Treatment, a section of the journal Frontiers in Medicine

Received: 30 August 2021
Accepted: 05 October 2021
Published: 17 November 2021

Citation:
Silva KNC, Pinheiro PCG, Gobatto ALN, Passos RH, Paradas BD, França LSA, Nonaka CKV, Barreto-Duarte B, Araújo-Pereira M, Tibúrcio R, Cruz AF, Martins GLS, Andrade BB, Castro-Faria-Neto HC, Rocco PRM and Souza BSF (2021) Immunomodulatory and Anti-fibrotic Effects Following the Infusion of Umbilical Cord Mesenchymal Stromal Cells in a Critically Ill Patient With COVID-19 Presenting Lung Fibrosis: A Case Report. Front. Med. 8:767261. doi: 10.3389/fmed.2021.767261

Oral Tolerance Induced By Heat Shock Protein 65-Producing Lactococcus Lactis Mitigates Inflammation In Leishmania Braziliensis Infection. Frontiers In Immunology

frontiers in Immunology

ORIGINAL RESEARCH
published: 24 June 2021
doi: 10.3389/fimmu.2021.647987

Oral Tolerance Induced by Heat Shock Protein 65-Producing *Lactococcus lactis* Mitigates Inflammation in *Leishmania braziliensis* Infection

Priscila Valera Guerra[1,2†], *Camila Mattos Andrade*[1†], *Ivanéia Valeriano Nunes*[1], *Brena Cardoso Gama*[1], *Rafael Tibúrcio*[1], *Washington Luis Conrado Santos*[3,4], *Vasco Ariston Azevedo*[5], *Natalia Machado Tavares*[1,6], *Juliana de Souza Rebouças*[7], *Tatiani Uceli Maioli*[8], *Ana Maria Caetano Faria*[6,9] *and Cláudia Ida Brodskyn*[1,6*]

[1] Laboratório da Interação Parasita-Hospedeiro e Epidemiologia (LAPHE) Instituto Gonçalo Moniz, Fundação Oswaldo Cruz, Salvador, Brazil, [2] Curso de Medicina, Centro Universitário Christus, Fortaleza, Brazil, [3] Laboratório de Patologia Estrutural e Molecular (LAPEM), Instituto Gonçalo Moniz, Fundação Oswaldo Cruz, Salvador, Brazil, [4] Departamento de Patologia e Medicina Legal Faculdade de Medicina da Universidade Federal da Bahia, Salvador, Brazil, [5] Departamento de Genética, Ecologia e Evolução, Instituto de Ciências Biomédicas, Universidade Federal de Minais Gerais, Belo Horizonte, Brazil, [6] Instituto de Investigação em Imunologia, Instituto Nacional de Ciência e Tecnologia (INCT), São Paulo, Brazil, [7] Instituto de Ciências Biológicas, Programa de Pós Graduação em Ciências da Saúde, Universidade de Pernambuco, Recife, Brazil, [8] Departamento de Nutrição, Escola de Enfermagem, Universidade Federal de Minas Gerais, Belo Horizonte, Brazil, [9] Departamento de Bioquímica e Imunologia, Instituto de Ciências Biológicas, Universidade Federal de Minas Gerais, Belo Horizonte, Brazil

Cutaneous leishmaniasis caused by *L. braziliensis* induces a pronounced Th1 inflammatory response characterized by IFN-γ production. Even in the absence of parasites, lesions result from a severe inflammatory response in which inflammatory cytokines play an important role. Different approaches have been used to evaluate the therapeutic potential of orally administrated heat shock proteins (Hsp). These proteins are evolutionarily preserved from bacteria to humans, highly expressed under inflammatory conditions and described as immunodominant antigens. Tolerance induced by the oral administration of Hsp65 is capable of suppressing inflammation and inducing differentiation in regulatory cells, and has been successfully demonstrated in several experimental models of autoimmune and inflammatory diseases. We initially administered recombinant *Lactococcus lactis* (*L. lactis*) prior to infection as a proof of concept, in order to verify its immunomodulatory potential in the inflammatory response arising from *L. braziliensis*. Using this experimental approach, we demonstrated that the oral administration of a recombinant *L. lactis* strain, which produces and secretes Hsp65 from *Mycobacterium leprae* directly into the gut, mitigated the effects of inflammation caused by *L. braziliensis* infection in association or not with PAM 3CSK4 (*N*-α-Palmitoyl-

OPEN ACCESS

Edited by:
Taun J. De Vries, VU University Amsterdam, Netherlands

Reviewed by:
Bastiaan P. Krom, VU University Amsterdam, Netherlands
Manuel Soto, Autonomous University of Madrid, Spain

***Correspondence:**
Cláudia Ida Brodskyn
claudia.brodskyn@fiocruz.br

[†]*These authors have contributed equally to this work and share first authorship*

Specialty section:
This article was submitted to Inflammation, a section of the journal Frontiers in Immunology

Received: *30 December 2020*
Accepted: *07 June 2021*
Published: *24 June 2021*

Citation:
Guerra PV, Andrade CM, Nunes IV, Gama BC, Tibúrcio R, Santos WLC, Azevedo VA, Tavares NM, Rebouças JS, Maioli T, Faria AMC and Brodskyn CI (2021) Oral Tolerance Induced by Heat Shock Protein 65-Producing Lactococcus lactis Mitigates Inflammation in Leishmania braziliensis Infection. Front. Immunol. 12:647987. doi: 10.3389/fimmu.2021.647987

In Vitro Differentiation of Human Dendritic Cells and their Markers in Leishmania Infection. Jove-Journal of Visualized Experiments

jove

In Vitro Differentiation of Human Dendritic Cells and their Markers in *Leishmania* Infection

Amanda R. Pitzão[*,1], Rafael Tibúrcio[*,1], Elaine Carvalho[1], Thalita Silva[1], Patrícia S. T. Veras[1], Natalia M. Tavares[1], Juliana P. B. de Menezes[1], Cláudia I. Brodskyn[1]

[1] Laboratory of Host-Parasite Interaction and Epidemiology, Gonçalo Moniz Institute

[*] These authors contributed equally

Corresponding Author

Cláudia I. Brodskyn
claudia.brodskyn@fiocruz.br

Citation

Pitzão, A.R., Tibúrcio, R., Carvalho, E., Silva, T., Veras, P.S.T., Tavares, N.M., de Menezes, J.P.B., Brodskyn, C.I. *In Vitro* Differentiation of Human Dendritic Cells and their Markers in *Leishmania* Infection. *J. Vis. Exp.* (182), e62794, doi:10.3791/62794 (2022).

Date Published

April 6, 2022

DOI

10.3791/62794

URL

jove.com/video/62794

Abstract

Leishmaniasis comprises a collection of clinical manifestations associated with the infection of obligate intracellular protozoans, *Leishmania*. The life cycle of *Leishmania* parasites consists of two alternating life stages (amastigotes and promastigotes), during which parasites reside within either arthropod vectors or vertebrate hosts, respectively. Notably, the complex interactions between *Leishmania* parasites and several cells of the immune system largely influence the outcome of infection. Importantly, although macrophages are known to be the main host niche for *Leishmania* replication, parasites are also phagocytosed by other innate immune cells, such as neutrophils and dendritic cells (DCs).

DCs play a major role in bridging the innate and adaptive branches of immunity and thus orchestrate immune responses against a wide range of pathogens. The mechanisms by which *Leishmania* and DCs interact remain unclear and involve aspects of pathogen capture, the dynamics of DC maturation and activation, DC migration to draining lymph node (dLNs), and antigen presentation to T cells. Although a large body of studies support the notion that DCs play a dual role in modulating immune responses against *Leishmania*, the participation of these cells in susceptibility or resistance to *Leishmania* remains poorly understood. After infection, DCs undergo a maturation process associated with the upregulation of surface major histocompatibility complex (MHC) II, in addition to costimulatory molecules (namely, CD40, CD80, and CD86).

Understanding the role of DCs in infection outcome is crucial to developing therapeutic and prophylactic strategies to modulate the immune response against *Leishmania*. This paper describes a method for the characterization of *Leishmania*-DC interaction. This detailed protocol provides guidance throughout the steps of DC differentiation, the characterization of cell surface molecules, and infection protocols, allowing scientists

Systemic Inflammation Associated with Immune Reconstitution Inflammatory Syndrome in Persons Living with HIV

life

MDPI

Review

Systemic Inflammation Associated with Immune Reconstitution Inflammatory Syndrome in Persons Living with HIV

Caian L. Vinhaes [1,2,3,†], Mariana Araujo-Pereira [1,2,4,†], Rafael Tibúrcio [1,2,4], Juan M. Cubillos-Angulo [1,2,4], Fernanda O. Demitto [2], Kevan M. Akrami [1,2,4,5] and Bruno B. Andrade [1,2,3,4,6,*]

1 Instituto Gonçalo Moniz, Fundação Oswaldo Cruz, Salvador 40296-710, Brazil; caianlea8@gmail.com (C.L.V.); araujopereira.mariana@gmail.com (M.A.-P.); rafael.santos@aluno.bahia.fiocruz.br (R.T.); j.cubillosangulo@gmail.com (J.M.C.-A.); Kevan.akrami@gmail.com (K.M.A.)
2 Multinational Organization Network Sponsoring Translational and Epidemiological Research (MONSTER) Initiative, Salvador 40210-320, Brazil; fernandademitto@gmail.com
3 Bahiana School of Medicine and Public Health, Bahia Foundation for the Development of Sciences, Salvador 40290-000, Brazil
4 Faculdade de Medicina, Universidade Federal da Bahia, Salvador 40110-100, Brazil
5 Divisions of Infectious Diseases and Pulmonary, Critical Care and Sleep Medicine, Department of Medicine, University of California, San Diego, CA 92093, USA
6 Curso de Medicina, Centro Universitário Faculdade de Tecnologia e Ciências (UniFTC), Salvador 41741-590, Brazil
* Correspondence: bruno.andrade@fiocruz.br; Tel.: +55-71-3176-2264
† These authors contributed equally to this work.

Abstract: Antiretroviral therapy (ART) has represented a major advancement in the care of people living with HIV (PLWHH), resulting in significant reductions in morbidity and mortality through immune reconstitution and attenuation of homeostatic disruption. Importantly, restoration of immune function in PLWH with opportunistic infections occasionally leads to an intense and uncontrolled cytokine storm following ART initiation known as immune reconstitution inflammatory syndrome (IRIS). IRIS occurrence is associated with the severe and rapid clinical deterioration that results in significant morbidity and mortality. Here, we detail the determinants underlying IRIS development in PLWH, compiling the available knowledge in the field to highlight details of the inflammatory responses in IRIS associated with the most commonly reported opportunistic pathogens. This review also highlights gaps in the understanding of IRIS pathogenesis and summarizes therapeutic strategies that have been used for IRIS.

Keywords: systemic inflammation; mycobacteria; HIV; immune reconstitution inflammatory syndrome (IRIS)

Citation: Vinhaes, C.L.; Araujo-Pereira, M.; Tibúrcio, R.; Cubillos-Angulo, J.M.; Demitto, F.O.; Akrami, K.M.; Andrade, B.B. Systemic Inflammation Associated with Immune Reconstitution Inflammatory Syndrome in Persons Living with HIV. *Life* **2021**, *11*, 65. https://doi.org/10.3390/life11010065

Received: 16 November 2020
Accepted: 14 January 2021
Published: 18 January 2021

1. Introduction

Globally, nearly 38 million people are living with HIV (PLWH) [1]. The most critical advancement in this epidemic was the development and increased access to antiretroviral therapy (ART), which led to significant reductions in morbimortality through immune reconstitution and attenuation of homeostatic disruption [2]. This has reduced the incidence and severity of opportunistic infections (OI) such as *Mycobacterium tuberculosis* (Mtb) and *Avium complex* (MAC), *Cytomegalovirus* (CMV), Kaposi sarcoma-associated herpesvirus (KSHV), hepatitis C (HCV) and B (HBV) virus, *Cryptococcus neoformans*, *Pneumocystis jirovecci* and *Toxoplasma gondii*. However, paradoxically in a subset of PLWH, ART initiation may trigger clinical worsening with pathologic immune activation against these OIs, characterized by uncontrolled cytokine production known as immune reconstitution inflammatory syndrome (IRIS) [2].

IRIS is defined as a condition occurring shortly after ART initiation (up to 3 months) marked by rapid clinical deterioration with uncontrolled inflammatory processes despite